# Everything You Always Wanted to Know About XVA Model Risk but Were Afraid to Ask

Lorenzo Silotto[*], Marco Scaringi[†], Marco Bianchetti[‡]

September 17, 2021

## Abstract

Valuation adjustments, collectively named XVA, play an important role in modern derivatives pricing to take into account additional risk factors, in particular counterparty and funding risk. XVA are an exotic price component, since they require the time simulation of multiple risk factors in order to compute the portfolio exposure including possible collateral guarantees, leading to a significant model risk and computational effort even in case of plain vanilla trades.

This work analyses the most critical XVA model risk factors, meant as those to which XVA are most sensitive, looking for an acceptable compromise between accuracy and performance. We adopt a realistic modelling framework, based on a market standard multi-curve G2++ model calibrated on real market data, considering both Variation and Initial Margin, different collateralization schemes, and the most common linear and non-linear interest rates derivatives. Moreover, we consider also an alternative analytical approach to XVA for uncollateralized Swaps.

We show that a crucial element of the framework is the construction of a parsimonious time grid capable of capturing all periodical spikes arising in collateralized exposure during the Margin Period of Risk. To this end, we propose a workaround to efficiently capture all spikes. Moreover, we show that there exists parameterizations of the framework which allow a reasonable balance between accuracy and computational time, a very important feature for practical applications. Furthermore, in order to address the valuation uncertainty associated with the existence of a range of different parameterizations, we calculate the XVA Model Risk Additional Valuation Adjustment according to the provisions of the EU Prudent Valuation regulation.

Finally, this work serves as an handbook containing step-by-step instructions for the implementation of a complete, realistic and robust modelling framework of collateralized exposure and XVA.

---

[*]Deloitte Consulting S.r.l., `silotto.lorenzo@gmail.com`

[†]Intesa Sanpaolo, Financial and Market Risk Management, `marco.scaringi@intesasanpaolo.com`

[‡]Intesa Sanpaolo, Financial and Market Risk Management, and University of Bologna, Department of Statistical Sciences "Paolo Fortunati", `marco.bianchetti@unibo.it`

# Contents

**Disclaimer**: the views expressed here are those of the authors and do not represent the opinions of their employers. They are not responsible for any use that may be made of these contents.

# 1 Introduction

The 2007 credit crunch crisis has made necessary to reconsider the methodologies used until that time to price over-the-counter (OTC) derivatives. For example, during the crisis a change of regime in the interest rate market was observed: basis spreads between interest rate derivatives characterised by different underlying rate tenors (e.g. IBOR 3M[1], IBOR 6M, etc.) exploded and the spread between Overnight Indexed Swap (OIS) rates and rates of longer tenors widened significantly. This change of regime has lead to an evolution of market practice with the introduction of multiple interest rate yield curves (multi-curve framework) and OIS discounting. Literature is very extensive in this field, a non-exhaustive list of references includes [1, 2, 3, 4, 5, 6, 7]. Such framework has been recently questioned by the interest benchmark reform and the progressive replacement of the old IBOR rates with the corresponding risk free rates. Benchmark reform impacts XVA as well, but in this paper it is not considered at all. We refer to [8] for a discussion around the impact of EONIA-€STR discounting switch on XVA.

Moreover, the crisis triggered the incorporation of additional risk factors within the usual risk-neutral valuation through a set of valuation adjustments, collectively named XVA. In particular, the Lehman Brothers bankruptcy triggered a greater awareness amongst market participants on counterparty credit risk, leading to its inclusion in derivatives pricing via Credit Valuation Adjustment (CVA)[2]. Post-crisis also the own risk of default began to be addressed (see e.g. [10, 11]) leading to bilateral CVA models and Debt Valuation Adjustment (DVA). Both CVA and DVA are also envisaged by the International Financial Reporting Standards (IFRS) 13 (see par. 42 and 56, [12]). In addition, the observed widening of funding spreads originated a parallel stream of literature (see e.g. [13, 14, 15]) focused on the inclusion of financing costs in derivatives pricing via Funding Valuation Adjustment (FVA) which, even nowadays, represents a source of debate in quantitative finance community given the possible overlap between its Funding Benefit Adjustment (FBA) component and DVA (see [16] and references therein). In a similar way, the Margin Valuation Adjustment (MVA) takes into account the costs of financing the Initial Margin (see e.g. [17]). Finally, due to the increasing regulatory capital requirements triggered by the crisis (Basel II, [18] and Basel III, [19]), the literature started to consider these capital costs in derivatives pricing through the Capital Valuation Adjustment (KVA) (see e.g. [20]). From regulatory capital requirements perspective, Basel III has set provisions only for CVA and DVA by introducing the CVA capital charge to cover potential losses associated with a deterioration in the credit worthiness of a counterparty, and by de-recognizing DVA from CET1 capital to ensure that an increase in the credit risk of a bank does not lead to an increase in its common equity due to a reduction in the value of its liabilities (see par. 14(b) and 75, [19]).

This paper focuses on CVA and DVA, whose calculation requires modelling the credit exposure along the lifetime of a derivative position. The credit crunch crisis has pushed regulators to mitigate the credit exposure for OTC derivatives. In particular, with regard to non-cleared OTC derivatives, in 2015 the Basel Committee on Banking Supervision (BCBS) and the International Organization of Securities Commissions (IOSCO) finalized a framework, introduced progressively from 2016, which requires institutions engaging in these transactions to bilaterally post Variation Margin (VM) and Initial Margin (IM) on a daily basis at a netting set level (see [21]). In particular, VM aims at covering the current exposure stemming from changes in the value of the portfolio by reflecting its current size, while IM aims at covering the potential future exposure that could arise, in the event of default of the counterparty, from changes in the value of the portfolio in the the period between last VM exchange and the close-out of the position. IM represented an element of innovation in bilateral derivatives markets and according to [21]

---

[1]IBOR denotes a generic Interbank Offered Rates.

[2]Which actually was explored before the crisis, see e.g. [9] and references therein.

4

shall be calculated through either a standardized schedule or an approved internal model. With the aim to prevent both potential disputes between counterparties related to IM determination with different internal models and the overestimation of margin requirements due to the non-risk-sensitive standard approach (see [22]), the International Swaps and Derivatives Association (ISDA) developed the Standard Initial Margin Model (SIMM), a uniform risk-sensitive model for calculating bilateral IM (see [23]), the first version of which was published in 2016.

These margin requirements mitigate credit exposure with impacts on CVA/DVA, therefore VM and IM have to be correctly modelled. Extensive literature exists regarding VM (see e.g. [24, 25, 26]). On the other hand, ISDA-SIMM dynamic IM modelling involves the simulation of several forward sensitivities and their aggregation according to a set of predefined rules, this poses difficult computation and implementation challenges. Different methods have been proposed to overcome such challenges: approximations based on normal distribution assumptions (see [27, 28]), approximated pricing formulas to speed up the calculation (see e.g. [29, 30]), adjoint algorithmic differentiation (AAD) for fast sensitivities calculation (see e.g. [31, 32]) and regression techniques to approximate IM (see e.g. [33, 34]). This paper focuses on the implementation of ISDA-SIMM avoiding as much as possible any approximation. Moreover, in calculating forward sensitivities we considered a finite-difference "bump-and-run" approach which, although computationally intensive compared to AAD, is still used in the financial industry when performances are not critical.

In general, XVA pricing is subject to significant model risk as it depends on many assumptions made for modelling and calculating the relevant quantities in a reasonable computation time. This model risk arises principally from the need to optimize the trade-off between accuracy and performance. In light of this, our paper is intended to answer to the following two interconnected questions:

1. which are the most critical model risk factors, meant as those to which exposure modelling and thus CVA/DVA are most sensitive?

2. Is there an acceptable compromise between accuracy and performance?

We address these questions by identifying all the relevant calculation parameters involved in the standard Monte Carlo approach for computing CVA/DVA and by analysing their impacts in terms of accuracy of the results and computational effort required. Specifically, we calculated CVA/DVA using real market data for both linear and non-linear interest rates derivatives for different collateralization schemes. Clearly, collateral simulation introduces a series of complexities which pose greater computational effort to obtain reliable results; we propose a possible solution which allows to obtain robust results in a reasonable time.

Our work extends the existing literature in the following regards. We provide a comprehensive description of the work-flow of an XVA desk, also tackling practical issues such as the calculation of the implied volatility in future scenarios. Furthermore, we consider a complete framework including different collateralization schemes and interest rates derivatives based on real market data. In this context, we generalize G2++ model to multi-curve framework also allowing for the time dependency of volatility parameters for both risk factor dynamics and pricing formulas for Swaps and Swaptions, reporting all mathematical details. In addition, we describe the implementation of ISDA-SIMM dynamic IM focusing on the principal methodological peculiarities. Regarding XVA pricing, we address the related model risk by analysing CVA and DVA sensitivities to the relevant calculation parameters and by applying the provisions of regulation [35, 36] regarding the calculation of Model Risk Additional Valuation Adjustment (MoRi AVA). Finally, we compare XVA for uncollateralized Swaps with those obtained through an alternative analytical approach.

The paper is organized as follows. In sec. 2 we introduce the notation, we briefly remind the basic theoretical framework and pricing formulas for the instruments analysed, we describe the

model used for simulating interest rates, and we remind CVA/DVA formulas describing both Monte Carlo and analytical approaches for their numerical calculation. In sec. 3 we introduce collateral and we describe the assumptions made for modelling VM and IM along with their calculation methodologies. In sec. 4 we describe the parameterization optimizing the trade-off between accuracy and performance and we show the results both in terms of credit exposure and CVA/DVA for the selected instruments. In sec. 5 we report the analyses conducted on model parameters in order to answer the questions above and we describe the calculation of the MoRi AVA. In sec. 6 we draw the conclusions.

## 2 Theoretical Framework

### 2.1 Pricing Approach

Assuming no arbitrage and the usual probabilistic framework $(\Omega, \mathcal{F}, \mathcal{F}_t, Q)$ with market filtration $\mathcal{F}_t$ and risk-neutral probability measure $Q$, the general pricing formula of a financial instrument with payoff $V(T)$ paid at time $T > t$ is

$$V(t) = V_0(t) + \text{XVA}(t), \tag{2.1}$$

$$V_0(t) = \mathbb{E}^Q \left[ D(t; T) V(T) \,|\, \mathcal{F}_t \right] = P(t; T) \mathbb{E}^{Q^T} \left[ V(T) \,|\, \mathcal{F}_t \right], \tag{2.2}$$

$$D(t; T) = \frac{B(t)}{B(T)} = e^{-\int_t^T r(u) du}, \tag{2.3}$$

$$P(t; T) = \mathbb{E}^Q \left[ D(t; T) \,|\, \mathcal{F}_t \right], \tag{2.4}$$

where the base value[3] (or mark to market) $V_0(t)$ in eq. 2.2 is interpreted as the price of the financial instrument under perfect collateralization[4], the discount (short) rate $r(t)$ in eq. 2.3 is the corresponding collateral rate, $B(t)$ is the collateral bank account growing at rate $r(t)$, $D(t; T)$ is the stochastic collateral discount factor, $P(t; T)$ is the Zero Coupon Bond (ZCB) price, and $Q^T$ is the $T$-forward probability measure associated to the numeraire $P(t; T)$. Valuation adjustments in eq. 2.1, collectively named XVA, represent a crucial and consolidated component in modern derivatives pricing which takes into account additional risk factors not included among the risk factors considered in the base value $V_0$ in eq. 2.2. These risk factors are typically related to counterparties default, funding, and capital, leading, respectively, to Credit/Debt Valuation Adjustment (CVA/DVA), Funding Valuation Adjustment (FVA), often split into Funding Cost/Benefit Adjustment (FCA/FBA), Margin Valuation Adjustment (MVA), Capital Valuation Adjustment (KVA). A complete discussion on XVA may be found e.g. in [16]. For XVA pricing we must consider the enlarged filtration $\mathcal{G}_t = \mathcal{F}_t \vee \mathcal{H}_t \supseteq \mathcal{F}_t$ where $\mathcal{H}_t = \sigma(\{\tau \le u\} : u \le t)$ is the filtration generated by default events (see e.g. [24, 25, 26]). More details on XVA pricing are discussed in sec. 2.4 below.

### 2.2 Instruments

In this section we briefly describe the financial instruments subject to our analyses along with their corresponding pricing formulas. In particular, our analyses rely on Interest Rate Swaps and physically settled European Swaptions both characterized by the following time schedules

---

[3]In order to ease the notation, for the rest of the paper we omit subscript 0 unless clearly necessary, denoting the base value simply with $V$.

[4]An ideal Credit Support Annex (CSA) ensuring a perfect match between the price $V_0(t)$ and the corresponding collateral at any time $t$. This condition is realised in practice with a real CSA minimizing any friction between the price and the collateral, i.e. with daily margination, cash collateral in the same currency of the trade, flat overnight collateral rate, zero threshold and minimum transfer amount (see sec. 3 for further details).

for the fixed and floating leg of the Swap

$$\begin{aligned}
&\mathbf{S} = \{S_0, \ldots, T_i, \ldots, S_m\}, \text{ fixed leg schedule,} \\
&\mathbf{T} = \{T_0, \ldots, T_j, \ldots, T_n\}, \text{ floating leg schedule,} \\
&S_0 = T_0,\ S_m = T_n.
\end{aligned} \tag{2.5}$$

### 2.2.1 Interest Rate Swap

We consider a generic Swap contract, which allows the exchange of a fixed rate $K$ against a floating rate, characterised by the time schedules $\mathbf{S}$ and $\mathbf{T}$ and the following payoffs for the fixed and floating legs, respectively,

$$\begin{aligned}
&\mathbf{Swaplet}_{\text{fix}}(S_i; S_{i-1}, S_i, K) = NK\tau_K(S_{i-1}, S_i), \\
&\mathbf{Swaplet}_{\text{float}}(T_j; T_{j-1}, T_j) = NR_x(T_{j-1}, T_j)\tau_R(T_{j-1}, T_j),
\end{aligned} \tag{2.6}$$

where $\tau_K$ and $\tau_R$ are the year fractions for fixed and floating rate conventions, respectively, and $R_x(T_{j-1}, T_j)$ is the underlying spot floating rate with tenor $x$, consistent with the time interval $[T_{j-1}, T_j]$.

The price of the Swap at time $t$ is given by the sum of the prices of fixed and floating cash flows occurring after $t$,

$$\begin{aligned}
&\mathbf{Swap}(t; \mathbf{T}, \mathbf{S}, K, \omega) = N\omega \left[ \sum_{j=\eta_L(t)}^{n} P(t; T_j)F_{x,j}(t)\tau_R(T_{j-1}, T_j) - KA(t; \mathbf{S}) \right], \\
&A(t; \mathbf{S}) = \sum_{i=\eta_K(t)}^{m} P(t; S_i)\tau_K(S_{i-1}, S_i),
\end{aligned} \tag{2.7}$$

where $N$ is the notional amount, $\omega = +/-1$ denotes a payer/receiver Swap (referred to the fixed leg), $\eta_L(t) = \min\{j \in \{1, ..., n\} \text{ s.t. } T_j \geq t\}$ and $\eta_K(t) = \min\{i \in \{1, ..., m\} \text{ s.t. } S_j \geq t\}$ are the first future cash flows in the Swap's schedules, $A(t; \mathbf{S})$ is the annuity, and $F_{x,j}(t)$ is the forward rate observed at time $t$, fixing at future time[5] $T_{j-1}$ and spanning the future time interval $[T_{j-1}, T_j]$, given by

$$F_{x,j}(t) = F_x(t; T_{j-1}, T_j) = \mathbb{E}^{Q^{T_j}}\left[ R_x(T_{j-1}, T_j) | \mathcal{F}_t \right]. \tag{2.8}$$

By construction, the forward rate $F_{x,j}(t)$ is a martingale under the forward measure $Q^{T_j}$ associated to the numeraire $P(t; T_j)$.

The par Swap rate $R_x^{\text{Swap}}(t; \mathbf{T}, \mathbf{S})$, i.e. the fixed rate $K$ such that the Swap is worth zero, is given by

$$R_x^{\text{Swap}}(t; \mathbf{T}, \mathbf{S}) = \frac{\sum_{j=\eta_L(t)}^{n} P(t; T_j)F_x, j(t)\tau_R(T_{j-1}, T_j)}{A(t; \mathbf{S})}. \tag{2.9}$$

The Swap's price in terms of the par Swap rate can be expressed as

$$\mathbf{Swap}(t; \mathbf{T}, \mathbf{S}, K, \omega) = N\omega\left[ R_x^{\text{Swap}}(t; \mathbf{T}, \mathbf{S}) - K \right] A(t; \mathbf{S}). \tag{2.10}$$

The underlying rate $R_x(T_{j-1}, T_j)$ is an IBOR with a tenor $x$ consistent with the time interval $[T_{j-1}, T_j]$ (e.g. $x = 6M$ for EURIBOR 6M and semi-annual coupons). IBOR forward rates $F_{x,j}(t)$ are computed from IBOR yield curves built from homogeneous market IRS quotes (i.e.

---

[5]If $T_{j-1} \leq t \leq T_j$ the rate has already fixed, hence $F_{x,j}(t) = R_x(T_{j-1}, T_j)$.

with the same underlying IBOR tenor $x$), using the corresponding OIS yield curve for discounting, a procedure commonly called multi-curve bootstrapping[6]. We can write the usual expression of forward rates

$$F_{x,j}(t) = \frac{1}{\tau_F(T_{j-1}, T_j)} \left[ \frac{P_x(t; T_{j-1})}{P_x(t; T_j)} - 1 \right],$$ (2.11)

where $\tau_F$ is the year fraction with the forward rate convention and $P_x(t; T_j)$ can be interpreted as the price of a risky ZCB issued by an average IBOR counterparty[7].

### 2.2.2 European Swaption

A physically settled European Swaption is a contract which gives to the holder the right to enter, at a given expiry time $T_e$, into a Swap contract starting at $T_0 \geq T_e$ and maturing at $T_m$ with time schedules $\mathbf{S}$ and $\mathbf{T}$. The payoff can be written as

$$\begin{aligned}
\mathbf{Swaption}(T_e; \mathbf{T}, \mathbf{S}, K, \omega) &= \max \left[ \mathbf{Swap}(T_e; \mathbf{T}, \mathbf{S}, K, \omega); 0 \right], \\
&= NA(T_e; \mathbf{S}) \max \left\{ \omega \left[ R_x^{\mathrm{Swap}}(T_e; \mathbf{T}, \mathbf{S}) - K \right]; 0 \right\}.
\end{aligned}$$ (2.12)

The market practice is to value physically settled European Swaptions through the Black formula, assuming a shifted log-normal driftless dynamics for the evolution of the Swap rate under its corresponding discounting Swap measure[8] $Q_S$ associated to the numeraire $A(t, \mathbf{S})$. Formally, the price of a physically settled European Swaption at time $t$ is given by

$$\begin{aligned}
\mathbf{Swaption}(t; \mathbf{T}, \mathbf{S}, K, \omega) &= N\mathbb{E}^Q \left\{ D(t; T_e) A(T_e; \mathbf{S}) \max \left[ \omega \left[ R_x^{\mathrm{Swap}}(T_e; \mathbf{T}, \mathbf{S}) - K \right]; 0 \right] | \mathcal{F}_t \right\}, \\
&= NA(t; \mathbf{S}) \mathbb{E}^{Q_S} \left\{ \max \left[ \omega \left[ R_x^{\mathrm{Swap}}(T_e; \mathbf{T}, \mathbf{S}) - K \right]; 0 \right] | \mathcal{F}_t \right\}, \\
&= NA(t; \mathbf{S}) \mathrm{Black} \left[ R_x^{\mathrm{Swap}}(t; \mathbf{T}, \mathbf{S}), K, \lambda_x, v_x(t; \mathbf{T}, \mathbf{S}), \omega \right],
\end{aligned}$$ (2.13)

where $\lambda_x$ is the constant log-normal shift, $v_x(t; \mathbf{T}, \mathbf{S}) = \int_t^{T_e} \sigma_x(u; \mathbf{T}, \mathbf{S})^2 du$ is the shifted log-normal implied forward variance, with $\sigma_x(t; T_e, \mathbf{T}, \mathbf{S}) = \sqrt{\frac{v_x(t; \mathbf{T}, \mathbf{S})}{\tau_x(t, T_e)}}$ being the shifted log-normal implied forward volatility.

## 2.3 G2++ Model

As regards interest rate simulation, due to its analytical tractability, we considered the Shifted two-factor Gaussian (Vasicek) model G2++, equivalent to the Hull-White Two-Factor Model, introduced in [39]. We generalized G2++ model in multi-curve framework also allowing for the time dependency of volatility parameters. In following sections we describe the instantaneous short rate process dynamics, pricing formulas for Swaps and European Swaptions, and the methodologies used for calibrating model parameters and for implementing Monte Carlo simulation. Pricing formulas are further described in app. B.

### 2.3.1 Short-Rates Dynamics

The dynamics of the instantaneous short rate process under the risk-neutral measure $Q$ is given by

$$r^c(t) = x(t) + y(t) + \varphi^c(t), \qquad r^c(0) = r_0^c,$$ (2.14)

---

[6]Since OIS and IBOR curves with different tenors are involved, see e.g. [37] for a detailed discussion.

[7]Namely an issuer with a credit risk equal to the average credit risk of the IBOR panel, see e.g. [38].

[8]Since $\mathbb{E}^Q \left[ D(t; T) V(T) | \mathcal{F}_t \right] = A(t; \mathbf{S}) \mathbb{E}^{Q_S} \left[ \frac{V(T)}{A(T; \mathbf{S})} \Big| \mathcal{F}_t \right]$.

where $c \in \{d, x\}$, with $d$ and $x$ denoting, respectively, the discount curve $\mathcal{C}_d$ and the forward curve $\mathcal{C}_x$. The processes $\{x_t\}_{t \geqslant 0}$ and $\{y_t\}_{t \geqslant 0}$ are defined as follows

$$dx(t) = -ax(t)dt + \sigma(t)dW_1(t), \qquad x(0) = 0, \tag{2.15}$$

$$dy(t) = -by(t)dt + \eta(t)dW_2(t), \qquad y(0) = 0, \tag{2.16}$$

where $(W_1, W_2)$ is a two dimensional Brownian motion with an instantaneous correlation $\rho$ such that

$$dW_1(t)dW_2(t) = \rho dt, \tag{2.17}$$

with $r_0^c$, $a$, $b$ positive constants, $-1 \leqslant \rho \leqslant 1$, $\sigma(t) = \sigma\Gamma(t)$, $\eta(t) = \eta\Gamma(t)$, with $\Gamma : \mathbb{R} \to \mathbb{R}^+$ piece-wise constant function written as $\Gamma = \sum_i \Gamma_i \chi_{[T_i, T_{i+1}]}$. The function $\varphi^c$ is deterministic and well defined in the time interval $[0, T^*]$. This modification of G2++ model represents the most parsimonious way to take into account the multi-curve dynamics of interest rates (see e.g. [6] for G1++ model).

By integrating eqs. 2.15 and 2.16 we obtain, for each $s < t$

$$
\begin{aligned}
r^c(t) = x(s)e^{-a(t-s)} + y(s)e^{-b(t-s)} \\
+ \sigma \int_s^t \Gamma(u)e^{-a(t-u)}dW_1(u) + \eta \int_s^t \Gamma(u)e^{-b(t-u)}dW_2(u) + \varphi^c(t),
\end{aligned}
\tag{2.18}
$$

from which we can see that $r^c(t)$, conditional on the sigma-field $\mathcal{F}_s$ generated by the pair $(x, y)$ up to time $s$, is normally distributed with mean ad variance, respectively,

$$\mathbb{E}\left(r^c(t)|\mathcal{F}_s\right) = x(s)e^{-a(t-s)} + y(s)e^{-b(t-s)} + \varphi^c(t), \tag{2.19}$$

$$\mathrm{Var}(r^c(t)|\mathcal{F}_s) = \frac{\sigma^2}{2a}\sum_{i=u}^{v}\Gamma_i^2 e^{-2at}e^{2a(T_{i+1}-T_i)} + \frac{\eta^2}{2b}\sum_{i=u}^{v}\Gamma_i^2 e^{-2bt}e^{2b(T_{i+1}-T_i)},$$

$$+ 2\frac{\rho\eta\sigma}{a+b}(1 - e^{-(a+b)t})\sum_{i=u}^{v}\Gamma_i^2 e^{(a+b)(T_{i+1}-T_i)}, \tag{2.20}$$

where for the variance we assumed, without loosing generality, that $T_u = s$ and $T_{v+1} = t$ for a certain $u$ and $v$ with $u < v$.

### 2.3.2 Interest Rate Swap and European Swaption Pricing

In [39] it is shown that in single-curve framework G2++ model admits closed pricing formulas for the price of Swaps and European Swaptions. In particular, Swap pricing is fairly straightforward since ZCB are known, while for an European Swaption it is necessary to compute an integral. We generalized G2++ pricing formulas in multi-curve framework also allowing for time dependent (piece-wise constant) volatility parameters in such a way to preserve the proofs in [39]. All details are reported in app. B.

### 2.3.3 Calibration

We calibrated G2++ model parameters on at-the-money (ATM) Swaption prices following a two-steps procedure:

1. Constant volatility calibration: calibration of $a, b, \sigma, \eta, \rho$ by minimizing the following objective function, which represents the distance between market prices $V^{\mathrm{mkt}}$ and model prices $V^{\mathrm{G2++}}$ for each combination of expiry $\{\xi_i\}_{i=1}^{M}$ and tenor $\{\mathfrak{T}_j\}_{j=1}^{N}$

$$\left\{\hat{a}, \hat{b}, \hat{\sigma}, \hat{\eta}, \hat{\rho}\right\} = \underset{\{a,b,\sigma,\eta,\rho\}}{\arg\min} \sum_{i=1}^{M}\sum_{j=1}^{N}\left(\frac{V^{\mathrm{G2++}}(a, b, \sigma, \eta, \rho; \xi_i, \mathfrak{T}_j)}{V^{\mathrm{mkt}}(\xi_i, \mathfrak{T}_j)} - 1\right)^2. \tag{2.21}$$

9

2. Time dependent volatility calibration: calibration of the function $\Gamma(t)$ which multiplies $\hat{\sigma}$ and $\hat{\eta}$ obtained from step above. We calibrated $\Gamma_i = \Gamma(\xi_i)$ through an iterative calibration which minimizes the following objective function for each expiry $\xi_i$ using $\{\hat{\Gamma}_k\}_{k=1}^{i-1}$ calibrated in the previous iterations

$$\hat{\Gamma}_i = \arg\min_{\Gamma_i} \sum_{j=1}^{N} \left( \frac{V^{\mathrm{G2++}}(\hat{a}, \hat{b}, \hat{\sigma}\Gamma_i, \hat{\eta}\Gamma_i, \hat{\rho}; \xi_i, \mathfrak{T}_j)}{V^{\mathrm{mkt}}(\xi_i, \mathfrak{T}_j)} - 1 \right)^2, \qquad i = 1, \ldots, M. \qquad (2.22)$$

### 2.3.4 Monte Carlo Simulation

Since G2++ is analytically tractable, it is possible to avoid unnecessary workloads by simulating the processes $x(t)$ and $y(t)$ under the $T$-forward measure $Q^T$ (see e.g. [40, 39]). In [39] the dynamics of $x(t)$ and $y(t)$ are rewritten under the $T$-forward measure $Q^T$ and explicit solutions for the stochastic differential equations are shown. Following the authors, we considered the following simulation scheme by using the exact transition density and generalizing for time-dependent volatility parameters

$$x(t) = x(s)e^{-a(t-s)} - M_x^T(s;t) + N_1(t-s), \qquad (2.23)$$
$$y(t) = y(s)e^{-b(t-s)} - M_y^T(s;t) + N_2(t-s), \qquad (2.24)$$

for $s \leq t \leq T$, where $M_x^T(s;t)$ and $M_y^T(s;t)$ are the drift components (see app. B), and $N(t-s)$ is a two-dimensional normal random vector with zero mean and covariance matrix (assuming $T_u = s$ and $T_{v+1} = t$)

$$\boldsymbol{\Sigma}(t-s) = \begin{bmatrix} \frac{\sigma^2}{2a} \sum_{i=u}^{v} \Gamma_i^2 e^{-2at} e^{2a(T_{i+1}-T_i)} & \frac{\rho\eta\sigma}{a+b} \left[ 1 - e^{-(a+b)t} \right] \sum_{i=u}^{v} \Gamma_i^2 e^{(a+b)(T_{i+1}-T_i)} \\ \frac{\rho\eta\sigma}{a+b} \left[ 1 - e^{-(a+b)t} \right] \sum_{i=u}^{v} \Gamma_i^2 e^{(a+b)(T_{i+1}-T_i)} & \frac{\eta^2}{2b} \sum_{i=u}^{v} \Gamma_i^2 e^{-2bt} e^{2b(T_{i+1}-T_i)} \end{bmatrix}$$
$$(2.25)$$

In detail, we defined a time grid $t = t_0 < \ldots < t_i < \cdots < t_{N_T} = T$ and we calculated the price of each instrument at a future time step $t_i$ (or mark to future) by simulating forward market risk factors using the pair $(x(t_i), y(t_i))$, obtained from the previously generated $(x(t_{i-1}), y(t_{i-1}))$ by applying eqs. 2.23 and 2.24, with $s = t_{i-1}$ and $t = t_i$, for $i = 1, \ldots, N_T$. It should be noticed that, for our purposes, we do not need to simulate $r(t)$ since the price of a Swap or an European Swaptions can be obtained directly through $x(t)$ and $y(t)$ (see app. B).

## 2.4 XVA Pricing

As mentioned before, our paper is focused on Credit Valuation Adjustment (CVA) and Debt Valuation Adjustment (DVA) which take into account the risks related to counterparties default. In particular, CVA is related to counterparty default, while DVA is related to own default. In this section we define these valuation adjustments and we describe both the adopted Monte Carlo approach and an alternative analytical approach limited to CVA/DVA calculation of Swaps.

### 2.4.1 Definitions

Let us consider the two parts of the contract as the Bank (B) and the Counterparty (C) assuming that both can default at instant $\tau_X$, $X \in \{B,C\}$.

In order to define CVA we suppose that $\tau_C < \tau_B < T$, i.e. C defaults before B and contract maturity $T$, and B has positive exposure with regard to C. In this case, B suffers a loss equal to the replacement cost of the position. CVA is therefore the discounted value of expected future loss suffered by B due to the default of C and it is a negative quantity in B's perspective.

On the other hand, to define DVA we consider the opposite situation: $\tau_B < \tau_C < T$, i.e. B

defaults before C and contract maturity $T$, and B has negative exposure with regard to C. In this case, C suffers a loss equal to the replacement cost of the position. DVA is therefore the discounted value of expected future loss suffered by C due to the default of B and it is a positive quantity in B's perspective. Formally

$$\text{CVA}(t) = -\mathbb{E}^Q \left[ D(t; \tau_{\text{C}}) LGD_{\text{C}}(\tau_{\text{C}}) \left[ H(\tau_{\text{C}}) \right]^+ \mathbb{1}_{\{t < \tau_{\text{C}} < \tau_{\text{B}} < T\}} \, | \mathcal{G}_t \right], \tag{2.26}$$

$$\text{DVA}(t) = -\mathbb{E}^Q \left[ D(t; \tau_{\text{B}}) LGD_{\text{B}}(\tau_{\text{B}}) \left[ H(\tau_{\text{B}}) \right]^- \mathbb{1}_{\{t < \tau_{\text{B}} < \tau_{\text{C}} < T\}} \, | \mathcal{G}_t \right], \tag{2.27}$$

$$H(\tau_{\text{X}}) = \mathbb{E}^Q_{\tau_{\text{X}}} \left[ V_0(\tau_{\text{X}}) \right] - C(\tau_{\text{X}}), \tag{2.28}$$

where $H(\tau_{\text{X}})$ denotes the exposure at time $\tau_{\text{X}} > t$ in the event of default of X, $V_0(\tau_{\text{X}})$ is the base value[9] of the instrument at time $\tau_{\text{X}}$, $C(\tau_{\text{X}})$ denotes generically the collateral available at time $\tau_{\text{X}}$ (see sec. 3 for a specific definition in relation with our purposes), and $LGD_{\text{X}}(\tau_{\text{X}}) = 1 - R_{\text{X}}(\tau_{\text{X}})$ is the Loss Given Default at time $\tau_{\text{X}}$, which represents the percentage amount of the exposure expected to be loss in case of X's default, with $R_{\text{X}}$ denoting the Recovery Rate.

Assuming independence among credit and interest rate processes and even among default instants $\tau_{\text{B}}$, $\tau_{\text{C}}$ and in absence of wrong way risk[10], the expectations in eqs. 2.26 and 2.27 can be represented as integrals over time,

$$\text{CVA}(t) = -\int_t^T \mathbb{E}^Q \left[ D(t; u) LGD_{\text{C}} \left[ H(u) \right]^+ | \mathcal{F}_t \right] \mathbb{E}^Q \left[ \mathbb{1}_{\{t < \tau_{\text{C}} < \tau_{\text{B}} < T\}} | \mathcal{H}_t \right] du,$$

$$= -LGD_{\text{C}} \int_t^T \mathbb{E}^Q \left[ D(t; u) \left[ H(u) \right]^+ | \mathcal{F}_t \right] S_{\text{B}}(t, u) dQ_{\text{C}}(t, u), \tag{2.29}$$

$$\text{DVA}(t) = -\int_t^T \mathbb{E}^Q \left[ D(t; u) LGD_{\text{B}} \left[ H(u) \right]^- | \mathcal{F}_t \right] \mathbb{E}^Q \left[ \mathbb{1}_{\{t < \tau_{\text{B}} < \tau_{\text{C}} < T\}} | \mathcal{H}_t \right] du,$$

$$= -LGD_{\text{B}} \int_t^T \mathbb{E}^Q \left[ D(t; u) \left[ H(u) \right]^- | \mathcal{F}_t \right] S_{\text{C}}(t, u) dQ_{\text{B}}(t, u), \tag{2.30}$$

where $S_{\text{X}}(t, u)$ is the survival probability of X until time $u$ valued at $t$ such that $S_{\text{X}}(t, u) = \mathbb{E}^Q \left[ \mathbb{1}_{\{\tau_{\text{X}} > u\}} | \mathcal{H}_t \right] = \mathbb{E}^Q \left[ e^{-\int_t^u \gamma_{\text{X}}(s) ds} | \mathcal{H}_t \right] = 1 - Q_{\text{X}}(t, u)$, with $\gamma_{\text{X}}$ denoting the stochastic hazard rate of X (see e.g. [39]); $dQ_{\text{X}}(t, u) = Q_{\text{X}}(t, u, u + du)$ is the marginal default probability of X referred to the infinitesimal time interval $[u, u + du]$ valued at $t$; $\mathcal{F}_t$ and $\mathcal{H}_t$ denote respectively the market filtration and the filtration generated by default events (see e.g. [24, 25, 26]). $LGD_{\text{X}}$ is assumed to be constant.

Similar formulas for other XVA can be found in e.g. [16]. Survival probabilities used for XVA are computed from default curves built from market CDS quotes through standard bootstrapping procedure.

### 2.4.2 Calculation Methodology

Our work is based on the standard Monte Carlo simulation approach to solve eqs. 2.29 and 2.30, which allows to calculate CVA and DVA for any instrument, both at trade and at netting set level, also in the presence of collateral agreements. This approach, whilst the most time-consuming for exposure quantification, allows us to easily cope with the various complexities related to XVA calculation.

First of all, it is necessary to discretize the integral along a time grid $t = t_0 < \ldots < t_i < \cdots < t_{N_T} = T$, with $T$ being instrument's maturity. Then, in order to simulate the relevant quantities over time, it is necessary to make assumptions regarding their stochastic dynamics.

---

[9]We assume "risk free" close-out at the base value, without any adjustment.

[10]Risk arising when the exposure with the counterparty is inversely related to the creditworthiness of the counterparty itself.

To this end, G2++ model admits closed pricing formulas for Swap and European Swaptions (see app. B) and as such, once simulated the processes $x(t_i)$ and $y(t_i)$ (see sec. 2.3.4), the exposure can be computed.

In light of what stated above, eqs. 2.29 and 2.30 can be discretized as follows (see e.g. [16])

$$\text{CVA}(t) \cong -LGD_C \sum_{i=1}^{N_T} \mathcal{H}^+(t;t_i)\mathcal{S}_B(t,t_i)\Delta\mathcal{Q}_C(t,t_i), \qquad (2.31)$$

$$\text{DVA}(t) \cong -LGD_B \sum_{i=1}^{N_T} \mathcal{H}^-(t;t_i)\mathcal{S}_C(t,t_i)\Delta\mathcal{Q}_B(t,t_i), \qquad (2.32)$$

with

$$\mathcal{H}^{\pm}(t;t_i) = \mathbb{E}^Q\left[D(t;t_i)\left[H(t_i)\right]^{\pm}|\mathcal{F}_t\right]$$
$$= P(t;t_i)\mathbb{E}^{Q^{t_i}}\left[\left[H(t_i)\right]^{\pm}|\mathcal{F}_t\right] \cong P(t;t_i)\frac{1}{N_{MC}}\sum_{m=1}^{N_{MC}}\left[H_m(t_i)\right]^{\pm} \qquad (2.33)$$

where $\mathcal{H}^+(t;t_i)$ is the Expected Positive Exposure (EPE) at time $t$, discretized on interval $(t_{i-1},t_i]$, $\mathcal{H}^-(t;t_i)$ is the Expected Negative Exposure (ENE), $H_m(t_i)$ is the exposure at time step $t_i$ for path $m$ (see eq. 3.1), $\mathcal{S}_x(t,t_i) = 1 - \mathcal{Q}_x(t,t_i)$ is the survival probability of X at time $t$, referred to time interval $[t,t_i]$ and $\Delta\mathcal{Q}_x(t,t_i) = \mathcal{Q}_x(t,t_i) - \mathcal{Q}_x(t,t_{i-1})$ is the marginal default probability of X at time $t$, referred to interval $(t_{i-1},t_i]$.

### 2.4.3 Analytical Formulas

For some derivatives, such as Swaps, it is possible to analytically solve eqs. 2.29 and 2.30 with considerable benefits in terms of computational time, but limited to uncollateralized case and at trade level. Nevertheless, this approach can be used with the aim to validate the results obtained through a Monte Carlo model (see sec. 5.5).

Starting from eq. 2.29, the CVA of an uncollateralized Swap at time $t$ can be written as (see e.g. [16])

$$\text{CVA}(t) = -LGD_C \int_t^T \mathbb{E}^Q\left\{D(t;u)\left[\mathbf{Swap}(u;\mathbf{T},\mathbf{S},K,\omega)\right]^+|\mathcal{F}_t\right\}S_B(t,u)dQ_C(t,u). \qquad (2.34)$$

By rewriting the price of the Swap in terms of Swap rate (eq. 2.10) and rearranging the terms, the equation above becomes

$$\text{CVA}(t) = -LGD_C \int_t^T N\mathbb{E}^Q\left\{D(t;u)A(u;\mathbf{S})\omega\left[R_x^{Swap}(u;\mathbf{T},\mathbf{S}) - K\right]^+|\mathcal{F}_t\right\}S_B(t,u)dQ_C(t,u),$$
$$= -LGD_C \int_t^T \mathbf{Swaption}(t;u,\mathbf{T},\mathbf{S},K,\omega)S_B(t,u)dQ_C(t,u), \qquad (2.35)$$

where $\mathbf{Swaption}(t;u,\mathbf{T},\mathbf{S},K,\omega)$ denotes the price at time $t$ of an European Swaption expiring at time $u$ on a Swap having tenor equal to $\mathcal{T} = T - u$.

Since $[A]^- = [-A]^+$, the analytical DVA can be obtained as

$$\text{DVA}(t) = -LGD_B \int_t^T \mathbb{E}^Q\left\{D(t;u)\mathbf{Swap}(u;\mathbf{T},\mathbf{S},K,\omega)^-|\mathcal{F}_t\right\}S_C(t,u)dQ_B(t,u),$$
$$= -LGD_B \int_t^T \mathbb{E}^Q\left\{D(t;u)\mathbf{Swap}(u;\mathbf{T},\mathbf{S},K,-\omega)^+|\mathcal{F}_t\right\}S_C(t,u)dQ_B(t,u), \qquad (2.36)$$
$$= -LGD_B \int_t^T \mathbf{Swaption}(t;u,\mathbf{T},\mathbf{S},K,-\omega)S_C(t,u)dQ_B(t,u).$$

By discretizing the above integrals along a time grid $t = t_0 < t_1 < \ldots < t_{N_T} = T$, with $T$ being the maturity of the Swap one obtains

$$\text{CVA}(t) \cong -LGD_{\text{C}} \sum_{i=1}^{N_T} \textbf{Swaption}(t; t_i, \textbf{T}, \textbf{S}, K, \omega) \mathcal{S}_{\text{B}}(t, t_i) \Delta \mathcal{Q}_{\text{C}}(t, t_i), \tag{2.37}$$

$$\text{DVA}(t) \cong -LGD_{\text{B}} \sum_{i=1}^{N_T} \textbf{Swaption}(t; t_i, \textbf{T}, \textbf{S}, K, -\omega) \mathcal{S}_{\text{C}}(t, t_i) \Delta \mathcal{Q}_{\text{B}}(t, t_i). \tag{2.38}$$

Thus, the CVA of a payer (receiver) Swap at time $t$ can be written as a weighted sum with weights represented by the values of a strip of co-terminal payer (receiver) European Swaptions expiring at time $t_i$ to enter in a Swap with tenor $\mathcal{T} = T - t_i$. Symmetrically, DVA can be obtained as a weighted sum over the values of a strip of receiver (payer) European Swaptions.

## 3 Collateral Modelling

With the aim to reduce the systemic risk posed by non-cleared OTC derivatives, BCBS-IOSCO framework (see [21]) requires institutions engaging in these transactions to post bilaterally Variation Margin (VM) and Initial Margin (IM) on a daily basis at a netting set level. On the one hand, VM aims at covering the current exposure stemming from changes in instrument's mark to market by reflecting its current size. On the other hand, IM aims at covering the potential future exposure that could arise, in the event of default of the counterparty, from changes in instrument's mark to market in the the period between last VM exchange and the close-out of the position; this time interval is known as Margin Period of Risk (MPoR).

This section introduces collateral and describes the assumptions made for calculating VM and IM, with a particular focus on ISDA-SIMM dynamic IM.

### 3.1 Collateral Management

ISDA Master Agreement represents the most common legal framework which governs bilateral OTC derivatives transactions. In particular, the Credit Support Annex (CSA) to ISDA Master Agreement provides the terms under which collateral is posted, along with rules for the resolution of collateral disputes. Certain CSA parameters affect the residual exposure, namely: eligible assets (cash, cash equivalent, government bonds), margin call frequency, threshold (K), defined as the maximum amount of allowed unsecured exposure before any margin call is made, and minimum transfer amount (MTA), defined as the minimum amount that can be transferred for each margin call.

Under perfect collateralization, counterparty risk is suppressed resulting in null CVA/DVA. Theoretically, this corresponds to an ideal CSA ensuring a perfect match between the price $V_0(t)$ and the corresponding collateral at any time $t$. This condition is approximated in practice with a CSA minimizing any friction between the mark to market and the collateral, i.e. cash collateral in the same currency of the trade, daily margination, flat overnight collateral rate, zero threshold and minimum transfer amount. Nevertheless, real CSA introduces some frictions causing divergences between the price and the corresponding collateral and hence a not negligible counterparty risk. For example, collateral transfers are not instantaneous events and may also takes several days to complete in case of disputes; for this reason, in the event of default, the collateral actually available to the non-defaulting party at the close-out date may differ from the prescribed one.

A simple way to capture these divergences is assuming that VM and IM available at time step $t_i$ depend on the price computed at time $t_i - l$, with $l$ being a lag parameter. In this way the

time interval $[t_i - l, t_i]$ represents the MPoR, with $t_i - l$ being the last date for which collateral was fully posted and $t_i$ the close-out date. This implies that, while both counterparties stop simultaneously to post collateral for the entire MPoR, contractual cash flows are fully paid. Although simplistic, this assumption can be deemed appropriate in relation to the purposes of our work (advanced models can be found in [41, 28]).

In practical terms, the inclusion of MPoR requires a secondary time grid, built by defining for each $t_i$ of the principal time grid a look-back time point $\tilde{t}_i = t_i - l$ such that $\tilde{t}_i > t_0$ at which collateral is computed, with $i = 1, \ldots, N_T$. Formally, from B's perspective the collateralized exposure $H_m(t_i)$ at time step $t_i$ for a generic path $m$, can be written as

$$H_m(t_i) = \begin{cases} \left[ V_{0,m}(t_i) - \text{VM}_m\left(t_i; V_{0,m}(\tilde{t}_i), \text{K}_{\text{VM}}, \text{MTA}_{\text{VM}}\right) - \text{IM}_m\left(t_i; V_{0,m}(\tilde{t}_i), \text{K}_{\text{IM}}, \text{MTA}_{\text{IM}}\right) \right]^+ & \text{if } V_{0,m}(t_i) > 0 \\ 0 & \text{if } V_{0,m}(t_i) = 0 \\ \left[ V_{0,m}(t_i) - \text{VM}_m\left(t_i; V_{0,m}(\tilde{t}_i), \text{K}_{\text{VM}}, \text{MTA}_{\text{VM}}\right) + \text{IM}_m\left(t_i; V_{0,m}(\tilde{t}_i), \text{K}_{\text{IM}}, \text{MTA}_{\text{IM}}\right) \right]^- & \text{if } V_{0,m}(t_i) < 0 \end{cases}$$
$$(3.1)$$

Here we assumed that a bilateral and symmetrical CSA is in place, VM is netted, and IM is posted into a segregated account as required by regulation (see [21]); therefore, from B's perspective VM can be positive (if posted by C) or negative (if posted by B), while IM is always positive.

## 3.2 Variation Margin

VM modelling is fairly straightforward as it depends on instrument's mark to market, together with $\text{K}_{\text{VM}}$ and $\text{MTA}_{\text{VM}}$. We calculated VM available at time step $t_i$ for a generic path $m$ through the following formula

$$\text{VM}_m\left(t_i; V_{0,m}(\tilde{t}_i), \text{K}_{\text{VM}}, \text{MTA}_{\text{VM}}\right) = \widehat{\text{VM}}_m(\tilde{t}_{i-1})$$
$$+ \mathbb{1}_{\left\{ \left| (V_{0,m}(\tilde{t}_i) - \text{K}_{\text{VM}})^+ - \widehat{\text{VM}}_m^+(\tilde{t}_{i-1}) \right| > \text{MTA}_{\text{VM}} \right\}} \left[ (V_{0,m}(\tilde{t}_i) - \text{K}_{\text{VM}})^+ - \widehat{\text{VM}}_m^+(\tilde{t}_{i-1}) \right]$$
$$+ \mathbb{1}_{\left\{ \left| (V_{0,m}(\tilde{t}_i) + \text{K}_{\text{VM}})^- - \widehat{\text{VM}}_m^-(\tilde{t}_{i-1}) \right| > \text{MTA}_{\text{VM}} \right\}} \left[ (V_{0,m}(\tilde{t}_i) + \text{K}_{\text{VM}})^- - \widehat{\text{VM}}_m^-(\tilde{t}_{i-1}) \right], \quad (3.2)$$

$$\widehat{\text{VM}}_m(\tilde{t}_{i-1}) = \frac{\text{VM}_m(\tilde{t}_{i-1})}{P(\tilde{t}_{i-1}, \tilde{t}_i)}, \quad (3.3)$$

where $\widehat{\text{VM}}_m(\tilde{t}_{i-1})$ is the value of VM just before its update at $\tilde{t}_i$, and the second and the third terms of eq. 3.2 correspond to the amount of VM posted at time step $\tilde{t}_i$ by C and B respectively. In particular, in the second term, C will update VM for the amount exceeding the threshold and VM already in place, provided that this amount is greater than the minimum transfer amount; the same holds for B in case of negative exposure (third term). We imposed null VM for $t_i = t_0$ and $t_i = t_{N_T}$.

## 3.3 Initial Margin

### 3.3.1 ISDA Standard Initial Margin Model

In 2013 ISDA, in cooperation with entities first impacted by bilateral margin requirements, started developing the Standard Initial Margin Model (SIMM) with the aim to provide market participant with a uniform risk-sensitive model for calculating bilateral IM (see [23]), preventing both potential disputes between counterparties related to IM determination with different internal models and the overestimation of margin requirements due to the use of the non-risk-sensitive standard approach (see [22]). The first version of the model was published in 2016. On an annual basis model parameters are recalibrated and the methodology is reviewed in order

to ensure that regulatory requirements are met. Since our work relies on market data at 28 December 2018, we considered ISDA-SIMM Version 2.1 which was effective from 1 December 2018 to 30 November 2019 (see [42]).

In general, ISDA-SIMM is a parametric VaR model based on Delta, Vega and Curvature (i.e. "pseudo" Gamma) sensitivities, defined across risk factors by asset class, tenor and expiry, computed in line with specific definitions. More in detail, each trade of a portfolio (under a certain CSA agreement) is assigned to a Product Class among Interest Rates & FX, Credit, Equity and Commodity. Since a given trade may have sensitivity to different risk factors, six Risk Classes are defined among Interest Rate, FX, Credit (Qualifying), Credit (non-Qualifying), Equity and Commodity. The margin contributions stemming from the different Risk Classes are combined by means of an aggregation function taking account of Risk Classes correlations. Formally, IM for a generic instrument can be written as

$$\mathrm{IM} = \sqrt{\sum_x \mathrm{M}_x^2 + \sum_x \sum_{s \neq x} \psi_{x,s} \mathrm{M}_x \mathrm{M}_s}, \tag{3.4}$$

$$\mathrm{M}_x = \mathrm{DeltaMargin}_x + \mathrm{VegaMargin}_x + \mathrm{CurvatureMargin}_x, \tag{3.5}$$

where $\mathrm{M}_x$ is the margin component for the Risk Class[11] $x$, with $x \in \{\text{Interest Rate, FX}, \dots\}$, and $\psi_{x,s}$ is the correlation matrix between Risk Classes. IM at portfolio level is obtained by adding together IM contributions from each trade (see [43, 42] for a complete description of the model and underlying assumptions).

In our case, Swaps and European Swaptions are assigned to the Interest Rates & FX Product Class and exposed only to Interest Rate (IR) Risk Class, thus $\mathrm{IM} = \mathrm{M}_{\mathrm{IR}}$. Moreover, for a Swap $\mathrm{IM} = \mathrm{DeltaMargin}_{\mathrm{IR}}$ given the linearity of its payoff. As discussed above, we imposed that collateral available at time step $t_i$ is function of instrument's value (sensitivities in IM case) at time $\tilde{t}_i = t_i - l$. Therefore, at time step $t_i$ and for a generic path $m$ the ISDA-SIMM dynamic IM is given by

$$\mathrm{IM}_m^{\mathrm{Swap}}(t_i) = \mathrm{DeltaMargin}_{\mathrm{IR},m}\left(t_i; V_m(\tilde{t}_i)\right), \tag{3.6}$$

$$\begin{aligned} \mathrm{IM}_m^{\mathrm{Swpt}}(t_i) = {} & \mathrm{DeltaMargin}_{\mathrm{IR},m}\left(t_i; V_m(\tilde{t}_i)\right) \\ & + \mathrm{VegaMargin}_{\mathrm{IR},m}\left(t_i; V_m(\tilde{t}_i)\right) + \mathrm{CurvatureMargin}_{\mathrm{IR},m}\left(t_i; V_m(\tilde{t}_i)\right). \end{aligned} \tag{3.7}$$

Finally, allowing for $\mathrm{K}_{\mathrm{IM}}$ and $\mathrm{MTA}_{\mathrm{IM}}$

$$\mathrm{IM}_m^p\left(t_i; V_m(\tilde{t}_i), \mathrm{K}_{\mathrm{IM}}, \mathrm{MTA}_{\mathrm{IM}}\right) = \mathbb{1}_{\left\{(\mathrm{IM}_m^p(t_i) - \mathrm{K}_{\mathrm{IM}})^+ > \mathrm{MTA}_{\mathrm{IM}}\right\}} \left[\left(\mathrm{IM}_m^p(t_i) - \mathrm{K}_{\mathrm{IM}}\right)^+\right], \quad p \in \{\mathrm{Swap, Swpt}\}. \tag{3.8}$$

Similar to VM, we imposed null IM for $t_i = t_0$ and $t_i = t_{N_T}$.

### 3.3.2 Calculation Methodology

The most challenging task underlying ISDA-SIMM dynamic IM is the simulation of forward sensitivities coherently with ISDA definitions, since the subsequent application of weights and aggregation functions is straightforward if we assume that parameters and aggregation rules do not change during the lifetime of the trade. In this section we report the methodology used for computing forward sensitivities, while the other steps to get the different margin components can be found in app. C.

---

[11]For Credit (Qualifying) Risk Class, which includes instruments whose price is sensitive to correlation between the defaults of different credits within an index or basket (e.g. CDO tranches), an additional margin component, i.e. the BaseCorrMargin shell be calculated (see [42]).

According to ISDA, Delta for the IR Risk Class is defined as price change with respect to a 1 bp shift up in a given tenor[12] of the interest rate curve, expressed in monetary terms. Moreover, ISDA specifies that if computed by the internal system at different tenors, Delta shall be linearly re-allocated onto the SIMM tenors. In general, the price of an instrument which depends on an interest rate curve $\mathcal{C}_c$ depends explicitly on the zero rates of the curve, which, in turn, depends on the market rates from which the curve is constructed via bootstrapping procedure (see e.g. [37]). Therefore, being $Z^c = [Z_1^c, \ldots, Z_{N_Z}^c]$ and $R^c = [R_1^c, \ldots, R_{N_R}^c]$, respectively, the zero rates and the market rates in correspondence of the term structure of the same curve $\mathcal{C}_c$, we calculated the sensitivity with respect to the $j$-th market rate $R_j^c$ at a generic time step $t_i$ as (to ease the notation we neglect subscripts referring to the path)

$$\Delta_j^x(t_i) = \frac{\partial V(t_i)}{\partial R_j^x(t_i)} = \sum_{k=1}^{N_Z^x} \frac{\partial V(t_i)}{\partial Z_k^x(t_i)} J_{j,k}^{x,x}(t_0), \qquad j = 1, \ldots, N_R^x, \qquad (3.9)$$

$$\Delta_j^d(t_i) = \frac{\partial V(t_i)}{\partial R_j^d(t_i)} = \sum_{k=1}^{N_Z^d} \frac{\partial V(t_i)}{\partial Z_k^d(t_i)} J_{j,k}^{d,d}(t_0) + \sum_{k=1}^{N_Z^x} \frac{\partial V(t_i)}{\partial Z_k^x(t_i)} J_{j,k}^{x,d}(t_0), \qquad j = 1, \ldots, N_R^d, \qquad (3.10)$$

where $x$ and $d$ denote, respectively, the forwarding curve $\mathcal{C}_x$ and the discounting curve $\mathcal{C}_d$,

$$J_{j,k}^{m,n}(t_0) = \frac{\partial Z_k^m(t_0)}{\partial R_j^n(t_0)}, \qquad (3.11)$$

is an element of the Jacobian matrix (with $m \neq n$), assumed to be constant for each $t_i > t_0$, and

$$\frac{\partial V(t_i)}{\partial Z_k^c(t_i)} \approx \frac{V\big(t_i; Z_k^c(t_i) + 0.0001\big) - V\big(t_i; Z_k^c(t_i)\big)}{0.0001}, \qquad (3.12)$$

is the zero rate Delta sensitivity at $t_i$. The last term of eq. 3.10 takes into account the indirect Delta sensitivity component of the forwarding zero curve to the discounting zero curve, due to the exogenous nature of the bootstrapping procedure. In line with ISDA prescriptions, for each tenor $j$ of the curve $\mathcal{C}_c$, we multiplied Delta sensitivity by shock size and linearly allocated this quantity onto the SIMM tenors, obtaining the (1-by-12) Delta vector

$$\Delta^c(t_i) = \left[ \Delta_{2w}^c(t_i), \ldots, \Delta_{30y}^c(t_i) \right]. \qquad (3.13)$$

We then calculated and aggregated the Weighted Sensitivities in order to get Delta Margin (see eqs. C.4 and C.6).

According to ISDA, Vega for the IR Risk Class is defined as price change with respect to a 1% shift up in ATM Black implied volatility $\sigma_x^{\text{Blk}}$, formally

$$\nu(t_i) = \frac{\partial V(t_i)}{\partial \sigma_x^{\text{Blk}}(t_i; T_e, \mathbf{T}, \mathbf{S})} \approx \frac{V\big(t_i; \sigma_x^{\text{Blk}}(t_i; T_e, \mathbf{T}, \mathbf{S}) + 0.01\big) - V\big(t_i; \sigma_x^{\text{Blk}}(t_i; T_e, \mathbf{T}, \mathbf{S})\big)}{0.01}. \qquad (3.14)$$

where we use superscript Blk to distinguish between Black implied volatility $\sigma_x^{\text{Blk}}$ and G2++ parameter $\sigma$.

Vega sensitivity shall be multiplied by implied volatility to obtain the Vega Risk for expiry $T_e$ and linearly allocated onto the SIMM expiries, which correspond to the tenors defined for Delta sensitivity. Since G2++ European Swaption pricing formula (see eq. B.12) does not provide for an explicit dependence on Black implied volatility, when performing time simulation Vega

---

[12]ISDA defines for both OIS and IBOR curves the following 12 tenors at which Delta shall be computed: 2w, 1m, 3m, 6m, 1y, 2y, 3y, 5y, 10y, 15y, 20y, 30y.

16

cannot be calculated according to the definition above. To overcome this limit we propose the following approximation

$$\frac{\partial V(t_i)}{\partial \sigma_x^{\text{Blk}}(t_i; T_e, \mathbf{T}, \mathbf{S})} \approx \frac{V\left(t_i; \sigma + \epsilon_\sigma, \eta + \epsilon_\eta\right) - V\left(t_i; \sigma, \eta\right)}{\hat{\sigma}_x^{\text{Blk}}(t_i; T_e, \mathbf{T}, \mathbf{S}) - \sigma_x^{\text{Blk}}(t_i; T_e, \mathbf{T}, \mathbf{S})}, \qquad (3.15)$$

where $\epsilon_\sigma$ and $\epsilon_\eta$ are shocks applied on G2++ model parameters governing the underlying process volatility, and implied volatilities $\hat{\sigma}_x^{\text{Blk}}(t_i)$ and $\sigma_x^{\text{Blk}}(t_i)$ are obtained respectively from European Swaption's prices $V(t_i; \sigma + \epsilon_\sigma, \eta + \epsilon_\eta)$ and $V(t_i; \sigma, \eta)$ by solving the shifted Black pricing formula (see eq. 2.13). In sec. 5.3 we report the analyses conducted to validate this approach and to select the values for the shocks $\epsilon_\sigma$, $\epsilon_\eta$ and the Black shift $\lambda_x$. In line with ISDA prescriptions, we multiplied Vega sensitivity by implied volatility $\sigma_x^{\text{Blk}}$ and linearly allocated the resulting Vega Risk onto the SIMM expiries, obtaining the (1-by-12) Vega Risk vector

$$\text{VR}(t_i) = [\text{VR}_{2\text{w}}(t_i), \dots, \text{VR}_{30\text{y}}(t_i)]. \qquad (3.16)$$

We then calculated and aggregated the Vega Risk Exposures to get Vega Margin (see eqs. C.9 and C.11).

Curvature for the IR Risk Class is calculated by using an approximation of the Vega-Gamma relationship (see [43]). The (1-by-12) Curvature Risk Vector

$$\text{CVR}(t_i) = [\text{CVR}_{2\text{w}}(t_i), \dots, \text{CVR}_{30\text{y}}(t_i)] \qquad (3.17)$$

is obtained multiplying the Vega Risk vector by a Scaling Function. We then aggregated the elements of Curvature Risk vector to get Curvature Margin (see eqs. C.14 and C.15).

# 4 Numerical Simulation

This section reports the results in terms of exposure and CVA/DVA obtained for various interest rate derivatives under three collateralization schemes: without collateral, with VM only and with both VM and IM. In particular, we considered 15 years payer Swaps, 30 years payer Swaps, 5x10 years payer and receiver Forward Swaps, and 5x10 years physically settled European payer and receiver Swaptions with different moneyness levels, listed in tab. 1.

## 4.1 Summary of Numerical Steps

We report below a summary of the numerical steps followed for simulating the exposure and computing CVA/DVA.

1. Discretization of the integrals in eqs. 2.29 and 2.30 along an equally spaced time grid $t = t_0 < \dots < t_i < \dots < t_{N_T} = T$ with granularity $\Delta t = t_i - t_{i-1}$ (see eqs. 2.31 and 2.32). In order to capture all spikes arising in collateralized exposure we added to the time grid a point within the interval $(T_j, T_j + l]$ for each floating coupon date $T_j$ $(j = 1, \dots, n)$[13], with $l$ being a lag parameter governing the length of MPoR (see sec. 5.1.2 for details).

2. Construction of a secondary time grid by defining for each time step $t_i$ a look-back time point $\tilde{t}_i = t_i - l$ at which compute the collateral actually available at $t_i$ (see sec. 3.1 for details).

3. Calibration of G2++ model parameters $p = \{a, \sigma, b, \eta, \rho, \Gamma_1, \dots, \Gamma_{14}\}$ on market ATM European Swaption prices according to the procedure described in sec. 2.3.3.

---

[13]For the instruments considered, fixed coupon dates are a subset of floating ones since taking place at the same time, otherwise the corresponding coupon dates should have been added to the time grid.

List of analysed instruments

| Instrument | $\omega$ | $K$ | Moneyness |
|---|---|---|---|
| | 1 | 0.0167 | out-of-the-money |
| 15Y Swap | 1 | 0.0117 | at-the-money |
| | 1 | 0.0067 | in-the-money |
| | 1 | 0.0188 | out-of-the-money |
| 30Y Swap | 1 | 0.0138 | at-the-money |
| | 1 | 0.0088 | in-the-money |
| | -1 | 0.0120 | out-of-the-money |
| 5x10Y Forward Swap | 1 | 0.0170 | at-the-money |
| | 1 | 0.0220 | out-of-the-money |
| | -1 | 0.0120 | out-of-the-money |
| 5x10Y Swaption | 1 | 0.0170 | at-the-money |
| | 1 | 0.0220 | out-of-the-money |

**Table 1:** Details on financial instruments analysed. All instruments are denominated in EUR, with $N = 100$ Mio, semi-annual floating leg tied to EURIBOR 6M and annual fixed leg. $\omega = +/-1$ stands for payer/receiver (referred to the fixed leg of the Swap).

4. Generation of the pairs $(x_m(t_i),\ y_m(t_i))$ and $(x_m(\tilde{t}_i),\ y_m(\tilde{t}_i))$ for each time step of both the principal and the secondary time grids and simulated path $m = 1, \ldots, N_{MC}$ according to the procedure described in sec. 2.3.4.

5. Calculation of exposure $H_m(t_i)$ for each time step $t_i$ and simulated path $m$ according to eq. 3.1. This requires to:

   a. compute instrument's mark to future $V_{0,m}(t_i)$ at $t_i$ (see pricing formulas in app. B);

   b. compute Variation Margin $\text{VM}_m(t_i)$ available at $t_i$, which is function of instrument's mark to future $V_{0,m}(\tilde{t}_i)$ at $\tilde{t}_i$ (see eq. 3.2);

   c. compute ISDA-SIMM dynamic Initial Margin $\text{IM}_m(t_i)$ available at $t_i$, which is function of instrument Delta $\Delta_m^c(\tilde{t}_i)$ and Vega $\nu_m(\tilde{t}_i)$ sensitivities at $\tilde{t}_i$ (see eq. 3.8 and sec. 3.3.2 for details on calculation methodology).

6. Calculation of EPE $\mathcal{H}^+(t;t_i)$ and ENE $\mathcal{H}^-(t;t_i)$ for each time step $t_i$ according to eq. 2.33.

7. Calculation of survival probabilities for each time step $t_i$ from default curves built from market CDS quotes through bootstrapping procedure.

8. Calculation of CVA and DVA via eqs. 2.31 and 2.32.

## 4.2 Model Setup

Aside from G2++ model parameters we can distinguish between calculation parameters and CSA parameters.

The former affect both the accuracy of the results and the calculation time required and are those related to Monte Carlo approach for calculating CVA/DVA. In particular, we are referring to the granularity of the time grid $\Delta t$ used for discretize the integrals, the number of simulated scenarios $N_{MC}$, and the parameters used for compute forward Vega sensitivities related to ISDA-SIMM dynamic IM (see eq. 3.15), namely the magnitude of the shocks on G2++ model parameters $\epsilon_\sigma$ and $\epsilon_\eta$, and the value of the Black shift $\lambda_x$ for implied volatility calculation.

CSA parameters affect the residual credit exposure and consequently CVA/DVA with no impacts

on the accuracy of the results, and are those related to collateral simulation. In particular, we are referring to threshold K, minimum transfer amount MTA, and to the length of MPoR $l$.

In selecting calculation parameters it is necessary to cope with the trade-off between accuracy and computational effort. The parameterization considered in this section (see tab. 2) is the one that optimizes this trade-off on the basis of specific analyses reported in sec. 5. Regarding CSA

Adopted model parameters

| Parameters Class | Parameter | Value |
|---|---|---|
| | $\Delta t$ | 1 month |
| | $N_{MC}$ | 5000 |
| Calculation parameters | $\epsilon_\sigma$ | 0.01 |
| | $\epsilon_\eta$ | 0.04 |
| | $\lambda_x$ | 0.06 |
| | $l$ | 2 days |
| CSA parameters | K | 0 EUR |
| | MTA | 0 EUR |
| | $a$ | 1.1664 |
| | $\sigma$ | 0.0501 |
| | $b$ | 0.0304 |
| | $\eta$ | 0.0084 |
| | $\rho$ | -1.0000 |
| | $\Gamma_1$ | 0.9530 |
| | $\Gamma_2$ | 0.9781 |
| | $\Gamma_3$ | 1.0895 |
| | $\Gamma_4$ | 1.0709 |
| G2++ parameters | $\Gamma_5$ | 1.0032 |
| | $\Gamma_6$ | 1.0776 |
| | $\Gamma_7$ | 1.0488 |
| | $\Gamma_8$ | 1.0186 |
| | $\Gamma_9$ | 1.1000 |
| | $\Gamma_{10}$ | 0.9608 |
| | $\Gamma_{11}$ | 1.0114 |
| | $\Gamma_{12}$ | 0.9553 |
| | $\Gamma_{13}$ | 0.9629 |
| | $\Gamma_{14}$ | 0.9340 |

**Table 2:** Adopted model parameters and respective values. Note that calculation parameters are those optimizing the trade-off between accuracy and calculation time (see sec. 5).

parameters, in order to get as close as possible to perfect collateralization case, we considered bilateral CSA with K = MTA = 0 both for VM and IM, with $l = 2$ days. In sec. 5.4 the impact of these parameters is assessed. With regard to the calibration of G2++ model parameters, we considered the market ATM European Swaption prices matrix in correspondence of the following expiries $\xi = \{2, 3, 4, 5, 6, 7, 8, 9, 10, 12, 15, 20, 25, 30\}$ and tenors $\mathfrak{T} = \{2, 3, 4, 5, 6, 7, 8, 9, 10, 15, 20, 25, 30\}$, both expressed in years (see app. A for details). Calibration errors in absolute percentage terms are shown in fig. 1.
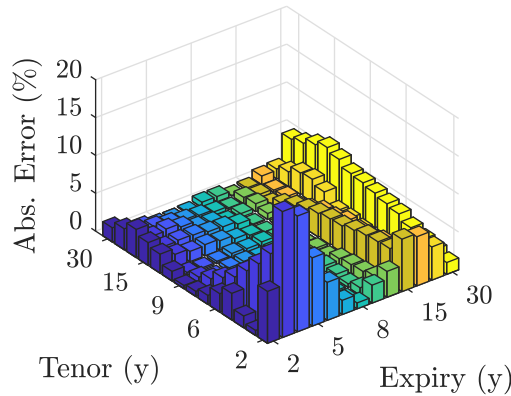
**Figure 1:** Calibration errors in absolute percentage terms.

## 4.3 Results

### 4.3.1 Exposure

The results in terms of EPE and ENE profiles are reported in figs. 2-5 and are aligned on what can be found in the literature (see e.g. [16]).

Focusing on uncollateralized exposures (top panels), the jagged shape observed for the Swaps (figs. 2 and 3) is due to the different coupons frequency (floating coupons received semi-annually, fixed coupons paid annually) which determines semi-annual jumps in instruments' mark to future at coupon dates. EPE is larger than ENE, in absolute terms, except for the out-of-the-money (OTM) 15 years Swap, due to the forward rates structure which causes expected floating leg values greater than those of the fixed leg. This is evident for in-the-money (ITM) Swaps for which ENE is also almost flat given the low probability to observe negative mark to futures. By comparing the exposures for different maturities, 30 years Swaps are clearly riskier due to the greater number of coupons to be exchanged. The analogous shape for the exposure is observed for the Forward Swaps when coupons payment starts, i.e. from $t = 5$ years (fig. 4). Here we can observe the asymmetric effect of forward rates on opposite transactions: the OTM payer Forward Swap displays larger EPE and less negative ENE compared to the OTM receiver one. Physically settled European Swaptions (fig. 5) are written on the same Forward Swaps, before the expiry the exposure is always positive and greater than the one of the corresponding underlying Forward Swap as the price is always positive. After the expiry, OTM paths are excluded as the exercise do not take place, determining smaller EPE and ENE (in absolute value) with respect to the corresponding underlying Forward Swap.

Focusing on exposures with VM (middle panels), a reduction of one order of magnitude can be observed. According to the assumptions made, VM tracks instrument's mark to future with a delay equal to the length of MPoR (2 days), which represents the only element of friction. This delay causes a material residual exposure characterized by spikes at coupon dates. In general, when only floating coupons are received, one can expect to observe downward spikes due to the fact that the counterparty make a payment for which B still has not returned VM. Conversely, upward spikes arise when fixed cash flows occur and are offset by the downward ones stemming from floating coupons. The magnitude of these spikes is determined by the simulated forward rates structure, e.g. the large upward spikes displayed at the early stage of payer Swaps' life are due to negative rates (see sec. 5.1.1 for details).

Focusing on exposures with VM and IM (bottom panels), EPE/ENE profiles display spikes with increasing magnitude approaching to maturity, which means that IM turns out to be inadequate to suppress completely the exposure due to its decreasing profile, as displayed in fig. 6.

20
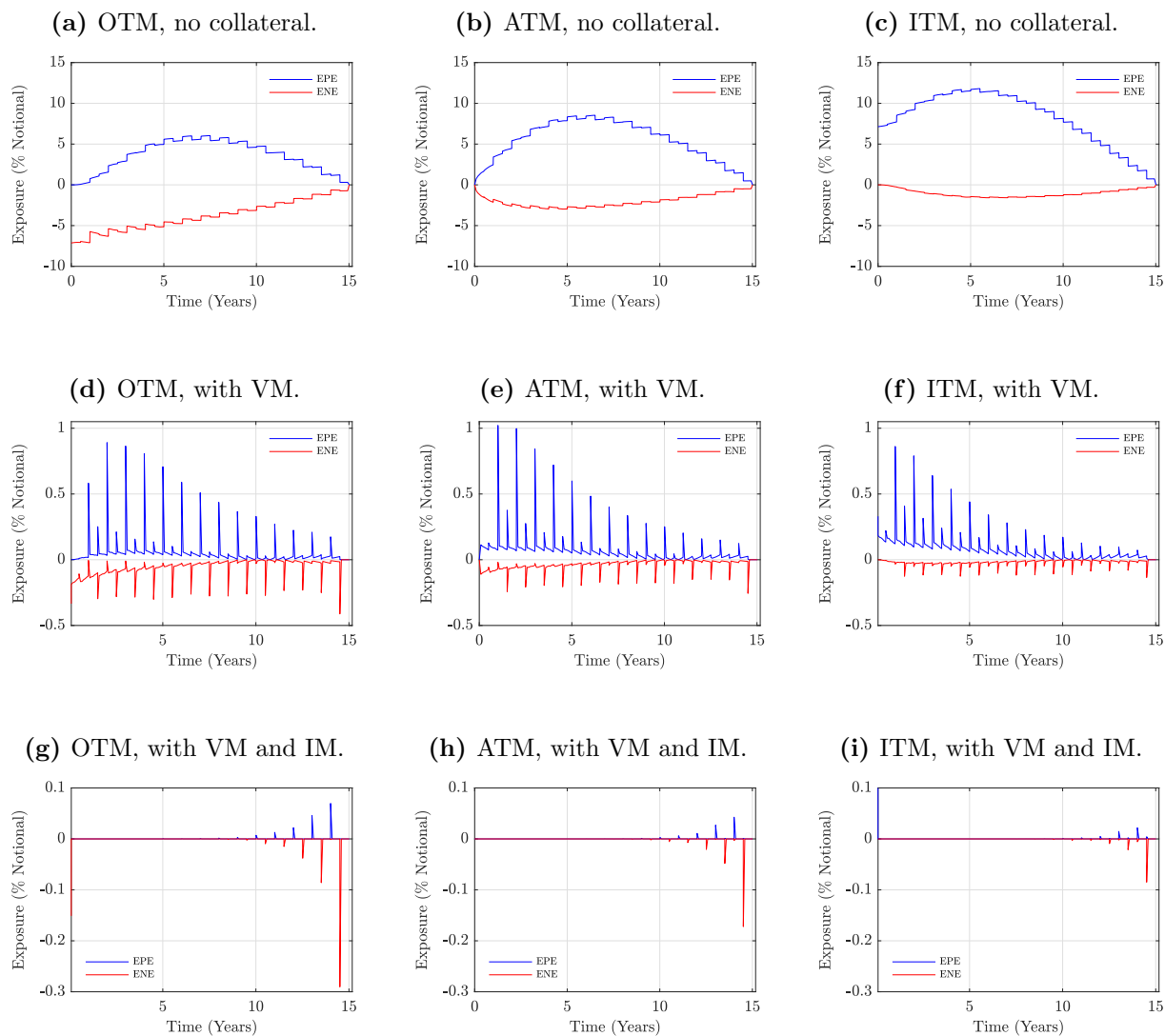
**Figure 2:** 15 years payer Swaps EUR 100 Mio notional, EPE and ENE profiles (blue and red solid lines respectively) for the collateralization schemes (top: no collateral, mid: VM, bottom: VM and IM) and moneyness (left: OTM, mid: ATM, right: ITM) considered. To enhance plots readability, we excluded collateralized EPE/ENE for time step $t_0$ as not mitigated by collateral. Model setup as in tab. 2. Quantities expressed as a percentage of the notional.

21
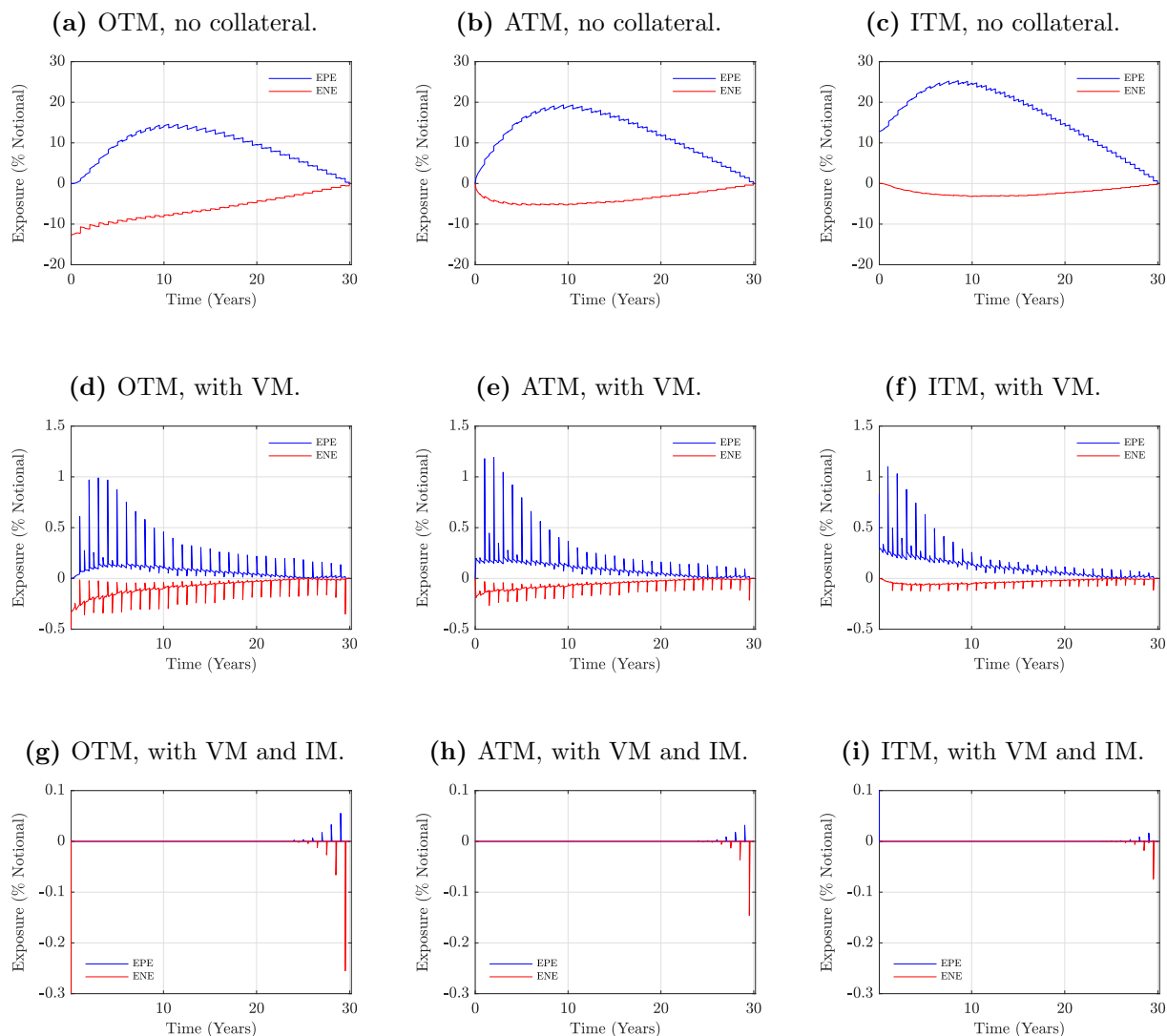
**Figure 3:** 30 years payer Swaps EUR 100 Mio notional, EPE and ENE profiles (blue and red solid lines respectively) for the collateralization schemes (top: no collateral, mid: VM, bottom: VM and IM) and moneyness (left: OTM, mid: ATM, right: ITM) considered. To enhance plots readability, we excluded collateralized EPE/ENE for time step $t_0$ as not mitigated by collateral. Model setup as in tab. 2. Quantities expressed as a percentage of the notional.

22
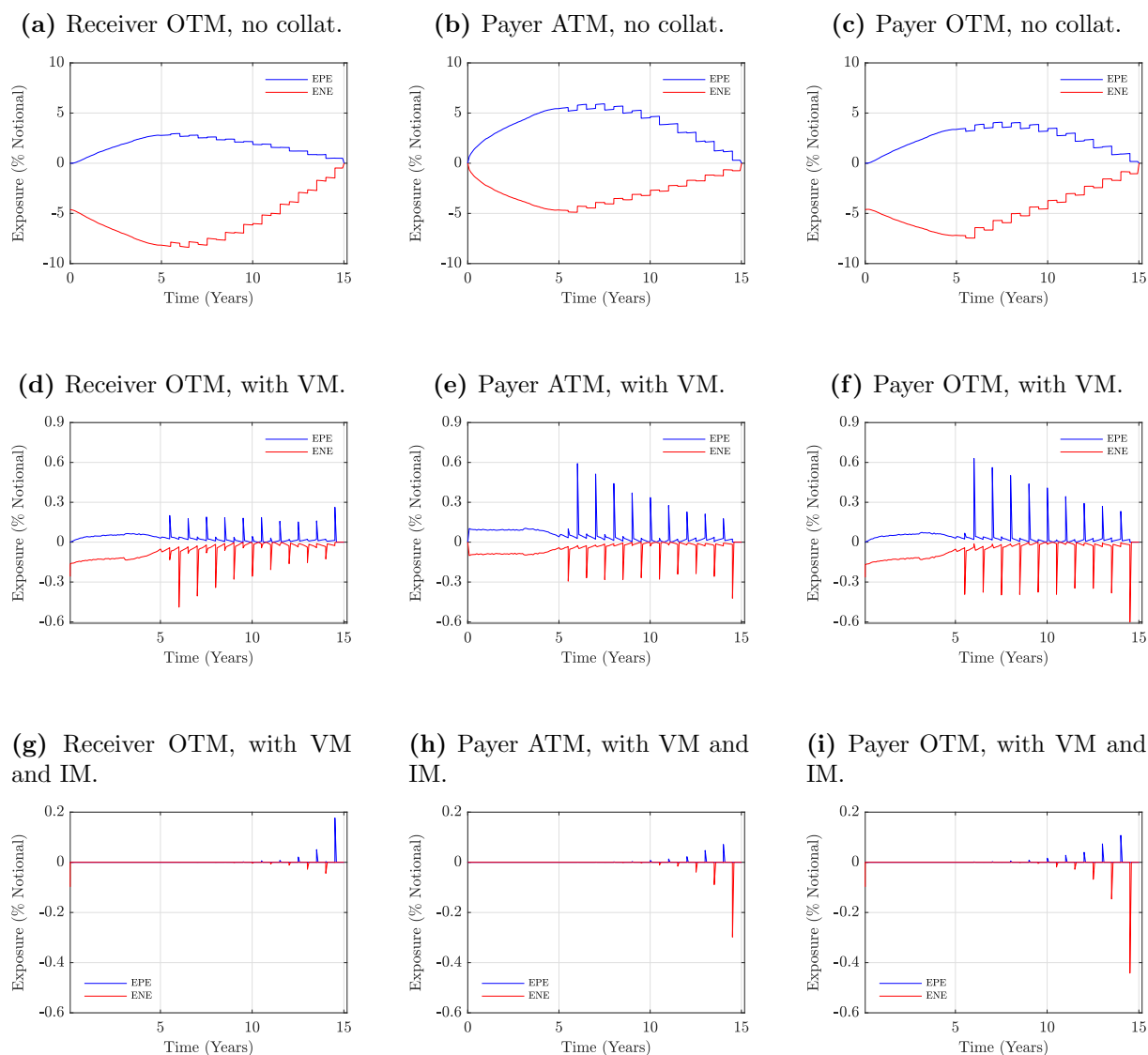
**Figure 4:** 5x10 years Forward Swaps EUR 100 Mio notional, EPE and ENE profiles (blue and red solid lines respectively) for the collateralization schemes (top: no collateral, mid: VM, bottom: VM and IM) and moneyness (left: reicever OTM, mid: payer ATM, right: payer OTM) considered. To enhance plots readability, we excluded collateralized EPE/ENE for time step $t_0$ as not mitigated by collateral. Model setup as in tab. 2. Quantities expressed as a percentage of the notional.

**(a)** Receiver OTM, no collat.  **(b)** Payer ATM, no collat.  **(c)** Payer OTM, no collat.

**(d)** Receiver OTM, with VM.  **(e)** Payer ATM, with VM.  **(f)** Payer OTM, with VM.

**(g)** Receiver OTM, with VM and IM.  **(h)** Payer ATM, with VM and IM.  **(i)** Payer OTM, with VM and IM.
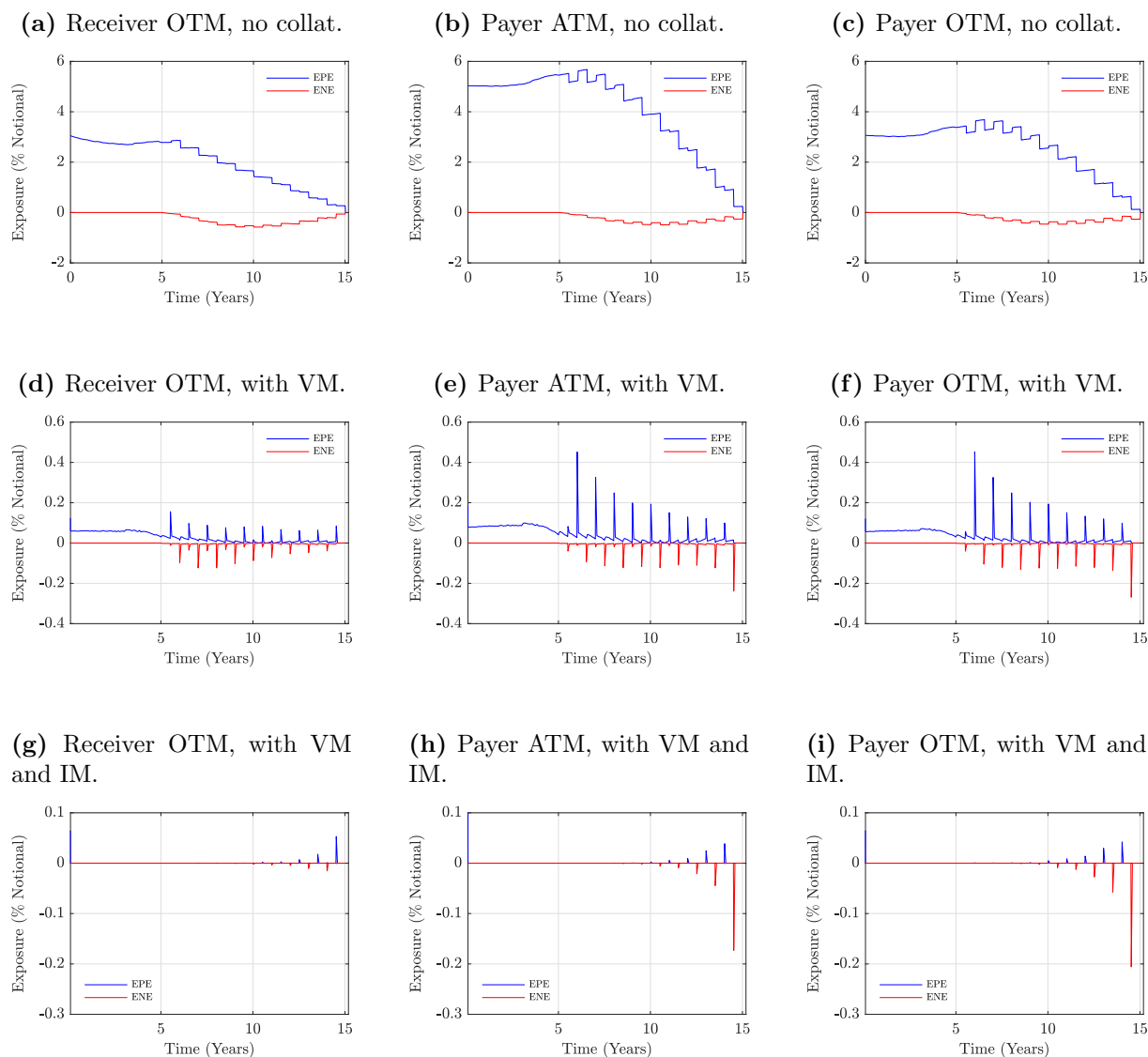
**Figure 5:** 5x10 years physically settled European Swaptions EUR 100 Mio notional, EPE and ENE profiles (blue and red solid lines respectively) for the collateralization schemes (top: no collateral, mid: VM, bottom: VM and IM) and moneyness (left: reicever OTM, mid: payer ATM, right: payer OTM) considered. To enhance plots readability, we excluded collateralized EPE/ENE for time step $t_0$ as not mitigated by collateral. Model setup as in tab. 2. Quantities expressed as a percentage of the notional.
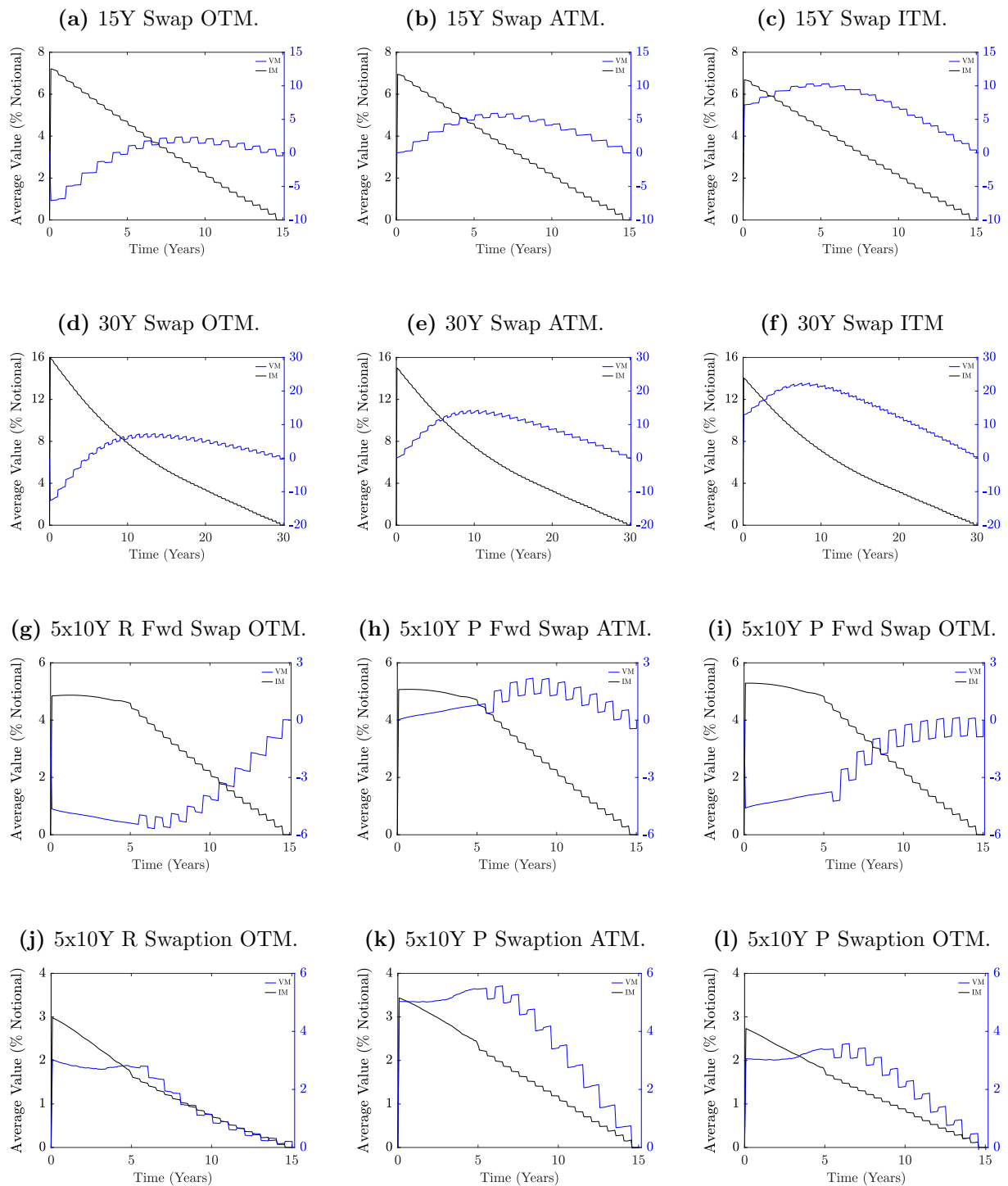
**Figure 6:** Average values for VM (blue lines, right-hand scale) and IM (black lines, left-hand scale) for instruments in tab. 1. Letter P and R distinguish between payer and receiver instruments where necessary. Model setup as in tab. 2. Quantities expressed as a percentage of the notional.

25

### 4.3.2 XVA

The results in terms of CVA/DVA reported in tab. 3 are driven by the elements above discussed.

Focusing on uncollateralized CVA/DVA, Swaps display larger CVA (DVA) figures for ITM (OTM) instruments due to the greater probability to observe positive (negative) mark to futures, also reflected in lower Monte Carlo errors. Moreover, CVA is larger than DVA except for the OTM 15 years Swap due to the simulated forward rates structure discussed above. Finally, analysing the results for different maturities, the higher risk of 30 years Swaps leads to larger adjustments compared to those maturing in 15 years. Analogous results are obtained for Forward Swaps. In this case, the asymmetric effect of simulated forward rates on opposite transactions causes larger CVA and smaller DVA for the OTM payer Forward Swap with respect to the OTM receiver one. Slightly lower (absolute) CVA values are observed for the corresponding physically settled European Swaptions since OTM paths are excluded after the exercise, while DVA values are considerably lower as negative exposure exists only after the expiry.

Focusing on CVA/DVA with VM only, the results show that the adjustments are reduced on average by approx. two orders of magnitude. In this case CVA/DVA are widely driven by spikes in exposure profiles which determine changes in certain relations previously identified. In particular, the 30 years OTM Swap displays greater DVA compared to CVA since ENE is larger than EPE between the spikes and their magnitude becomes larger for ENE by approaching the maturity (where default probability increases). The same can be observed for the 5x10 years ATM Forward Swap.

Focusing on CVA/DVA with VM and IM, the results show that the adjustments are reduced on average by approx. four orders of magnitude with respect to uncollateralized case. CVA/DVA are entirely due to the spikes closest to maturity which are not fully suppressed by IM. Largest DVA compared to CVA are observed for payer instruments for which wide spikes are observed in ENE as the difference between fixed rate and floating rate are greater. For the same reason receiver instruments display larger CVA figures.

CVA and DVA for the instruments in tab. 1

| Collateral | Instrument | Moneyness | $\omega$ | CVA | DVA |
|---|---|---|---|---|---|
| None | 15Y Swap | OTM | 1 | $-779\,085\,(\pm\ \ 6\%)$ | $884\,382\,(\pm\ \ 6\%)$ |
| | 15Y Swap | ATM | 1 | $-1\,172\,938\,(\pm\ \ 4\%)$ | $475\,324\,(\pm\ \ 9\%)$ |
| | 15Y Swap | ITM | 1 | $-1\,681\,190\,(\pm\ \ 4\%)$ | $240\,662\,(\pm 12\%)$ |
| | 30Y Swap | OTM | 1 | $-2\,630\,312\,(\pm\ \ 5\%)$ | $2\,218\,071\,(\pm\ \ 7\%)$ |
| | 30Y Swap | ATM | 1 | $-3\,756\,886\,(\pm\ \ 4\%)$ | $1\,233\,129\,(\pm 10\%)$ |
| | 30Y Swap | ITM | 1 | $-5\,173\,086\,(\pm\ \ 3\%)$ | $650\,447\,(\pm 14\%)$ |
| | 5x10Y Fwd Swap | OTM | -1 | $-387\,131\,(\pm\ \ 9\%)$ | $1\,373\,951\,(\pm\ \ 4\%)$ |
| | 5x10Y Fwd Swap | ATM | 1 | $-821\,210\,(\pm\ \ 5\%)$ | $714\,338\,(\pm\ \ 7\%)$ |
| | 5x10Y Fwd Swap | OTM | 1 | $-530\,527\,(\pm\ \ 7\%)$ | $1\,134\,273\,(\pm\ \ 5\%)$ |
| | 5x10Y Swaption | OTM | -1 | $-390\,339\,(\pm\ \ 9\%)$ | $43\,011\,(\pm 17\%)$ |
| | 5x10Y Swaption | ATM | 1 | $-818\,308\,(\pm\ \ 5\%)$ | $36\,418\,(\pm 17\%)$ |
| | 5x10Y Swaption | OTM | 1 | $-519\,394\,(\pm\ \ 7\%)$ | $34\,825\,(\pm 18\%)$ |
| VM | 15Y Swap | OTM | 1 | $-6506\,(\pm\ \ 9\%)$ | $10\,384\,(\pm\ \ 9\%)$ |
| | 15Y Swap | ATM | 1 | $-8856\,(\pm\ \ 8\%)$ | $6814\,(\pm 12\%)$ |
| | 15Y Swap | ITM | 1 | $-10\,787\,(\pm\ \ 7\%)$ | $3479\,(\pm 17\%)$ |
| | 30Y Swap | OTM | 1 | $-23\,462\,(\pm\ \ 9\%)$ | $32\,185\,(\pm 10\%)$ |
| | 30Y Swap | ATM | 1 | $-30\,123\,(\pm\ \ 8\%)$ | $21\,316\,(\pm 13\%)$ |
| | 30Y Swap | ITM | 1 | $-35\,292\,(\pm\ \ 7\%)$ | $11\,695\,(\pm 18\%)$ |
| | 5x10Y Fwd Swap | OTM | -1 | $-5130\,(\pm 13\%)$ | $13\,975\,(\pm\ \ 8\%)$ |
| | 5x10Y Fwd Swap | ATM | 1 | $-8322\,(\pm\ \ 9\%)$ | $9862\,(\pm 10\%)$ |
| | 5x10Y Fwd Swap | OTM | 1 | $-5899\,(\pm 11\%)$ | $13\,458\,(\pm\ \ 8\%)$ |
| | 5x10Y Swaption | OTM | -1 | $-4969\,(\pm 12\%)$ | $633\,(\pm 24\%)$ |
| | 5x10Y Swaption | ATM | 1 | $-7831\,(\pm\ \ 9\%)$ | $665\,(\pm 23\%)$ |
| | 5x10Y Swaption | OTM | 1 | $-5744\,(\pm 10\%)$ | $624\,(\pm 24\%)$ |
| VM and IM | 15Y Swap | OTM | 1 | $-7\,(\pm 24\%)$ | $12\,(\pm 14\%)$ |
| | 15Y Swap | ATM | 1 | $-4\,(\pm 32\%)$ | $7\,(\pm 20\%)$ |
| | 15Y Swap | ITM | 1 | $-2\,(\pm 43\%)$ | $4\,(\pm 30\%)$ |
| | 30Y Swap | OTM | 1 | $-2\,(\pm 20\%)$ | $4\,(\pm 11\%)$ |
| | 30Y Swap | ATM | 1 | $-1\,(\pm 27\%)$ | $2\,(\pm 15\%)$ |
| | 30Y Swap | ITM | 1 | $-1\,(\pm 37\%)$ | $1\,(\pm 22\%)$ |
| | 5x10Y Fwd Swap | OTM | -1 | $-7\,(\pm 19\%)$ | $4\,(\pm 31\%)$ |
| | 5x10Y Fwd Swap | ATM | 1 | $-7\,(\pm 23\%)$ | $13\,(\pm 14\%)$ |
| | 5x10Y Fwd Swap | OTM | 1 | $-12\,(\pm 20\%)$ | $20\,(\pm 11\%)$ |
| | 5x10Y Swaption | OTM | -1 | $-12\,(\pm 28\%)$ | $7\,(\pm 50\%)$ |
| | 5x10Y Swaption | ATM | 1 | $-13\,(\pm 30\%)$ | $38\,(\pm 17\%)$ |
| | 5x10Y Swaption | OTM | 1 | $-17\,(\pm 30\%)$ | $46\,(\pm 16\%)$ |

**Table 3:** CVA and DVA for instruments in tab. 1 for the three collateralization schemes considered, $3\sigma$ confidence intervals in parentheses. Model setup as in tab. 2. Quantities expressed in EUR.

# 5 Model Validation

Previous sections suggest that the numerical calculation of CVA/DVA requires various assumptions for modelling and computing the relevant quantities. Since affecting the stability of the results, these assumptions are source of model risk to be properly addressed.

The purpose of this section is twofold: on the one hand, we want to validate the framework adopted in sec. 4 by assessing its robustness and selecting a parameterization which optimizes the trade-off between accuracy and performance, on the other hand, we want to identify the most significant sources of model risk involved in exposure modelling and hence CVA/DVA calculation. To ease the presentation we report the results only for a subset of the instruments in tab. 1, mainly the 15 years ATM payer Swap and the 5x10 years ATM physically settled European payer Swaption. Analogous results are obtained for the other instruments.

## 5.1 Time Grid Construction

The numerical solution of eqs. 2.29 and 2.30 involves the discretization of the integral along a grid of valuation dates in correspondence of which the exposure is computed. In selecting the length of time steps $\Delta t$ it is necessary to optimize the trade-off between precision and computational effort. In fact, an high granularity reduces the discretization error but makes the calculation unfeasible due to long time required. Furthermore, the inclusion in the model of the MPoR requires to discretize the aforementioned equations in such a way to capture all periodical spikes in Swap's collateralized exposure which have material impact on CVA/DVA.

In this section we first analyse the nature of spikes in collateralized exposure when a daily grid is used and their impact on CVA/DVA. We then propose a possible workaround which allows to capture all spikes at lower granularities, at the end we report the results of a convergence analysis aimed at finding a granularity which ensures a good compromise between precision and computational time.

### 5.1.1 Spikes Analysis

Spikes arising in collateralized exposure are due to the MPoR since it implies that the collateral available at time step $t_i$ depends on instrument's mark to future at time step $\tilde{t}_i = t_i - l$, assumed to be the last date for which VM and IM were fully posted (see sec. 3.1). The granularity of the time grid used to discretize the integrals in eqs. 2.29 and 2.30 determines the existence of spikes in collateralized exposure profile, in fact a time grid with daily granularity is able to capture all spikes as shown in fig. 7, which displays EPE/ENE profiles for the 15 years ATM payer Swap (left-hand side panel) and the 5x10 years ATM physically settled European payer Swaption (right-hand side panel) for the three collateralization schemes considered. As can be seen, when only VM is considered, spikes emerge at inception as no collateral is posted, and at coupon dates as sudden changes in mark to future are captured by VM with a delay due to MPoR. When also IM is considered, spikes closest to maturity persist due to the downward profile of IM.

We further investigated the nature of these spikes by focusing on the 15 years ATM payer Swap's Expected Exposure (EE)[14] without collateral and with VM, displayed in fig. 8. Left-hand side panels show that both the jagged shape of uncollalteralized EE (fig. 8a) and the spikes in EE with VM (fig. 8b) are determined by sudden changes in the average values of Swap legs right after coupon payments. Right-hand side panels show a focus around $t = 1y$, when both fixed and floating coupons take place: after these cash flows, the average value of floating leg increases and fixed leg one decreases, resulting in a positive jump in uncollateralized EE at $t = $

---

[14]The Expected Exposure (EE) is defined as: $\mathcal{H}(t, t_i) = P(t; t_i) \frac{1}{N_{MC}} \sum_{m=1}^{N_{MC}} H_m(t_i)$.

**(a)** EPE and ENE Swap no collateral.

**(b)** EPE and ENE Swaption no collateral.

**(c)** EPE and ENE Swap with VM.

**(d)** EPE and ENE Swaption with VM.

**(e)** EPE and ENE Swap with VM and IM.

**(f)** EPE and ENE Swaption with VM and IM.
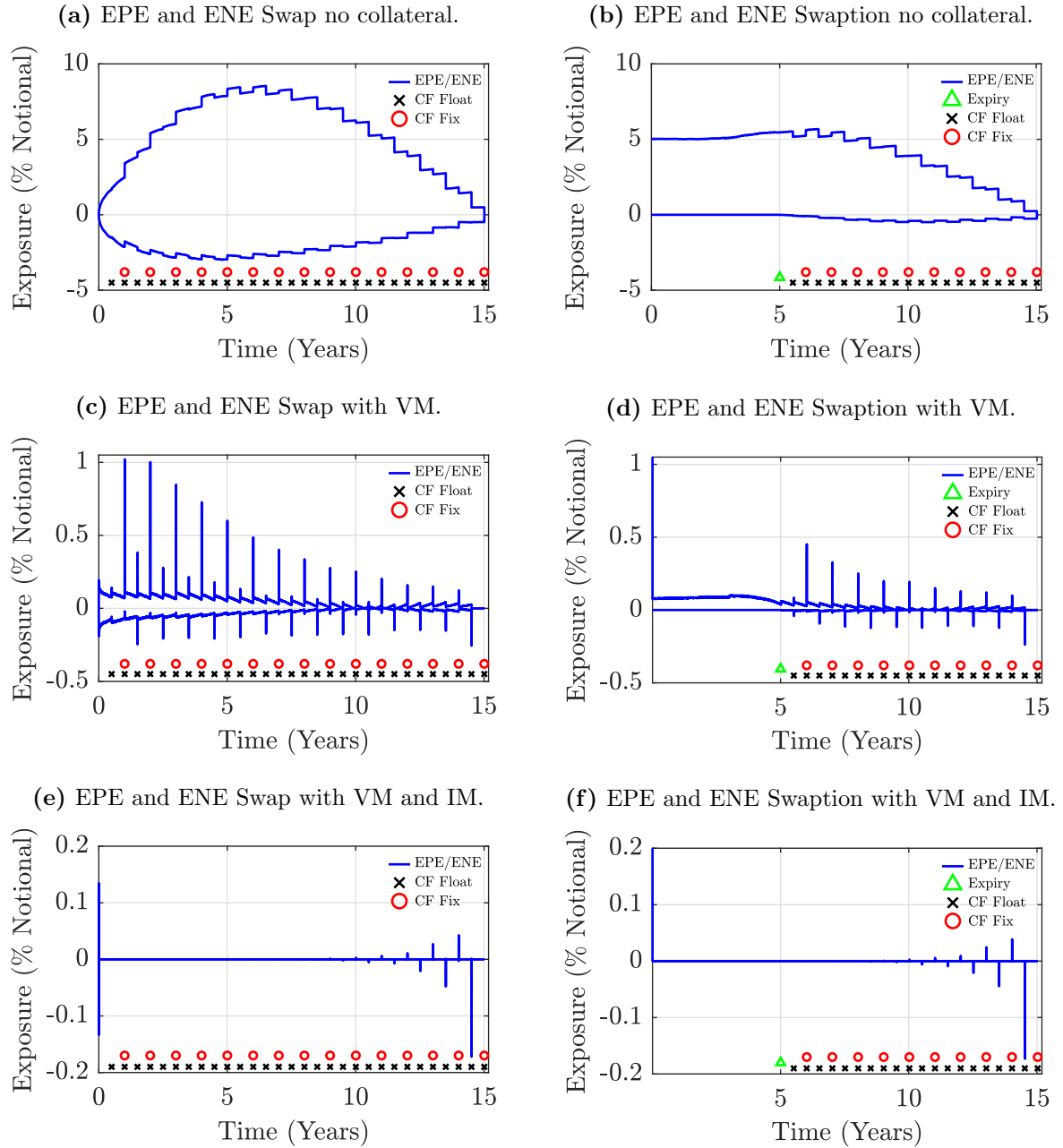
**Figure 7:** 15 years ATM payer Swap (left-hand side) and 5x10 years ATM physically settled European payer Swaption (right-hand side) EUR 100 Mio notional, EPE and ENE profiles (blue solid lines) on a daily grid for the three collateralization schemes considered (top: no collateral, mid: VM, bottom: VM and IM). Black crosses correspond to floating leg coupon dates (semiannual frequency), red circles correspond to fixed coupon dates (annual frequency), green triangles correspond to Swaption's expiry. Spikes in collateralized exposure at inception and at coupon dates are an effect of MPoR. To enhance Swaption's plots readability, we excluded collateralized EPE for time steps $t_0$ and $t_1$ as not mitigated by collateral (mid and bottom right-hand panels), in particular $EPE(t_0)$ corresponds to Swaption's price $5\,030\,423$ EUR (approx. 5% of the notional). Other model parameters as in tab. 2. Quantities expressed as a percentage of the notional.

**(a)** EE no collateral and Swap legs.

**(b)** Jump in EE no collateral.

**(c)** EE with VM and Swap legs.
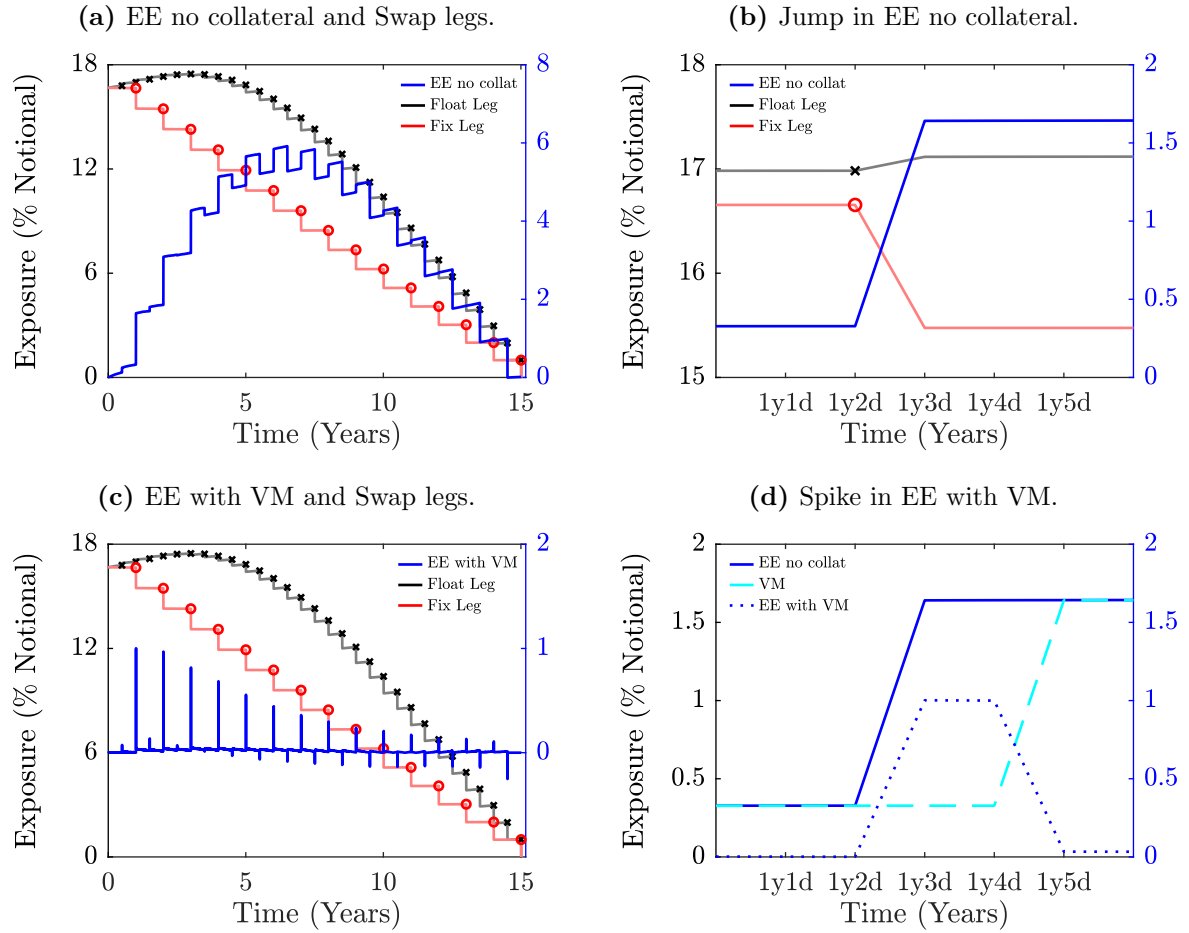
**(d)** Spike in EE with VM.

**Figure 8:** 15 years ATM payer Swap EUR 100 Mio notional, analysis on spikes in EE with VM. Top left-hand side panel displays floating and fixed legs average values (black and red solid lines respectively, black crosses: floating coupon dates, red circles: fixed coupon dates, left-hand scale) and uncollateralized EE (blue solid line, right-hand scale), which is positive since floating leg is always greater than fixed leg. Bottom left-hand side panel displays EE with VM (blue solid line, right-hand scale). Top right-hand side panel displays the jump in uncollateralized EE (blue solid line, right-hand scale) right after fixed and floating coupons payment taking place at $t = 1y2d$, and given by a simultaneous increase in floating leg and drop in fixed one (black and red solid lines respectively, left-hand scale). Bottom right-hand side panel displays the spike in EE with VM (blue dotted line) occurring right after fixed and floating coupons payment due to the fact that VM (cyan dashed line) captures the jump in uncollateralized EE (blue solid line) with a delay equal to the length of the MPoR. Daily grid considered, other model parameters as in tab. 2. Quantities expressed as a percentage of the notional.

1y3d (fig. 8c). This jump is captured by VM at $t = 1\text{y}5\text{d}$, this delay of 2 days due to MPoR causes an upward spike in EE with VM (fig. 8d). The direction and magnitude depend on the simulated forward rates structure and on whether fixed or floating coupon payments take place. Focusing on semiannual floating coupons paid by C, two different behaviours can be observed during the lifetime of the Swap. The first three floating coupons determine positive jumps in uncollateralized EE and upward spikes in EE with VM. This is due to the fact that the simulated forward rates are on average negative until 2.5 years implying that, until that time, these coupons are actually paid by B. Once forward rates revert to positive values, negative jumps in uncollateralized EE and downward spikes in EE with VM arise in correspondence of the remaining floating coupons (figs. 8a and 8b).

When also annual fixed coupons paid by B take place, positive jumps in uncollateralized EE and upward spikes with decreasing magnitude in EE with VM can be observed. Negative rates cause wide spikes in correspondence of the first two fixed and floating coupons due to the simultaneous increase in the average value of floating leg and decrease in the fixed leg one, in B's perspective, right after coupons payment (figs. 8c and 8d).

The impact of spikes on total CVA and DVA is significant: with only VM the contribution is respectively of 7% and 4% for the 15 years ATM payer Swap and of 2% and 16% for the 5x10 years ATM physically settled European payer Swaption. With also IM the exposure between spikes is suppressed, therefore CVA and DVA are completely attributable to spikes.

### 5.1.2 Parsimonious Time Grid

Although a daily grid represents the best discrete approximation of the integrals in eqs. 2.29 and 2.30, it is very limited in terms of computational time required, as can be seen from the last column of tab. 4. The most time consuming component is represented by IM which involves the calculation of several forward sensitivities for each path (see sec. 3.3.2). Computational time lengthens further for Swaptions due to the numerical resolution of G2++ pricing formula (see eq. B.12). The calculation of CVA/DVA using a daily grid is clearly unfeasible, this forced us to consider a lower granularity.

A standard less granular evenly spaced time grid may produce biased CVA/DVA values if not capable of capturing all spikes in collateralized exposure. In fact, the spike due to the coupon occurring at time $T_j$ would emerge only if the time grid includes a point $t_i$ falling within the interval $(T_j, T_j + l]$. A possible workaround to make sure to capture all spikes could be to add to a standard time grid the set of points $\{T_j + 1\text{d}\}_{j=1}^{n}$, where $T_j$ is the $j$-th floating coupon date and $n$ is the number of floating coupons[15]; we will refer to this augmented grid as the joint grid. The comparison between EPE/ENE for the 15 years ATM payer Swap, obtained through standard and joint grids with monthly granularity for the three collateralization schemes considered, is shown in fig. 9. The 5x10 years ATM physically settled European payer Swaption displays same results and is not reported. As can be seen, uncollateralized exposure is similar for both grids, while standard grid fails to capture spikes in collateralized exposure since no time point within the interval $(T_j, T_j + l]$ is included for each coupon date $T_j$. Moreover, with no spikes, IM suppresses completely the residual exposure resulting in null CVA/DVA. Instead, all spikes are captured by the joint grid which allows to correctly model the collateralized exposure with considerable time-saving benefits.

With the aim to optimize the trade-off between precision and computation time, we investigated CVA/DVA convergence with respect to different granularities for the joint grid, setting the results obtained with the daily grid as benchmark. In particular, we considered monthly, quarterly, semiannual and annual time steps. The results for the 15 years ATM payer Swap and

---

[15]For the instruments considered, fixed coupon dates are a subset of floating ones since taking place at the same time, otherwise the corresponding coupon dates should have been added to the time grid.

**(a)** Standard grid EPE and ENE no collateral.



**(b)** Joint grid EPE and ENE no collateral.



**(c)** Standard grid EPE and ENE with VM.



**(d)** Joint grid EPE and ENE with VM.



**(e)** Standard grid EPE and ENE with VM and IM.



**(f)** Joint grid EPE and ENE with VM and IM.
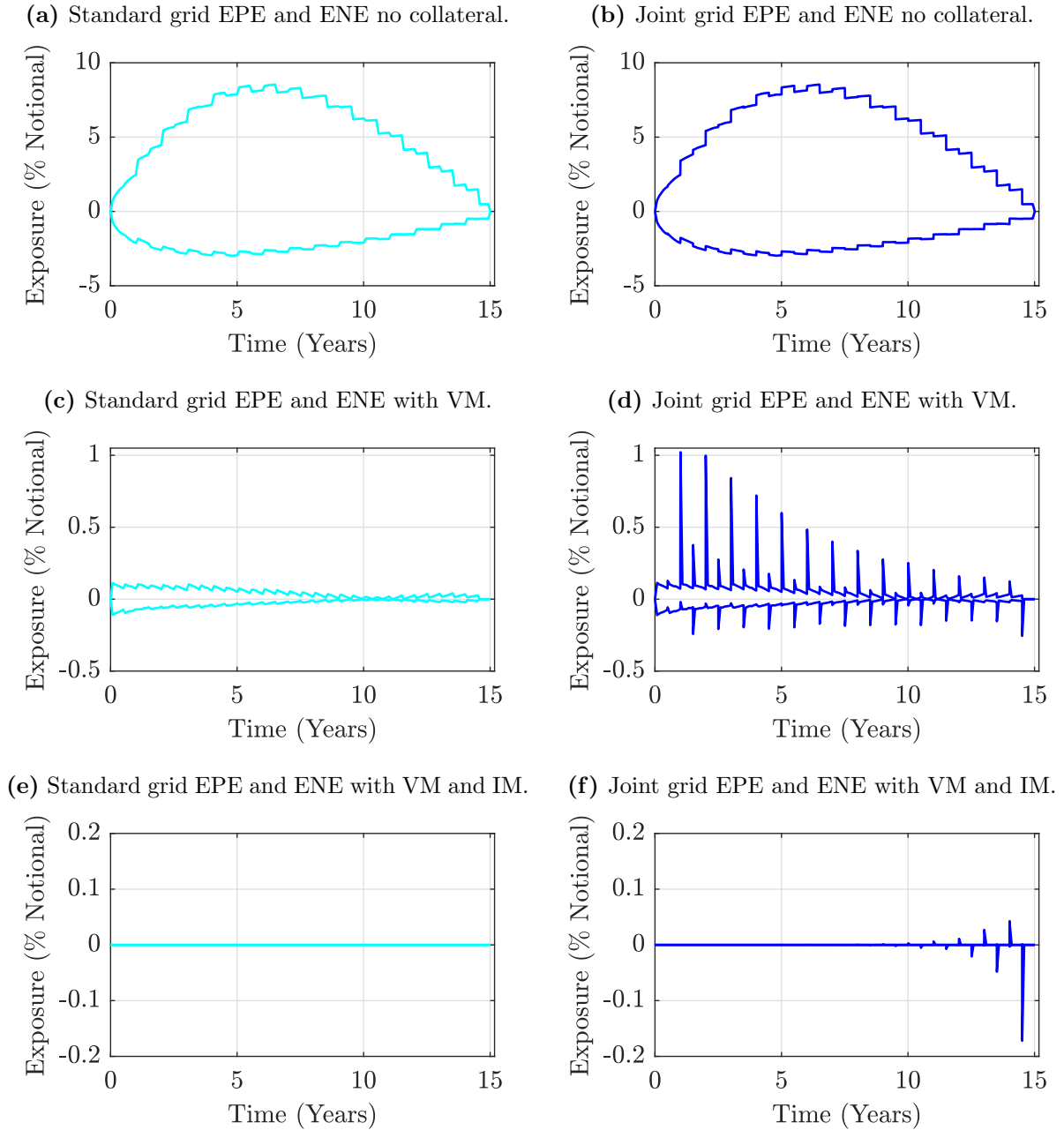


**Figure 9:** 15 years ATM payer Swap EUR 100 Mio notional, comparison between EPE and ENE profiles obtained with standard grid (left-hand side) and joint grid (right-hand side) with monthly granularity for the three collateralization schemes considered (top: no collateral, mid: VM, bottom: VM and IM). The graphs show that it is possible to capture spikes in collateralized exposure by adding to the standard grid the set of time points $\{T_j + 1\mathrm{d}\}_{j=1}^{n}$, where $T_j$ is the $j$-th floating coupon date and $n$ is the number of floating coupons. Other model parameters as in tab. 2. Quantities expressed as a percentage of the notional.

the 5x10 years ATM physically settled European payer Swaption, for the three collateralization schemes considered are reported in tab. 4. For uncollateralized case, CVA and DVA converge

CVA and DVA convergence with respect to time grid granularity

| Instrument | Collateral | $\Delta t$ | CVA | DVA | Time (min) |
|---|---|---|---|---|---|
| Swap | None | 12M | $-1\,119\,629\,(\pm\ \ 4\%)$ | $485\,660\,(\pm\ \ 8\%)$ | 0.45 |
| | | 6M | $-1\,170\,271\,(\pm\ \ 4\%)$ | $478\,016\,(\pm\ \ 9\%)$ | 0.60 |
| | | 3M | $-1\,172\,139\,(\pm\ \ 4\%)$ | $476\,789\,(\pm\ \ 9\%)$ | 0.90 |
| | | 1M | $-1\,172\,938\,(\pm\ \ 4\%)$ | $475\,324\,(\pm\ \ 9\%)$ | 2.10 |
| | | 1D | $-1\,173\,296\,(\pm\ \ 4\%)$ | $474\,469\,(\pm\ \ 9\%)$ | 54.80 |
| | VM | 12M | $-13\,894\,(\pm 10\%)$ | $22\,452\,(\pm 11\%)$ | 0.90 |
| | | 6M | $-7025\,(\pm\ \ 8\%)$ | $5597\,(\pm 12\%)$ | 1.20 |
| | | 3M | $-8138\,(\pm\ \ 8\%)$ | $6338\,(\pm 12\%)$ | 1.80 |
| | | 1M | $-8856\,(\pm\ \ 8\%)$ | $6814\,(\pm 12\%)$ | 4.20 |
| | | 1D | $-9374\,(\pm\ \ 8\%)$ | $7118\,(\pm 12\%)$ | 109.60 |
| | VM and IM | 12M | $-16\,(\pm 93\%)$ | $1098\,(\pm 17\%)$ | 12.38 |
| | | 6M | $-4\,(\pm 32\%)$ | $7\,(\pm 20\%)$ | 16.50 |
| | | 3M | $-4\,(\pm 32\%)$ | $7\,(\pm 20\%)$ | 24.75 |
| | | 1M | $-4\,(\pm 32\%)$ | $7\,(\pm 20\%)$ | 57.75 |
| | | 1D | $-6\,(\pm 27\%)$ | $16\,(\pm 15\%)$ | 1507.01 |
| Swaption | None | 12M | $-775\,964\,(\pm\ \ 6\%)$ | $41\,357\,(\pm 16\%)$ | 4.32 |
| | | 6M | $-815\,745\,(\pm\ \ 5\%)$ | $36\,705\,(\pm 17\%)$ | 6.07 |
| | | 3M | $-817\,396\,(\pm\ \ 5\%)$ | $36\,544\,(\pm 17\%)$ | 9.75 |
| | | 1M | $-818\,308\,(\pm\ \ 5\%)$ | $36\,418\,(\pm 17\%)$ | 23.57 |
| | | 1D | $-819\,616\,(\pm\ \ 5\%)$ | $36\,367\,(\pm 17\%)$ | 640.03 |
| | VM | 12M | $-6933\,(\pm 11\%)$ | $7363\,(\pm 16\%)$ | 8.02 |
| | | 6M | $-6940\,(\pm\ \ 9\%)$ | $638\,(\pm 22\%)$ | 11.27 |
| | | 3M | $-7481\,(\pm\ \ 9\%)$ | $649\,(\pm 23\%)$ | 17.77 |
| | | 1M | $-7831\,(\pm\ \ 9\%)$ | $665\,(\pm 23\%)$ | 43.77 |
| | | 1D | $-7734\,(\pm\ \ 9\%)$ | $527\,(\pm 25\%)$ | 1188.63 |
| | VM and IM | 12M | $-16\,(\pm 66\%)$ | $1102\,(\pm 18\%)$ | 119.63 |
| | | 6M | $-13\,(\pm 30\%)$ | $38\,(\pm 17\%)$ | 168.13 |
| | | 3M | $-13\,(\pm 30\%)$ | $38\,(\pm 17\%)$ | 265.13 |
| | | 1M | $-13\,(\pm 30\%)$ | $38\,(\pm 17\%)$ | 653.15 |
| | | 1D | $-38\,(\pm\ \ 3\%)$ | $12\,(\pm 19\%)$ | 17\,738.07 |

**Table 4:** 15 years ATM payer Swap and 5x10 years ATM physically settled European payer Swaption EUR 100 Mio notional, CVA and DVA convergence with respect to joint grid granularity for the three collateralization schemes considered, $3\sigma$ confidence intervals in parentheses. Other model parameters as in tab. 2. Quantities expressed in EUR.

for both instruments at low granularities, i.e. $\Delta t = 6M$. In case of collateralization, reliable results are obtained with $\Delta t = 1M$. Focusing on performance, a monthly grid allows on average a 95% reduction in computational time compared to a daily grid. In light of this analysis we set $\Delta t = 1M$ since offering a good compromise between accuracy and performance.

## 5.2  XVA Monte Carlo Convergence

Monte Carlo method for quantifying EPE/ENE in eq. 2.33, although the most complex and computational intensive approach, allows to easily cope with the complexities inherent XVA

calculation such as collateralization. Also in this case it is necessary to avoid unnecessary workloads by selecting a number of paths that optimizes the trade-off between precision and computational time. For this reason we investigated CVA/DVA convergence with respect to the number of simulated scenarios.

In this analysis we assumed CVA/DVA calculated with $N_{MC} = 10^6$ as proxies for "exact" values to be used as benchmark and assessed the convergence by computing CVA/DVA with a smaller number of scenarios using the same seed. Furthermore, in order to investigate Monte Carlo error we built for each time step $t_i$ the following $3\sigma$ upper and lower bounds on EPE/ENE

$$\mathcal{H}_{\mathrm{UB}}^{\pm}(t_0; t_i) = \mathcal{H}(t_0; t_i)^{\pm} + 3\frac{\sigma_{\mathcal{H}^{\pm}(t_0;t_i)}}{\sqrt{N_{MC}}}, \tag{5.1}$$

$$\mathcal{H}_{\mathrm{LB}}^{\pm}(t_0; t_i) = \mathcal{H}(t_0; t_i)^{\pm} - 3\frac{\sigma_{\mathcal{H}^{\pm}(t_0;t_i)}}{\sqrt{N_{MC}}}, \tag{5.2}$$

with

$$\sigma_{\mathcal{H}^{\pm}(t_0;t_i)} = \sqrt{\frac{1}{N_{MC}-1}\sum_{m=1}^{N_{MC}} \left[P(t_0; t_i)\left[H_m(t_i)\right]^{\pm} - \mathcal{H}^{\pm}(t_0; t_i)\right]^2}. \tag{5.3}$$

Therefore, we used these quantities to get the following confidence interval for CVA/DVA

$$\mathrm{CVA}_{\mathrm{UB,LB}}(t_0) = -LGD_{\mathrm{C}}\sum_{i=1}^{N_T}\mathcal{H}_{\mathrm{UB,LB}}^{+}(t_0; t_i)\mathcal{S}_{\mathrm{B}}(t_0, t_i)\Delta\mathcal{Q}_{\mathrm{C}}(t_0, t_i), \tag{5.4}$$

$$\mathrm{DVA}_{\mathrm{UB,LB}}(t_0) = -LGD_{\mathrm{B}}\sum_{i=1}^{N_T}\mathcal{H}_{\mathrm{UB,LB}}^{-}(t_0; t_i)\mathcal{S}_{\mathrm{C}}(t_0, t_i)\Delta\mathcal{Q}_{\mathrm{B}}(t_0, t_i). \tag{5.5}$$

Figs. 10 and 11 display convergence diagrams of CVA (left-hand side) and DVA (right-hand side) showing the dependence of Monte Carlo error upon the number of simulated scenarios for the 15 years ATM payer Swap and the 5x10 years ATM physically settled European payer Swaption respectively, for the three collateralization schemes considered. Furthermore, we show the convergence rate in terms of absolute percentage difference with respect to "exact" value proxies. As can be seen, for both instruments CVA/DVA converge to "exact" values proxies for all collateralization schemes, with small absolute percentage differences even for few paths (i.e. $N_{MC} = 1000$). Higher differences can be observed for VM and IM case (bottom panels) due to small CVA/DVA values; nevertheless, $N_{MC} \geq 5000$ ensures an absolute percentage difference below the 5% for the Swap and 6% for the Swaption. As regards computational time, since it scales linearly with the number of simulated paths, with $N_{MC} \geq 5000$ the benefits in terms of precision would be exceeded by the costs in terms of time required for the calculation, particularly for IM. In light of this, we set $N_{MC} = 5000$ since offering a good compromise between accuracy and performance.

34

**(a)** CVA no collateral.

**(b)** DVA no collateral.

**(c)** CVA with VM.

**(d)** DVA with VM.

**(e)** CVA with VM and IM.

**(f)** DVA with VM and IM.
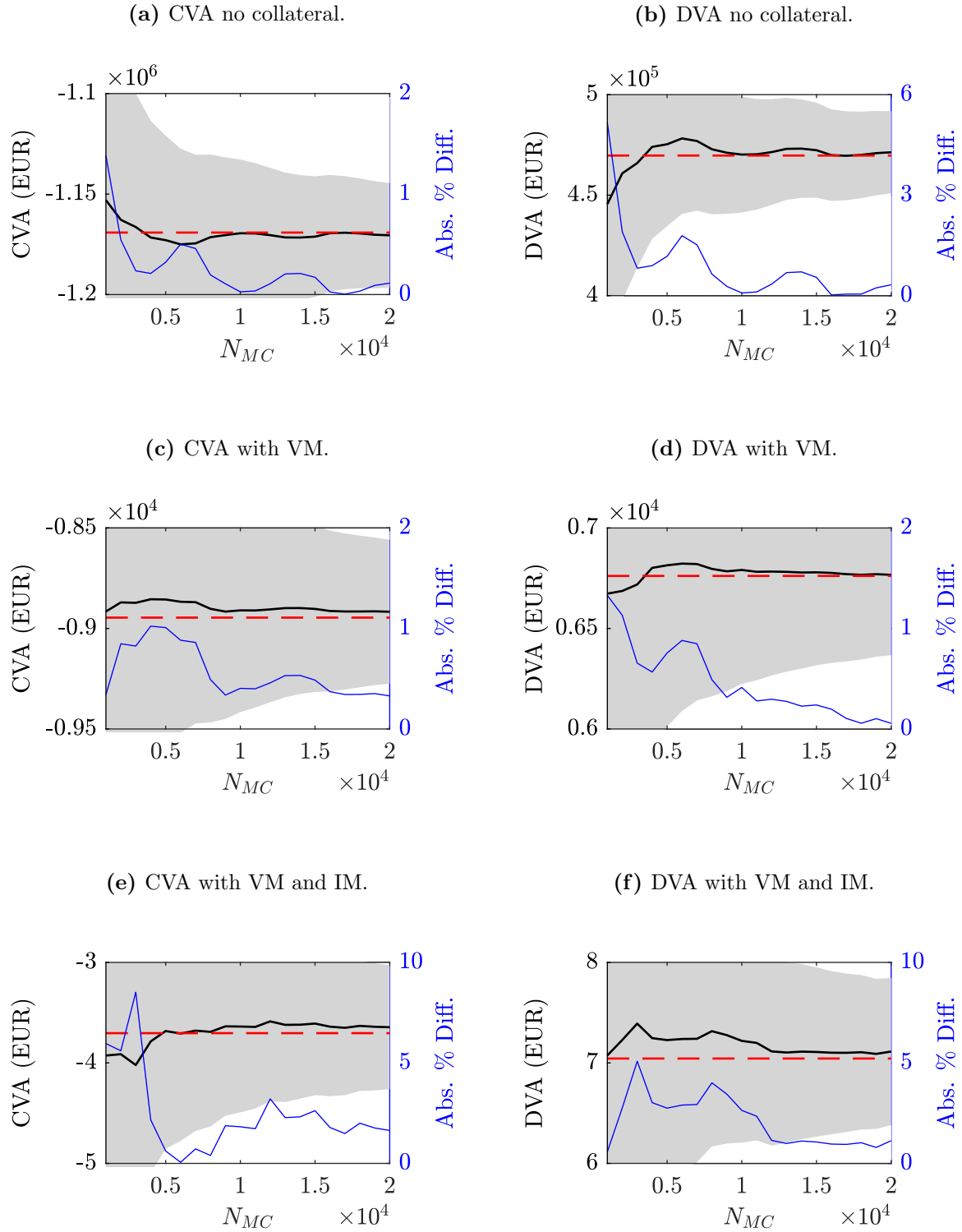
**Figure 10:** 15 years ATM payer Swap EUR 100 Mio notional, CVA (left-hand side) and DVA (right-hand side) convergence diagrams versus number of simulated scenarios for the three collateralization schemes considered (top: no collateral, mid: VM, bottom: VM and IM). Left-hand scale, black line: simulated CVA/DVA, grey area: $3\sigma$ confidence interval, dashed red line: "exact" value proxies. Right-hand scale, blue line: convergence rate in terms of absolute percentage difference with respect to "exact" values. We omit confidence interval for "exact" values proxies since small. CVA/DVA converge to "exact" values for all collateralization schemes, with small absolute percentage differences even for few paths (i.e. $N_{MC} = 1000$). Model parameters other than $N_{MC}$ as in tab. 2. Quantities expressed in EUR.

35

**(a)** CVA no collateral.

**(b)** DVA no collateral.

**(c)** CVA with VM.

**(d)** DVA with VM.

**(e)** CVA with VM and IM.

**(f)** DVA with VM and IM.
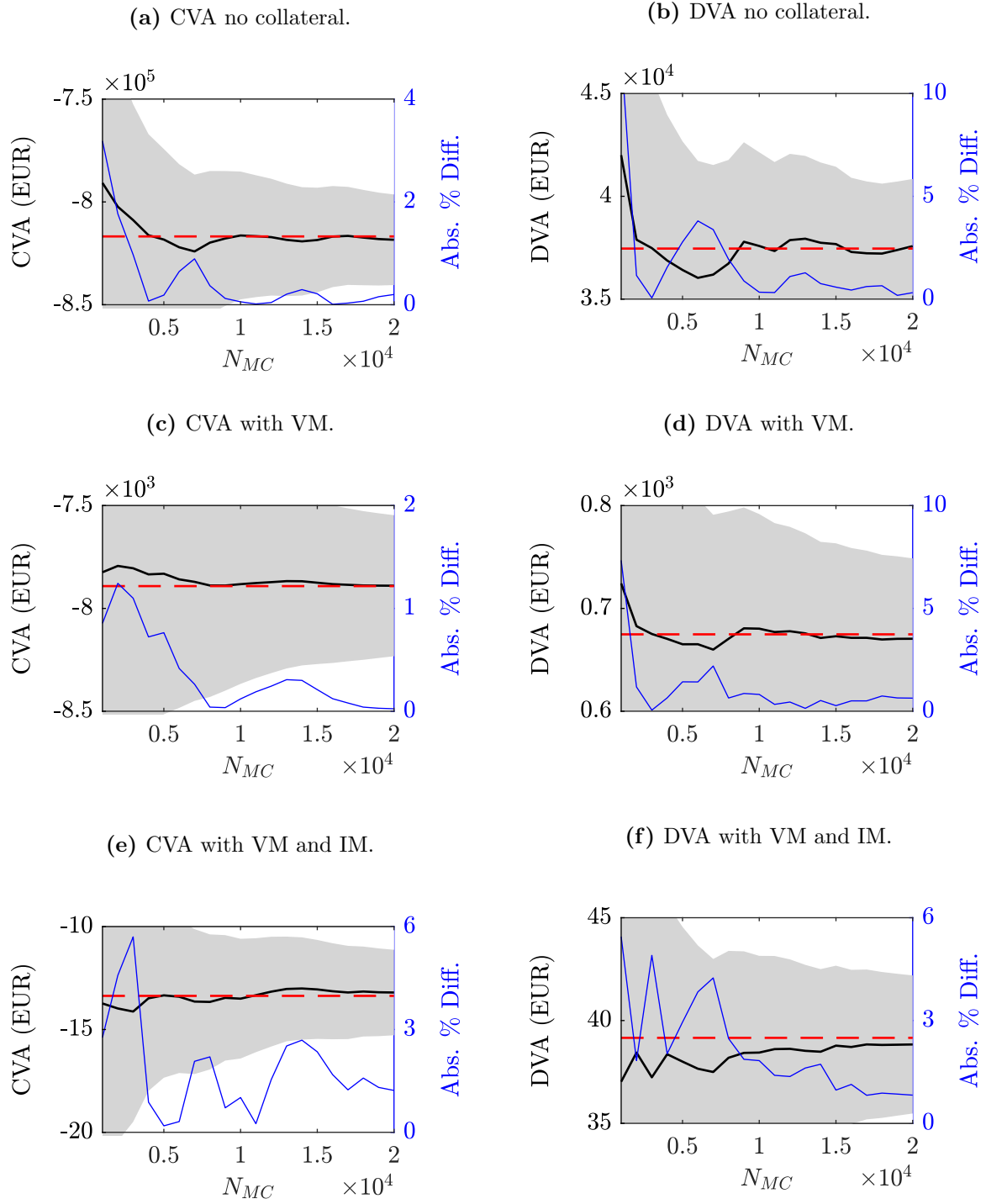
**Figure 11:** 5x10 years ATM physically settled European payer Swaption EUR 100 Mio notional, CVA (left-hand side) and DVA (right-hand side) convergence diagrams versus number of simulated scenarios for the three collateralization schemes considered (top: no collateral, mid: VM, bottom: VM and IM). Left-hand scale, black line: simulated CVA/DVA, grey area: $3\sigma$ confidence interval, dashed red line: "exact" value proxies. Right-hand scale, blue line: convergence rate in terms of absolute percentage difference with respect to "exact" values. We omit confidence interval for "exact" values proxies since small. Analogous considerations of fig. 10. Model parameters other than $N_{MC}$ as in tab. 2. Quantities expressed in EUR.

## 5.3 Forward Vega Sensitivity Calculation

In this section we report the analyses conducted to validate the approach adopted for calculating Vega sensitivity when simulating ISDA-SIMM dynamic IM. The results are shown for the 5x10 years ATM physically settled European payer Swaption, same considerations apply to the other Swaptions in tab. 1.

### 5.3.1 Shocks on G2++ Parameters

ISDA defines Vega sensitivity as the price change with respect to a 1% shift up in ATM Black implied volatility. Since G2++ European Swaption pricing formula does not provide for an explicit dependence on Black implied volatility (see eq. B.12), Vega cannot be calculated according to ISDA definition for future time steps. The approximation proposed in sec. 3.3.2 allows to calculate forward Vega by shifting up G2++ model parameters governing the underlying process volatility. In order validate this approach we compared Vega obtained at time step $t_0$ (i.e. valuation date) through eq. 3.15 with a "market" Vega and a "model" Vega, both consistent with ISDA prescriptions.

Specifically, for the 5x10 years ATM physically settled European payer Swaption we computed the following three Vega sensitivities

$$\nu_1(t_0) = \frac{V^{\text{Blk}}\big(t_0; \sigma_{6\text{m}}^{\text{Blk}}(t_0; 5, 10) + 0.01\big) - V^{\text{Blk}}\big(t_0; \sigma_{6\text{m}}^{\text{Blk}}(t_0; 5, 10)\big)}{0.01}, \qquad (5.6)$$

$$\nu_2(t_0) = \frac{V^{\text{G2++}}\big(t_0; \hat{p}\big) - V^{\text{G2++}}\big(t_0; p\big)}{0.01}, \qquad (5.7)$$

$$\nu_3(t_0) = \frac{V^{\text{G2++}}\big(t_0; \sigma + \epsilon_\sigma, \eta + \epsilon_\eta\big) - V^{\text{G2++}}\big(t_0; \sigma, \eta\big)}{\hat{\sigma}_{6\text{m}}^{\text{Blk}}(t_0; 5, 10) - \sigma_{6\text{m}}^{\text{Blk}}(t_0; 5, 10)}, \qquad (5.8)$$

where $\nu_1$ denotes "market" Vega obtained by shifting up ATM Black implied volatility quote by 1% and re-pricing the Swaption via Black pricing formula; $\nu_2$ denotes "model" Vega obtained by shifting up the ATM Black implied volatility matrix by 1%, re-pricing market Swaptions via Black pricing formula, re-calibrating G2++ parameters on these prices, and computing the price of the Swaption using re-calibrated parameters $\hat{p} = \{\hat{a}, \hat{\sigma}, \hat{b}, \hat{\eta}, \hat{\rho}, \hat{\Gamma}_1, \ldots, \hat{\Gamma}_{14}\}$. $\nu_3$ denotes Vega obtained according to the approximation outlined in sec. 3.3.2, i.e. by applying the shocks $\epsilon_\sigma$ and $\epsilon_\eta$ on G2++ parameters governing the underlying process volatility and computing Black implied volatilities by inverting Black pricing formula. In addition, we tested eq. 5.8 for different

Prices, Vega sensitivities and Vega Risks for the three different calculation approaches

| Approach | G2++ parameters | $V$ | $\hat{V}$ | $\nu(t_0)$ | VR |
|---|---|---|---|---|---|
| eq. 5.6 | None | 4 968 574 | 5 183 980 | 21 540 601 | 4 857 191 |
| eq. 5.7 | $\hat{p}$ | 5 030 423 | 5 248 595 | 21 817 192 | 4 982 139 |
| | $p, \epsilon_\sigma = 0.01, \epsilon_\eta = 0.01$ | 5 030 423 | 5 080 649 | 21 546 611 | 4 920 350 |
| | $p, \epsilon_\sigma = 0.02, \epsilon_\eta = 0.02$ | 5 030 423 | 5 155 984 | 21 535 711 | 4 917 861 |
| eq. 5.8 | $p, \epsilon_\sigma = 0.04, \epsilon_\eta = 0.04$ | 5 030 423 | 5 231 313 | 21 524 697 | 4 915 345 |
| | $p, \epsilon_\sigma = 0.10, \epsilon_\eta = 0.10$ | 5 030 423 | 5 532 576 | 21 479 486 | 4 905 021 |
| | $p, \epsilon_\sigma = 0.01, \epsilon_\eta = 0.04$ | 5 030 423 | 5 249 476 | 21 522 024 | 4 914 735 |

**Table 5:** 5x10 years ATM physically settled European payer Swaption EUR 100 Mio notional, comparison between prices $V(t_0)$ and $\hat{V}(t_0)$, Vega sensitivity $\nu(t_0)$ and Vega Risk $\text{VR}(t_0)$ at time step $t_0$ for the calculation approaches and parameterizations considered. Note that we denote with $\hat{V}(t_0)$ the prices obtained with shifted inputs.

values of $\epsilon_\sigma$ and $\epsilon_\eta$, considering both $\epsilon_\sigma = \epsilon_\eta$ and $\epsilon_\sigma \neq \epsilon_\eta$. In the latter case, we recovered shocks values from the re-calibrated parameters $\hat{\sigma}$ and $\hat{\eta}$ of eq. 5.7, which correspond respectively to $\epsilon_\sigma = 1\%$ and $\epsilon_\eta = 4\%$. The results of the comparison are reported in tab. 5. As can be seen, Vega sensitivities are aligned among the three approaches and the different shocks values examined. This means that at time step $t_0$ the approximation proposed produces Vega sensitivity and Vega Risk[16] values consistent with those obtained by applying ISDA definition, therefore we assumed that it can be adopted also for future time steps. As regards the choice of shocks sizes, in order to avoid any arbitrary elements, we computed forward Vega by using the re-calibrated $\hat{\sigma}$ and $\hat{\eta}$, corresponding to $\epsilon_\sigma = 1\%$ and $\epsilon_\eta = 4\%$.

### 5.3.2 Implied Volatility Calculation

When performing time simulation it may happen that for some extreme paths the value of the Black shift $\lambda_x$ observed at time step $t_0$ results to be too small to retrieve positive Swap rates in future time steps avoiding Black formula inversion (see fig. 12). In order to ensure Vega
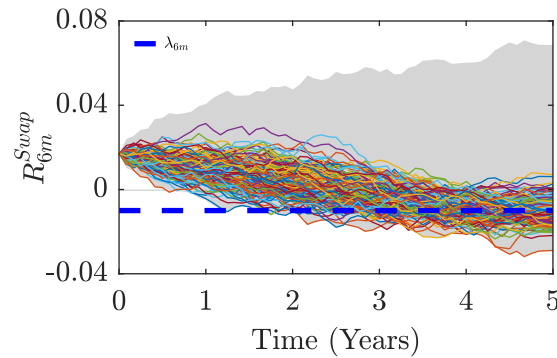


**Figure 12:** Grey area represents the cloud of forward Swap rate stochastic trajectories. Coloured paths are the ones for which the value of the Swap rate falls below the Black shift for at least one time step

sensitivity calculation for each time step and path, we propose to consider Black shift values larger than those observed on the market at time step $t_0$. To this end, we analysed the impact of different Black shift values on Black implied volatility, Vega sensitivity and Vega Risk. The results for the 5x10 years ATM physically settled European payer Swaption are reported in tab. 6. As can be seen, although a large impact on Black implied volatility and Vega sensitivity,

Black implied volatility, Vega sensitivity and Vega Risk for different Black shifts

| $\lambda_{6m}$ | $\sigma_{6m}^{Blk}$ | $\nu$ | VR |
|---|---|---|---|
| 0.01 | 0.2284 | 21 522 024 | 4 914 735 |
| 0.04 | 0.1302 | 38 342 983 | 4 992 724 |
| 0.06 | 0.0793 | 63 259 702 | 5 016 378 |
| 0.08 | 0.0629 | 79 814 066 | 5 021 578 |
| 0.10 | 0.0521 | 96 350 056 | 5 024 345 |

**Table 6:** 5x10 years ATM physically settled European payer Swaption EUR 100 Mio notional, comparison between Black implied volatility $\sigma_{6m}^{Blk}(t_0)$, Vega sensitivity $\nu(t_0)$ and Vega Risk $VR(t_0)$ at time step $t_0$ for different Black shift values $\lambda_{6m}$. Calculation approach as in eq. 5.8, with $\epsilon_\sigma = 0.01$ and $\epsilon_\eta = 0.04$.

the impact on Vega Risk is negligible as it is given by the product of the two quantities (see eq. C.8). More in detail, compared to the value observed at time step $t_0$, i.e. $\lambda_{6m} = 0.01$, the

---

[16]Vega Risk is the product between Vega sensitivity and Black implied volatility (see eq. C.8).

various Black shifts considered produce Vega Risk values differing up to a maximum of 2%. This leads us to conclude that $\lambda_x$ values larger than those observed at $t_0$ ensure the inversion of the Black formula for each path with an acceptable loss of accuracy in Vega Risk. For this reason we set $\lambda_{6m} = 0.06$.

## 5.4 XVA Sensitivities to CSA Parameters

The aim of this section is to analyse the impacts of CSA parameters on XVA figures by assessing if collateralized CVA/DVA converges to uncollateralized ones for increasing values of threshold K and minimum transfer amount MTA, keeping other model parameters as in tab. 2. The results with respect to the length of MPoR $l$ are not reported since no significant impacts were found. In carrying out the analysis we distinguished between the following three collateralization schemes:

1. CVA/DVA with VM only;

2. CVA/DVA with VM and IM, with K and MTA applied on VM only;

3. CVA/DVA with VM and IM, with K and MTA applied on both VM and IM.

Convergence diagrams for the 15 years ATM payer Swap are shown in figs. 13 and 14. In particular, left-hand side panels show CVA/DVA convergence with respect to K, with MTA = 0 EUR and $l = 2$ days; conversely, right-hand side panels show the convergence with respect to MTA, with K = 0 EUR and $l = 2$ days. As can be seen, case 1. (top panels) and case 3. (bottom panels) display similar results except for small values of K and MTA, thus IM is ineffective when significant frictions are considered. Instead, case 2. (middle panels) displays collateralized CVA/DVA not converging to uncollateralized ones, this means that without frictions IM is effective in reducing residual credit exposure. Furthermore, the results suggest that K leads to a faster convergence to uncollateralized figures compared to MTA; e.g. in case 1. K = 5 Mio EUR leads to an increase in absolute terms of approx. 5700% in CVA and 3600% in DVA with respect to the reference case (see tab. 2), while MTA = 5 Mio EUR leads to an increase of approx. 1300% in CVA and 1100% in DVA. As expected, K introduces an higher degree of friction since determining the maximum amount of allowed unsecured exposure; on the other hand, MTA governs only the minimum amount for each margin call, therefore significant impacts can be observed only for large values (see eqs. 3.2 and 3.8). The 5x10 years ATM physically settled European payer Swaption displays same results and is not reported.

A focus on the effects of K on collateralized exposure is shown in fig. 15, which displays EPE/ENE for the 15 years Swap (left-hand side panels) and the 5x10 years ATM physically settled European payer Swaption (right-hand side panels) for the three collateralization schemes above, for different values of K (with MTA = 0 EUR and $l = 2$ days). Focusing on the Swap with VM (top panel), the average EPE (ENE) over the time steps, expressed as a percentage of the notional, is equal to 0.08%, 0.62% and 2.56% (−0.04%, −0.31% and −1.12%), respectively for threshold values of 0, 1 and 5 EUR Mio. By adding IM with no threshold (middle panel), large part of residual exposure is suppressed: average EPE (ENE) is equal to 0.00%, 0.04% and 0.91% (0.00%, −0.02% and −0.25%) of the notional. By considering threshold also on IM (bottom panel), average EPE (ENE) is equal to 0.00%, 0.14% and 2.46% (0.00%, −0.06% and −0.97%) of the notional meaning that, as K increases, IM looses its effectiveness and EPE/ENE approach to those with only VM.

**(a)** CVA with VM for different K, no MTA.
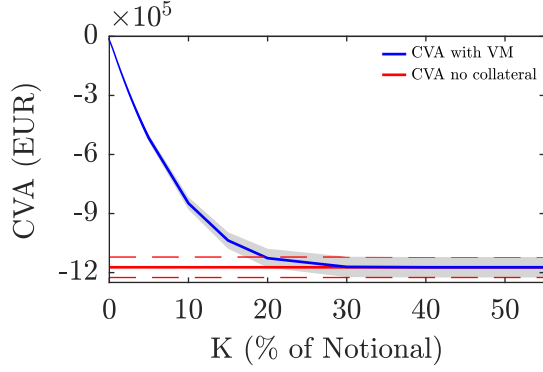


**(b)** CVA with VM for different MTA, no K.
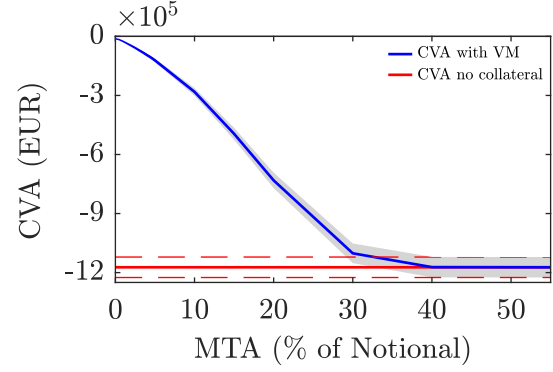


**(c)** CVA with VM and IM for different K on VM only, no MTA.
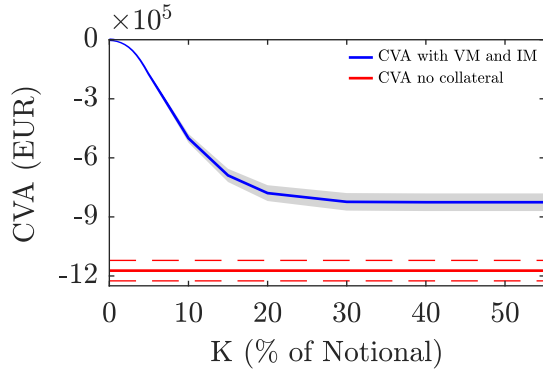


**(d)** CVA with VM and IM for different MTA on VM only, no K.
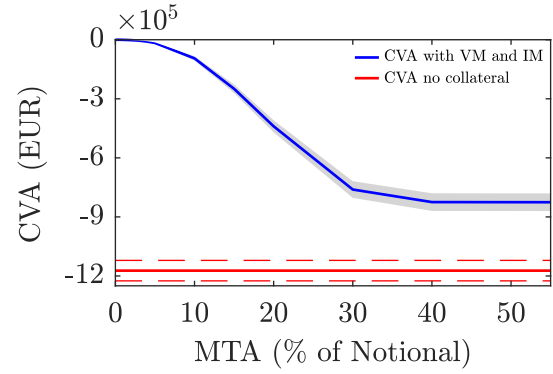


**(e)** CVA with VM and IM for different K on VM and IM, no MTA.
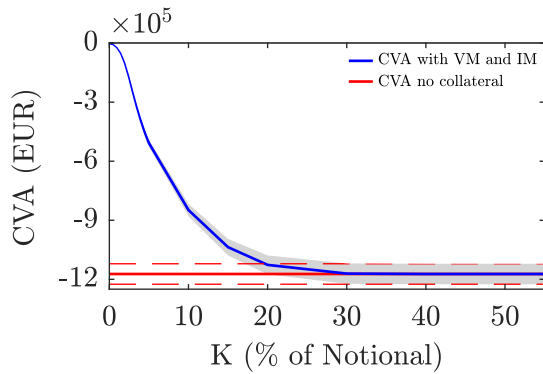


**(f)** CVA with VM and IM for different MTA on VM and IM, no K.
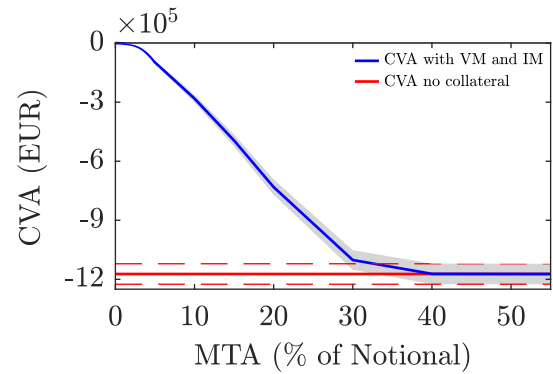


**Figure 13:** 15 years ATM payer Swap EUR 100 Mio notional, collateralized CVA convergence to uncollateralized case with respect to threshold (K, left-hand side) and minimum transfer amount (MTA, right-hand side), keeping other model parameters as in tab. 2. Top panels: CVA with VM, mid panels: CVA with VM and IM with K/MTA only on VM, bottom panels: CVA and with VM and IM with K/MTA on both margins. Grey areas: collateralized CVA $3\sigma$ confidence intervals, dashed lines: $3\sigma$ uncollateralized CVA confidence intervals. Convergence to uncollateralized CVA is reached for top and bottom panels for smaller values of K compared to MTA, to confirm that K introduces higher friction.

**(a)** DVA with VM for different K, no MTA.

**(b)** DVA with VM for different MTA, no K.

**(c)** DVA with VM and IM for different K on VM only, no MTA.

**(d)** DVA with VM and IM for different MTA on VM only, no K.

**(e)** DVA with VM and IM for different K on VM and IM, no MTA.

**(f)** DVA with VM and IM for different MTA on VM and IM, no K.
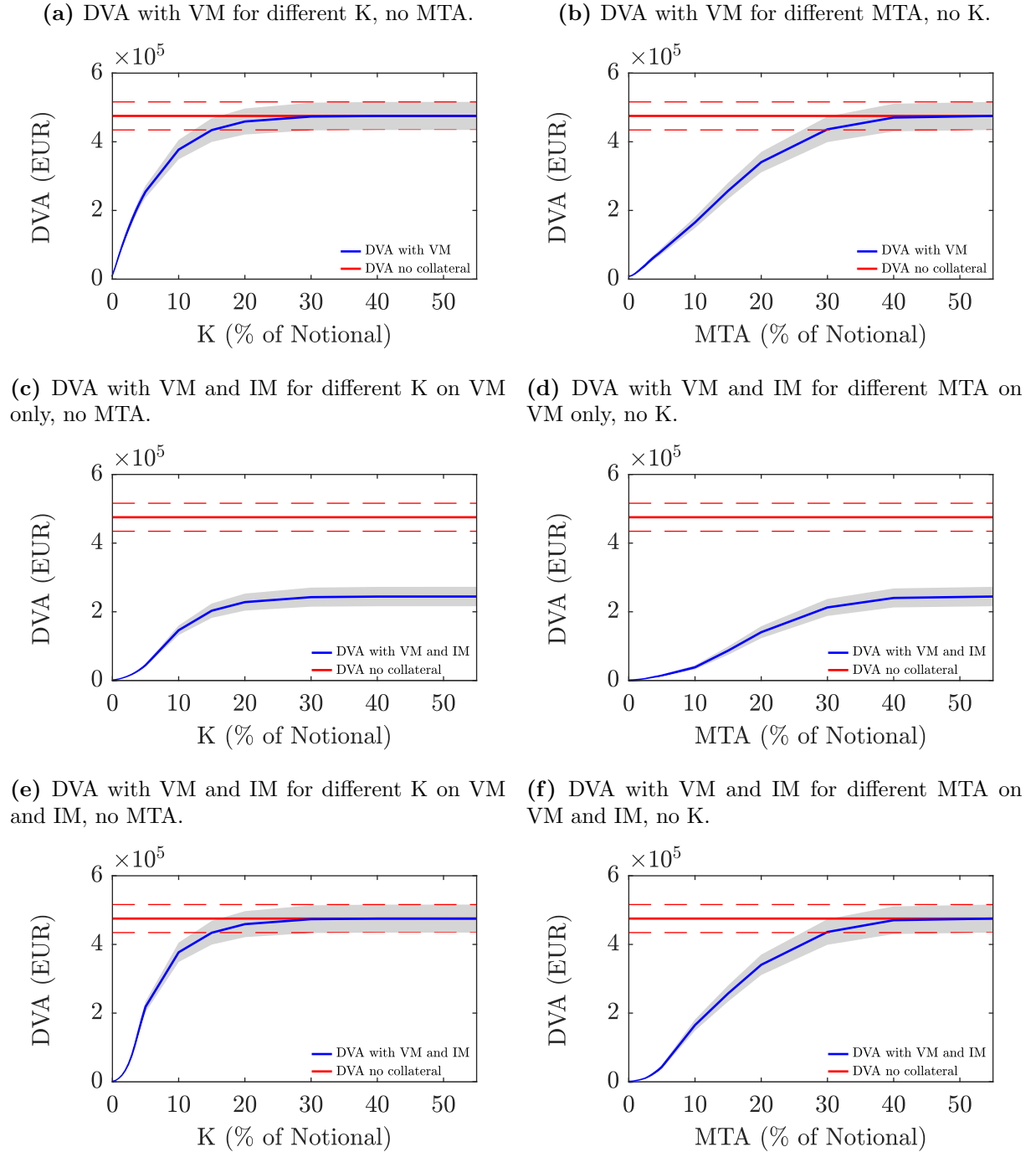
**Figure 14:** 15 years ATM payer Swap EUR 100 Mio notional, collateralized DVA convergence to uncollateralized case with respect to threshold (K, left-hand side) and minimum transfer amount (MTA, right-hand side), keeping other model parameters as in tab. 2. Top panels: DVA with VM, mid panels: DVA with VM and IM with K/MTA only on VM, bottom panels: DVA and with VM and IM with K/MTA on both margins. Grey areas: collateralized DVA $3\sigma$ confidence intervals, dashed lines: $3\sigma$ uncollateralized DVA confidence intervals. Analogous considerations of fig.13.

41

**(a)** EPE and ENE Swap with VM, no MTA.

**(b)** EPE and ENE Swaption with VM, no MTA.

**(c)** EPE and ENE Swap with VM and IM, K on VM only, no MTA.

**(d)** EPE and ENE Swaption with VM and IM, K on VM only, no MTA.

**(e)** EPE and ENE Swap with VM and IM, K on VM and IM, no MTA.

**(f)** EPE and ENE Swaption with VM and IM, K on VM and IM, no MTA.
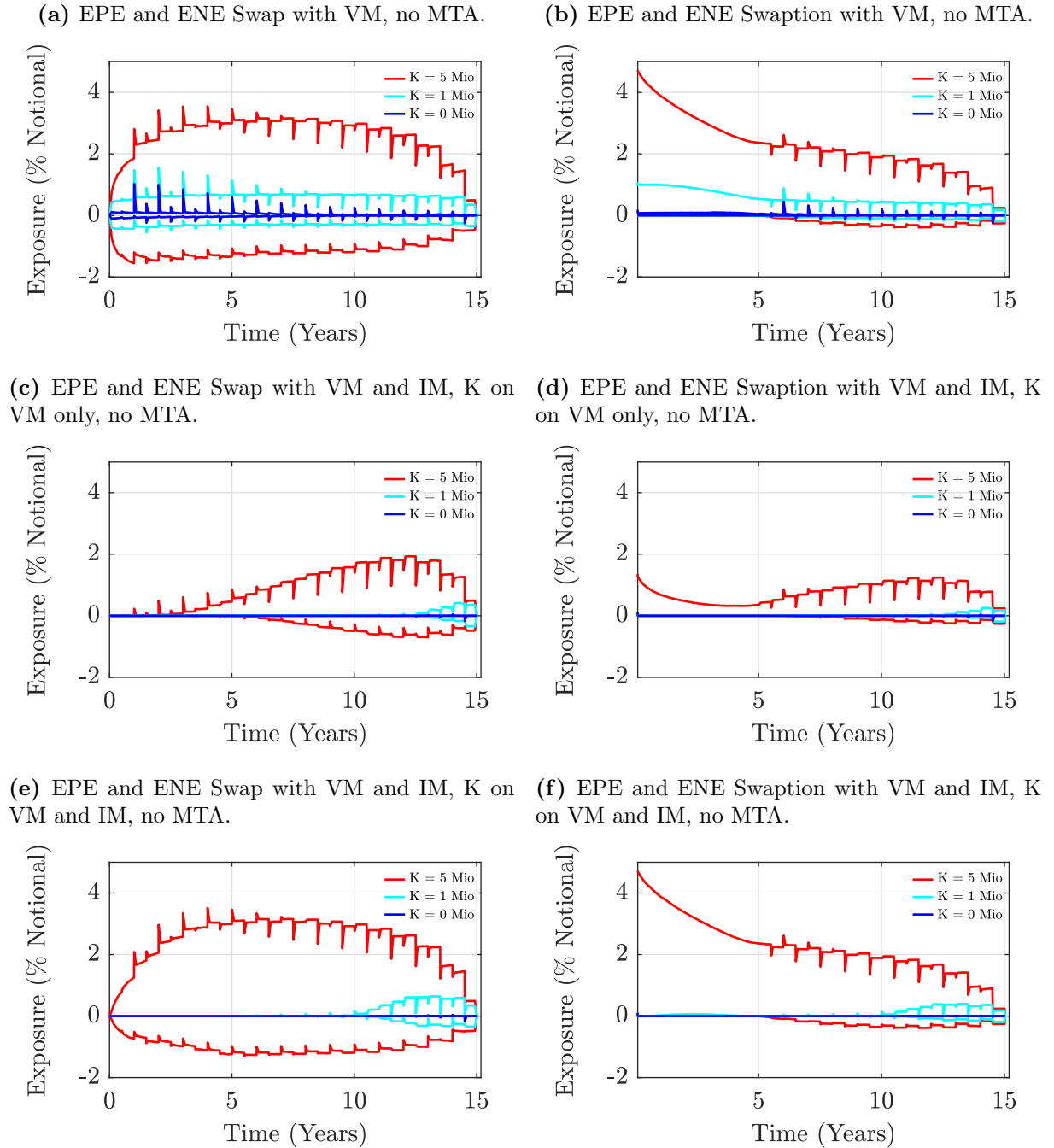
**Figure 15:** 15 years ATM payer Swap (left-hand side) and 5x10 years ATM physically settled European payer Swaption (right-hand side) EUR 100 Mio notional, collateralized EPE/ENE profiles for different values of threshold: K=0 Mio (blue lines), K = 1 Mio (cyan lines) and K = 5 Mio (red lines). Top panels: exposure with VM, mid panels: exposure with VM and IM with K only on VM, bottom panels: exposure with VM and IM with K on both margins. The residual exposure increases with K and IM becomes ineffective for large K. To enhance Swaption's plots readability, we excluded collateralized EPE for time step $t_0$ as not mitigated by collateral, in particular EPE($t_0$) corresponds to Swaption's price: $5\,030\,423$ EUR (approx. 5% of the notional). Other model parameters as in tab. 2. Quantities expressed as a percentage of the notional.

## 5.5 Monte Carlo Versus Analytical XVA

In sec. 2.4.3 we have shown that analytical solutions for eqs. 2.29 and 2.30 are available for uncollateralized Swaps. In particular, CVA and DVA of a payer (receiver) Swap can be interpreted as an integral over the values of a strip of co-terminal European payer (receiver) Swaptions and European receiver (payer) Swaptions, respectively (see eqs. 2.35 and 2.36). The numerical solution of eqs. 2.35 and 2.36 involves the discretization of the integrals on a

Comparison between CVA/DVA obtained with analytical approach and Monte Carlo approach

| Item | $\Delta t$ | Analytical G2++ | Analytical Black | MC |
|---|---|---|---|---|
| CVA ATM Swap | 12M | $-1\,091\,604$* | $-1\,016\,082$ | $-1\,119\,629\,(\pm 4\%)$ |
| | 6M | $-1\,157\,012$* | $-1\,077\,346$ | $-1\,170\,271\,(\pm 4\%)$ |
| | 3M | $-1\,147\,871$* | $-1\,067\,726$ | $-1\,172\,139\,(\pm 4\%)$ |
| | 1M | $-1\,152\,567$* | $-1\,072\,231$ | $-1\,172\,938\,(\pm 4\%)$ |
| | 1D | $-1\,156\,083$* | $-1\,075\,398$ | $-1\,173\,296\,(\pm 4\%)$ |
| DVA ATM Swap | 12M | $454\,023$* | $432\,373$ | $485\,660\,(\pm 8\%)$ |
| | 6M | $471\,340$* | $449\,890$* | $478\,016\,(\pm 9\%)$ |
| | 3M | $468\,884$* | $447\,358$* | $476\,789\,(\pm 9\%)$ |
| | 1M | $468\,721$* | $447\,369$* | $475\,324\,(\pm 9\%)$ |
| | 1D | $469\,562$* | $448\,170$* | $474\,469\,(\pm 9\%)$ |
| CVA OTM Swap | 12M | $-744\,144$* | $-698\,128$* | $-732\,977\,(\pm 6\%)$ |
| | 6M | $-783\,485$* | $-735\,481$ | $-778\,892\,(\pm 6\%)$ |
| | 3M | $-773\,913$* | $-725\,498$ | $-779\,280\,(\pm 6\%)$ |
| | 1M | $-774\,432$* | $-726\,025$ | $-779\,085\,(\pm 6\%)$ |
| | 1D | $-775\,955$* | $-727\,392$ | $-778\,991\,(\pm 6\%)$ |
| DVA OTM Swap | 12M | $788\,254$ | $793\,430$ | $892\,169\,(\pm 6\%)$ |
| | 6M | $833\,226$* | $840\,902$* | $880\,117\,(\pm 6\%)$ |
| | 3M | $839\,022$* | $847\,065$* | $882\,972\,(\pm 6\%)$ |
| | 1M | $846\,586$* | $855\,381$* | $884\,382\,(\pm 6\%)$ |
| | 1D | $851\,479$* | $860\,467$* | $885\,227\,(\pm 6\%)$ |

**Table 7:** 15 years ATM payer Swap and 15 years OTM payer Swap EUR 100 Mio notional, comparison between CVA/DVA obtained with analytical approach and Monte Carlo approach. The strip of co-terminal Swaptions has been computed through G2++ pricing formula in the third column and through Black formula in the fourth column. Results included in MC error marked with an asterisk. In absolute terms, analytical formulas underestimate CVA and DVA values. The results obtained with G2++ always included in MC error (only one exception: DVA OTM Swap 12M granularity). Considerable differences are observed with analytical Black.

grid of time points (see eqs. 2.37 and 2.38), with impacts in terms of precision of the results related to its granularity. Therefore, as for Monte Carlo model, we tested analytical formulas for different time steps frequencies. Moreover, given the model independent nature of this approach, we calculated Swaptions prices through both G2++ and Black formulas. The purpose is twofold: one one hand we want to test the results of the Monte Carlo approach, on the other hand we want to quantify the model risk stemming from the use of two alternative pricing formulas. More in detail, we calculated G2++ Swaptions prices by applying eq. B.12 and G2++ parameters in tab. 2. Regarding Black pricing formula, the most complex step regards the determination of implied volatility for the strip of co-terminal Swaptions. Starting from market Swaptions prices cube, we calibrated SABR parameters (see [44]) on each smile section (i.e. tenor-expiry combination) obtaining a SABR parameters cube; hence, we determined the implied volatility for each co-terminal Swaption using the SABR approximated closed formula

linearly interpolating/extrapolating on calibrated parameters cube in correspondence of the tenor-expiry combination of each co-terminal Swaption.

The analysis has been carried out considering the 15 years ATM payer Swap and the 15 years OTM payer Swap. The results shown in tab. 7 suggest that, with respect to Monte Carlo approach (last column), analytical formulas underestimate CVA and DVA values in absolute terms. Moreover, the results obtained with analytical G2++ (third column) are always included in Monte Carlo error (marked with an asterisk), with the only exception represented by the DVA of the OTM Swap with annual time grid granularity, to confirm the robustness of the results of the Monte Carlo model. As regards the results obtained with a different dynamic (fourth column), considerable differences are observed, particularly in CVA which is included in Monte Carlo error only in one case, to demonstrate that a not negligible model risk exists. In terms of computational performance, the advantage of the analytical approach is several orders of magnitude greater than that of Monte Carlo approach: with a daily grid robust results can be obtained in only 1 minute, meaning that, for an uncollateralized Swap, the analytical approach can replace the Monte Carlo approach whereas performance is critical.

## 5.6 XVA Model Risk

According to the Regulation (EU) No 575/2013 (see [35]), financial institutions are required to apply prudent valuation to fair-valued positions (Art. 105). For prudent valuation is meant the calculation of specific Additional Valuation Adjustments (AVA), to be deducted from the Common Equity Tier 1 (CET1) capital (Art. 34), necessary to adjust the fair-value of a financial instrument in order to achieve a prudent value with an appropriate degree of certainty. The prudent value has to be computed considering the valuation risk factors listed in Art. 105 (par. 10-11) in order to mitigate the risk of losses deriving from the valuation uncertainty of the exit price of a financial instrument. These valuation risk factors are linked to the corresponding AVA described in the Commission Delegated Regulation (EU) 2016/101 (see [36]), where the degree of certainty is set at 90%.

In particular, the Model Risk (MoRi) AVA is envisaged in Art. 11 of [36] and comprises the valuation uncertainty linked to the potential existence of a range of different models or model calibrations used by market participants. This may occur e.g. when a unique model recognized as a clear market standard for computing the price of a certain financial instrument does not exist, or when a model allows for different parameterizations or numerical solution algorithms. Accordingly, for MoRi AVA the prudent value at a 90% confidence level corresponds to the 10th percentile of the distribution of the plausible prices obtained from different models/parameterizations[17].

In this section we apply this framework to XVA by calculating a MoRi AVA based on the different models and parameterizations discussed in the sections above. In particular, we computed MoRi AVA $\text{AVA}^{\text{MoRi}}(t_0)$ at time $t_0$ starting from the following definition and avoiding the aggregation coefficient

$$\text{AVA}^{\text{MoRi}}(t_0) = V(t_0; M) - \text{PV}(t_0; M^*), \tag{5.9}$$

where:

- $V(t_0; M) = V_0(t_0) + \text{XVA}(t_0; M)$ is the fair-value of the instrument, intended as the price obtained from the target XVA framework $M$, i.e. the model and the corresponding parameters which optimizes the trade-off between accuracy and performance (as reported in tab. 2);

---

[17]Notice that we conventionally adopt positive/negative prices for assets/liabilities.

44

- $\text{PV}(t_0; M^*) = V_0(t_0) + \text{XVA}(t_0; M^*)$ is the prudent value obtained from the alternative XVA framework $M^* \in \{M_1, \ldots, M_N\}$, which produces the price corresponding to the $10^{\text{th}}$ percentile of the prices distribution obtained from the set of $N + 1$ XVA frameworks. In other words, $M^*$ ensures that one can exit the position at a price equal to or larger than $\text{PV}(t_0; M^*)$ with a degree of certainty equal to or larger than $90\%$[18].

In light of this, and since we are not considering the valuation uncertainty related to the base value $V_0(t_0)$, eq. 5.9 becomes

$$\text{AVA}^{\text{MoRi}}(t_0) = \text{XVA}(t_0; M) - \text{XVA}(t_0; M^*). \tag{5.10}$$

We built the XVA distribution by leveraging on the outcomes of the analyses described in the sections above. In particular, we considered XVA obtained from both standard and joint grids with different granularities $\Delta t$ (see sec. 5.1), different numbers of simulated paths $N_{MC}$ (see sec. 5.2), and analytical approach for uncollateralized Swaps with different time steps frequencies and pricing formulas for the strip of co-terminal Swaptions (see sec. 5.5).

We report in tabs. 8 and 9 the XVA distributions for the uncollateralized 15 years ATM payer Swap and for the uncollateralized 5x10 years ATM physically settled European payer Swaption, respectively. Similar results were obtained for the other collateralization schemes. Focusing on the Swap in tab. 8, in addition to the target XVA framework $M$ we considered $N = 37$ alternative frameworks. The one producing a prudent XVA at $90\%$ confidence level is framework $M_3$, namely the Monte Carlo model with the following parameterization: joint grid, $\Delta t = 1M$ and $N_{MC} = 3000$, at which corresponds $\text{XVA}(t_0; M_3) = -700\,463$ EUR (denoted by double asterisk in tab. 8). The related MoRi AVA obtained from eq. 5.10 is $\text{AVA}^{\text{MoRi}}(t_0) = 2849$ EUR, which corresponds to $0.41\%$ of $\text{XVA}(t_0; M)$. With reference to the Swaption in tab. 9, the framework producing prudent XVA at $90\%$ confidence level is framework $M_2$, namely the Monte Carlo model with the following parameterization: joint grid, $\Delta t = 1M$ and $N_{MC} = 6000$, at which corresponds $\text{XVA}(t_0; M_2) = -786\,025$ EUR (denoted by double asterisk in tab. 9). The related MoRi AVA is $\text{AVA}^{\text{MoRi}}(t_0) = 4135$ EUR, which corresponds to $0.53\%$ of $\text{XVA}(t_0; M)$.

---

[18]Notice that, according to our conventions, $\text{PV}(t_0) \leq V(t_0)$.

15 years ATM payer Swap, no collateral

| $M_j$ | Model | Parameters | | | CVA | DVA | XVA |
|---|---|---|---|---|---|---|---|
| | | Time grid | $\Delta t$ | $N_{MC}$ | | | |
| $M_1$ | MC | Joint | 1M | 1000 | $-1\,153\,010$ | $445\,537$ | $-707\,473$ |
| $M_2$ | MC | Joint | 1M | 2000 | $-1\,162\,820$ | $460\,853$ | $-701\,967$ |
| $M_3$ | MC | Joint | 1M | 3000 | $-1\,166\,416$ | $465\,953$ | $-700\,463^{**}$ |
| $M_4$ | MC | Joint | 1M | 17 000 | $-1\,169\,232$ | $469\,590$ | $-699\,642$ |
| $M_5$ | MC | Joint | 1M | 16 000 | $-1\,169\,479$ | $469\,905$ | $-699\,574$ |
| $M_6$ | MC | Joint | 1M | 18 000 | $-1\,169\,580$ | $470\,026$ | $-699\,554$ |
| $M_7$ | MC | Joint | 1M | 19 000 | $-1\,170\,243$ | $470\,898$ | $-699\,345$ |
| $M_8$ | MC | Joint | 1M | 9000 | $-1\,170\,432$ | $471\,101$ | $-699\,331$ |
| $M_9$ | MC | Joint | 1M | 10 000 | $-1\,169\,500$ | $470\,184$ | $-699\,316$ |
| $M_{10}$ | MC | Joint | 1M | 11 000 | $-1\,169\,599$ | $470\,326$ | $-699\,273$ |
| $M_{11}$ | MC | Joint | 1M | 20 000 | $-1\,170\,511$ | $471\,327$ | $-699\,184$ |
| $M_{12}$ | MC | Joint | 1M | 12 000 | $-1\,170\,445$ | $471\,424$ | $-699\,021$ |
| $M_{13}$ | MC | Joint | 1M | 15 000 | $-1\,171\,196$ | $472\,365$ | $-698\,831$ |
| $M_{14}$ | MC | Joint | 1D | 5000 | $-1\,173\,296$ | $474\,469$ | $-698\,826$ |
| $M_{15}$ | MC | Joint | 1M | 8000 | $-1\,171\,461$ | $472\,833$ | $-698\,628$ |
| $M_{16}$ | MC | Joint | 1M | 13 000 | $-1\,171\,579$ | $473\,037$ | $-698\,542$ |
| $M_{17}$ | MC | Joint | 1M | 14 000 | $-1\,171\,638$ | $473\,143$ | $-698\,495$ |
| $M_{18}$ | MC | Joint | 1M | 4000 | $-1\,171\,633$ | $474\,013$ | $-697\,620$ |
| $M$ | MC | Joint | 1M | 5000 | $-1\,172\,938$ | $475\,324$ | $-697\,614^{*}$ |
| $M_{19}$ | MC | Joint | 1M | 7000 | $-1\,174\,536$ | $476\,932$ | $-697\,604$ |
| $M_{20}$ | MC | Standard | 1M | 5000 | $-1\,172\,940$ | $475\,340$ | $-697\,601$ |
| $M_{21}$ | MC | Joint | 1M | 6000 | $-1\,175\,033$ | $478\,215$ | $-696\,818$ |
| $M_{22}$ | MC | Joint | 3M | 5000 | $-1\,172\,139$ | $476\,789$ | $-695\,350$ |
| $M_{23}$ | MC | Standard | 3M | 5000 | $-1\,172\,144$ | $476\,839$ | $-695\,304$ |
| $M_{24}$ | MC | Joint | 6M | 5000 | $-1\,170\,271$ | $478\,016$ | $-692\,255$ |
| $M_{25}$ | MC | Standard | 6M | 5000 | $-1\,170\,249$ | $478\,016$ | $-692\,233$ |
| $M_{26}$ | Analytical G2++ | Standard | 1D | NA | $-1\,156\,083$ | $469\,562$ | $-686\,520$ |
| $M_{27}$ | Analytical G2++ | Standard | 6M | NA | $-1\,157\,012$ | $471\,340$ | $-685\,672$ |
| $M_{28}$ | Analytical G2++ | Standard | 1M | NA | $-1\,152\,567$ | $468\,721$ | $-683\,846$ |
| $M_{29}$ | Analytical G2++ | Standard | 3M | NA | $-1\,147\,871$ | $468\,884$ | $-678\,987$ |
| $M_{30}$ | Analytical G2++ | Standard | 12M | NA | $-1\,091\,604$ | $454\,023$ | $-637\,581$ |
| $M_{31}$ | MC | Joint | 12M | 5000 | $-1\,119\,629$ | $485\,660$ | $-633\,968$ |
| $M_{32}$ | MC | Standard | 12M | 5000 | $-1\,116\,254$ | $488\,095$ | $-628\,159$ |
| $M_{33}$ | Analytical Black | Standard | 6M | NA | $-1\,077\,346$ | $449\,890$ | $-627\,456$ |
| $M_{34}$ | Analytical Black | Standard | 1D | NA | $-1\,075\,398$ | $448\,170$ | $-627\,229$ |
| $M_{35}$ | Analytical Black | Standard | 1M | NA | $-1\,072\,231$ | $447\,369$ | $-624\,862$ |
| $M_{36}$ | Analytical Black | Standard | 3M | NA | $-1\,067\,726$ | $447\,358$ | $-620\,369$ |
| $M_{37}$ | Analytical Black | Standard | 12M | NA | $-1\,016\,082$ | $432\,373$ | $-583\,709$ |
| $\text{XVA}(t_0; M)$ | | | | | | | $-697\,614$ |
| $\text{XVA}(t_0; M_3)$ | | | | | | | $-700\,463$ |
| $\text{AVA}^{\text{MoRi}}(t_0)$ | | | | | | | $2849$ |

**Table 8:** 15 years ATM payer Swap EUR 100 Mio notional, no collateral. Distribution of plausible XVA; each row represents a different combination of model and parameters. XVA obtained from target framework $M$ optimizing the trade-off between accuracy and performance denoted by an asterisk while prudent XVA at a confidence level of 90% obtained from framework $M_3$ denoted by double asterisk.

46

5x10 years ATM payer Swaption, no collateral

| | XVA framework | | | | CVA | DVA | XVA |
|---|---|---|---|---|---|---|---|
| $M_j$ | Model | Parameters | | | | | |
| | | Time grid | $\Delta t$ | $N_{MC}$ | | | |
| $M_1$ | MC | Joint | 1M | 7000 | $-824\,079$ | $36\,192$ | $-787\,887$ |
| $M_2$ | MC | Joint | 1M | 6000 | $-822\,059$ | $36\,034$ | $-786\,025^{**}$ |
| $M_3$ | MC | Joint | 1D | 5000 | $-819\,616$ | $36\,367$ | $-783\,249$ |
| $M_4$ | MC | Joint | 1M | 8000 | $-819\,809$ | $36\,733$ | $-783\,075$ |
| $M$ | MC | Joint | 1M | 5000 | $-818\,308$ | $36\,418$ | $-781\,890^{*}$ |
| $M_5$ | MC | Standard | 1M | 5000 | $-818\,293$ | $36\,426$ | $-781\,867$ |
| $M_6$ | MC | Joint | 1M | 14000 | $-819\,182$ | $37\,741$ | $-781\,441$ |
| $M_7$ | MC | Joint | 3M | 5000 | $-817\,396$ | $36\,544$ | $-780\,851$ |
| $M_8$ | MC | Joint | 1M | 15000 | $-818\,526$ | $37\,677$ | $-780\,849$ |
| $M_9$ | MC | Joint | 1M | 20000 | $-818\,405$ | $37\,577$ | $-780\,828$ |
| $M_{10}$ | MC | Standard | 3M | 5000 | $-817\,335$ | $36\,565$ | $-780\,770$ |
| $M_{11}$ | MC | Joint | 1M | 19000 | $-818\,061$ | $37\,390$ | $-780\,671$ |
| $M_{12}$ | MC | Joint | 1M | 13000 | $-818\,459$ | $37\,938$ | $-780\,521$ |
| $M_{13}$ | MC | Joint | 1M | 18000 | $-817\,336$ | $37\,215$ | $-780\,121$ |
| $M_{14}$ | MC | Joint | 1M | 9000 | $-817\,778$ | $37\,790$ | $-779\,988$ |
| $M_{15}$ | MC | Joint | 1M | 16000 | $-816\,860$ | $37\,294$ | $-779\,566$ |
| $M_{16}$ | MC | Joint | 1M | 4000 | $-816\,207$ | $36\,877$ | $-779\,330$ |
| $M_{17}$ | MC | Joint | 1M | 11000 | $-816\,663$ | $37\,339$ | $-779\,324$ |
| $M_{18}$ | MC | Joint | 1M | 17000 | $-816\,521$ | $37\,229$ | $-779\,292$ |
| $M_{19}$ | MC | Joint | 1M | 12000 | $-817\,132$ | $37\,870$ | $-779\,261$ |
| $M_{20}$ | MC | Joint | 6M | 5000 | $-815\,745$ | $36\,705$ | $-779\,040$ |
| $M_{21}$ | MC | Standard | 6M | 5000 | $-815\,610$ | $36\,737$ | $-778\,873$ |
| $M_{22}$ | MC | Joint | 1M | 10000 | $-816\,317$ | $37\,584$ | $-778\,733$ |
| $M_{23}$ | MC | Joint | 1M | 3000 | $-808\,845$ | $37\,481$ | $-771\,364$ |
| $M_{24}$ | MC | Joint | 1M | 2000 | $-802\,335$ | $37\,890$ | $-764\,445$ |
| $M_{25}$ | MC | Joint | 1M | 1000 | $-790\,761$ | $41\,999$ | $-748\,761$ |
| $M_{26}$ | MC | Joint | 12M | 5000 | $-775\,964$ | $41\,357$ | $-734\,606$ |
| $M_{27}$ | MC | Standard | 12M | 5000 | $-772\,699$ | $42\,047$ | $-730\,651$ |
| $\mathrm{XVA}(t_0; M)$ | | | | | | | $-781\,890$ |
| $\mathrm{XVA}(t_0; M_2)$ | | | | | | | $-786\,025$ |
| $\mathrm{AVA}^{\mathrm{MoRi}}(t_0)$ | | | | | | | $4135$ |

**Table 9:** 5x10 years ATM physically settled European payer Swaption EUR 100 Mio notional, no collateral. Distribution of plausible XVA; each row represents a different combination of model and parameters. XVA obtained from target framework $M$ optimizing the trade-off between accuracy and performance denoted by an asterisk while prudent XVA at a confidence level of 90% obtained from framework $M_2$ denoted by double asterisk.

# 6 Conclusions

We have shown that an XVA desk has to cope with a significant model risk, especially for collateralized trades. In fact, collateral simulation implies a greater computational effort, particularly when a "bump-and-run" approach is used for computing ISDA-SIMM dynamic IM. For this reason, it becomes necessary to avoid unnecessary workloads that would make the calculation unfeasible. A decrease in computing time can be obtained through additional modelling choices which turn out to be additional sources of model risk. In this context we have found a parameterization that offers an acceptable compromise between accuracy and performance.

We have seen that a crucial element is the construction of a parsimonious time grid capable of capturing all periodical spikes arising in collateralized Swap's exposure during the MPoR, having a material impact on CVA/DVA. To this end, we proposed a workaround which ensures to capture all spikes with an acceptable loss of precision in a reasonable time.

Regarding the number of simulated scenarios, we observed a convergence to "exact" value proxies even for a limited number of simulated paths, leaving room for an ulterior saving of computational time if necessary.

Further assumptions are required for the calculation of G2++ forward Vega sensitivities according to ISDA-SIMM prescriptions. In this case, the related model risk has been addressed by making sure that the proposed approximation produces results aligned with two alternative approaches both consistent with ISDA-SIMM definition at time $t_0$ (i.e. valuation date) and by avoiding any arbitrary elements in the choice of the associated parameters.

Furthermore, we have shown that analytical formulas represent a useful tool for validating the results obtained through Monte Carlo approach provided that the same interest rates dynamic is considered, and can also be used for obtain reliable CVA/DVA for an uncollateralized Swap. Also in this case, model risk should be correctly addressed since different dynamics lead to different results.

Finally, the valuation uncertainty stemming from CVA/DVA pricing has been considered by calculating the related Model Risk Additional Valuation Adjustment (AVA) as envisaged in regulation [35, 36].

This work can be extended in different directions. The performance of the XVA framework can be enhanced by applying more advanced techniques, e.g. adjoint algorithmic differentiation (AAD) or Chebyshev decomposition to speed up and stabilize sensitivities calculation. The exposure engine can be extended to include other valuation adjustments, e.g. Funding Valuation Adjustment (FVA) and Margin Valuation Adjustment (MVA). More payoffs can be implemented and XVA can be computed at portfolio level.

# Appendices

## A  Market Data

The following tables report the market data considered in our work at 28 December 2018.

EURIBOR 6M curve Zero Coupon Bonds

| $t$ (d) | $P(0;t)$ | $t$ (d) | $P(0;t)$ | $t$ (d) | $P(0;t)$ | $t$ (d) | $P(0;t)$ | $t$ (d) | $P(0;t)$ |
|---:|---:|---:|---:|---:|---:|---:|---:|---:|---:|
| 0 | 1.0000 | 311 | 1.0020 | 738 | 1.0036 | 5484 | 0.8355 | 10 597 | 0.6644 |
| 6 | 1.0000 | 339 | 1.0022 | 917 | 1.0033 | 5849 | 0.8195 | 10 965 | 0.6551 |
| 12 | 1.0001 | 370 | 1.0024 | 1102 | 1.0022 | 6214 | 0.8039 | 11 329 | 0.6461 |
| 19 | 1.0001 | 402 | 1.0025 | 1466 | 0.9977 | 6580 | 0.7890 | 11 693 | 0.6373 |
| 26 | 1.0002 | 430 | 1.0027 | 1831 | 0.9902 | 6947 | 0.7747 | 12 058 | 0.6287 |
| 38 | 1.0003 | 461 | 1.0028 | 2197 | 0.9800 | 7311 | 0.7612 | 12 424 | 0.6201 |
| 66 | 1.0005 | 493 | 1.0030 | 2562 | 0.9675 | 7675 | 0.7484 | 12 789 | 0.6117 |
| 95 | 1.0006 | 522 | 1.0031 | 2929 | 0.9531 | 8041 | 0.7361 | 13 156 | 0.6034 |
| 125 | 1.0008 | 552 | 1.0032 | 3293 | 0.9374 | 8406 | 0.7246 | 13 520 | 0.5953 |
| 157 | 1.0010 | 584 | 1.0033 | 3658 | 0.9208 | 8771 | 0.7136 | 13 885 | 0.5873 |
| 186 | 1.0012 | 614 | 1.0034 | 4023 | 0.9037 | 9138 | 0.7031 | 14 250 | 0.5796 |
| 217 | 1.0014 | 644 | 1.0035 | 4388 | 0.8863 | 9502 | 0.6932 | 14 615 | 0.5721 |
| 248 | 1.0016 | 675 | 1.0035 | 4753 | 0.8690 | 9867 | 0.6834 | 18 268 | 0.5046 |
| 278 | 1.0018 | 705 | 1.0036 | 5120 | 0.8520 | 10 232 | 0.6738 | 21 920 | 0.4461 |

**Table 10:** EURIBOR 6M Zero Coupon Curve.


OIS curve Zero Coupon Bonds

| $t$ (d) | $P(0;t)$ | $t$ (d) | $P(0;t)$ | $t$ (d) | $P(0;t)$ | $t$ (d) | $P(0;t)$ | $t$ (d) | $P(0;t)$ |
|---:|---:|---:|---:|---:|---:|---:|---:|---:|---:|
| 0 | 1.0000 | 248 | 1.0025 | 675 | 1.0059 | 5120 | 0.8689 | 10 232 | 0.6942 |
| 3 | 1.0000 | 278 | 1.0028 | 705 | 1.0061 | 5484 | 0.8530 | 10 597 | 0.6850 |
| 5 | 1.0001 | 311 | 1.0031 | 738 | 1.0062 | 5849 | 0.8375 | 10 965 | 0.6758 |
| 6 | 1.0001 | 339 | 1.0033 | 1102 | 1.0063 | 6214 | 0.8224 | 12 789 | 0.6325 |
| 12 | 1.0001 | 370 | 1.0036 | 1466 | 1.0033 | 6580 | 0.8079 | 14 615 | 0.5930 |
| 19 | 1.0002 | 402 | 1.0039 | 1831 | 0.9975 | 6947 | 0.7939 | 18 268 | 0.5250 |
| 26 | 1.0003 | 430 | 1.0042 | 2197 | 0.9888 | 7311 | 0.7807 | 21 920 | 0.4655 |
| 38 | 1.0004 | 461 | 1.0044 | 2562 | 0.9778 | 7675 | 0.7682 | | |
| 66 | 1.0007 | 493 | 1.0047 | 2929 | 0.9648 | 8041 | 0.7562 | | |
| 95 | 1.0009 | 522 | 1.0049 | 3293 | 0.9501 | 8406 | 0.7448 | | |
| 125 | 1.0012 | 552 | 1.0052 | 3658 | 0.9346 | 8771 | 0.7340 | | |
| 157 | 1.0016 | 584 | 1.0054 | 4023 | 0.9183 | 9138 | 0.7235 | | |
| 186 | 1.0019 | 614 | 1.0056 | 4388 | 0.9018 | 9502 | 0.7135 | | |
| 217 | 1.0022 | 644 | 1.0058 | 4753 | 0.8853 | 9867 | 0.7037 | | |

**Table 11:** OIS Zero Coupon Curve (EONIA).

| $\xi/\mathfrak{T}$ | 2 | 3 | 4 | 5 | 6 | 7 | 8 | 9 | 10 | 15 | 20 | 25 | 30 |
|---|---|---|---|---|---|---|---|---|---|---|---|---|---|
| 2 | 95 | 155 | 216 | 273 | 331 | 386 | 437 | 488 | 537 | 746 | 933 | 1108 | 1270 |
| 3 | 143 | 222 | 297 | 373 | 447 | 518 | 585 | 651 | 713 | 975 | 1221 | 1445 | 1653 |
| 4 | 185 | 279 | 371 | 460 | 548 | 632 | 715 | 793 | 865 | 1170 | 1459 | 1723 | 1976 |
| 5 | 221 | 328 | 432 | 534 | 634 | 731 | 824 | 913 | 996 | 1338 | 1666 | 1964 | 2250 |
| 6 | 248 | 367 | 481 | 594 | 705 | 810 | 912 | 1008 | 1101 | 1472 | 1832 | 2156 | 2471 |
| 7 | 271 | 399 | 523 | 644 | 763 | 876 | 986 | 1095 | 1200 | 1598 | 1980 | 2331 | 2674 |
| 8 | 290 | 427 | 560 | 690 | 818 | 940 | 1058 | 1171 | 1281 | 1705 | 2106 | 2487 | 2853 |
| 9 | 306 | 451 | 591 | 727 | 861 | 992 | 1116 | 1236 | 1355 | 1801 | 2227 | 2623 | 3007 |
| 10 | 320 | 473 | 620 | 765 | 904 | 1041 | 1170 | 1297 | 1427 | 1902 | 2344 | 2755 | 3164 |
| 12 | 342 | 503 | 663 | 816 | 967 | 1116 | 1257 | 1397 | 1528 | 2042 | 2516 | 2973 | 3390 |
| 15 | 368 | 544 | 713 | 879 | 1042 | 1198 | 1351 | 1505 | 1658 | 2225 | 2748 | 3230 | 3678 |
| 20 | 395 | 587 | 768 | 950 | 1131 | 1299 | 1469 | 1635 | 1794 | 2434 | 2961 | 3467 | 3927 |
| 25 | 417 | 620 | 812 | 1003 | 1188 | 1365 | 1537 | 1711 | 1878 | 2556 | 3086 | 3606 | 4082 |
| 30 | 432 | 640 | 842 | 1042 | 1229 | 1407 | 1571 | 1737 | 1906 | 2601 | 3136 | 3667 | 4164 |

**Table 12:** Quoted ATM Swaption Straddles (Physically settled LCH, $N = 10000$ EUR), expiries and tenors in years on rows and columns respectively.

| $t$ (d) | B | C |
|---|---|---|
| 180 | 91 | 24 |
| 360 | 105 | 29 |
| 720 | 125 | 48 |
| 1080 | 146 | 72 |
| 1440 | 163 | 99 |
| 1800 | 181 | 126 |
| 2520 | 200 | 159 |
| 3600 | 216 | 183 |
| 5400 | 219 | 195 |
| 7200 | 222 | 202 |
| 10 800 | 227 | 213 |

**Table 13:** CDS spread term structure for both counterparties (in bps).

# B   G2++ Swap and European Swaption Pricing

We present the generalization of G2++ pricing formulas for Swap and European Swaption in multi-curve framework and with time dependent (piece-wise constant) volatility parameters. In [39] it is shown that in single-curve framework European Swaption admits a closed formula. We derive European Swaption pricing formula in multi-curve framework by relying on the original derivation, expressing the multi-curve Swap price in a way which is formally equivalent to the single-curve one.

In single-curve framework, the price at time $t$ of an European Swaption expiring at $T_e$ under the forward measure $Q^{T_e}$ can be written as (we omit the filtration $\mathcal{F}_t$ in order to simplify the

presentation)

$$\textbf{Swaption}(t; \mathbf{T}, \mathbf{S}, K, \omega) = NP(t; T_e)\mathbb{E}^{Q^{T_e}} \left\{ \max \left[ \textbf{Swap}^{\text{SC}}(T_e; \mathbf{T}, \mathbf{S}, K, \omega, c); 0 \right] \right\},$$

$$= NP(t, T_e)\mathbb{E}^{Q^{T_e}} \left\{ \max \left[ \omega \left( P(T_e; T_0) - \sum_{i=1}^{m} c_i P(T_e; S_i) \right); 0 \right] \right\},$$

(B.1)

where $c_i = K\tau(S_{i-1}, S_i)$ for $i = 1, ..., m-1$ and $c_m = 1 + K\tau(S_{m-1}, S_m)$, with $S_m = T_n$. As already mentioned, [39] provides a closed formula for the expected value above under the G2++ model.

It can be shown that, in multi-curve framework, the price at time $t$ of a Swap's floating coupon payment under the G2++ model is given by

$$\textbf{Swaplet}_{\text{float}}(t; T_{j-1}, T_j) = N\mathbb{E}^{Q} \left[ D(t; T_j)R_x(T_{j-1}, T_j)\tau_R(T_{j-1}, T_j) \right]$$

$$= N \left[ \frac{\phi^d(T_{j-1}; T_j)}{\phi^x(T_{j-1}; T_j)} P_d(t; T_{j-1}) - P_d(t; T_j) \right],$$

(B.2)

where $\phi^c(t; T) = \exp\left\{ -\int_t^T \varphi^c(u)du \right\}$, $c \in \{d, x\}$ with $d$ and $x$ denoting respectively the discount $\mathcal{C}_d$ and the forward $\mathcal{C}_x$ curves.

*Proof.*

$$\mathbb{E}^{Q} \left[ D(t; T_j)R_x(T_{j-1}, T_j)\tau_R(T_{j-1}, T_j) \right]$$

$$= \mathbb{E}^{Q} \left[ D(t; T_j) \frac{1 - P_x(T_{j-1}; T_j)}{P_x(T_{j-1}; T_j)} \right]$$

$$= \mathbb{E}^{Q} \left[ \phi^d(t; T_j) \exp\left\{ -\int_t^{T_j} x(s) + y(s)ds \right\} \left( \frac{1}{P_x(T_{j-1}; T_j)} - 1 \right) \right]$$

$$= \mathbb{E}^{Q} \left[ \frac{\phi^d(t; T_j)}{\phi^x(T_{j-1}; T_j)} \exp\left\{ -\int_t^{T_{j-1}} x(s) + y(s)ds \right\} \right.$$

$$\left. \cdot \frac{\mathbb{E}^{Q}_{T_{j-1}} \left[ \exp\left\{ -\int_{T_{j-1}}^{T_j} x(s) + y(s)ds \right\} \right]}{\mathbb{E}^{Q}_{T_{j-1}} \left[ \exp\left\{ -\int_{T_{j-1}}^{T_j} x(s) + y(s)ds \right\} \right]} \right] - P_d(t; T_j)$$

(B.3)

$$= \mathbb{E}^{Q} \left[ \frac{\phi^d(t; T_j)}{\phi^x(T_{j-1}; T_j)} \exp\left\{ -\int_t^{T_{j-1}} x(s) + y(s)ds \right\} \right] - P_d(t, T_j)$$

$$= \mathbb{E}^{Q} \left[ \frac{\phi^d(t; T_{j-1})\phi^d(T_{j-1}; T_j)}{\phi^x(T_{j-1}; T_j)} \exp\left\{ -\int_t^{T_{j-1}} x(s) + y(s)ds \right\} \right] - P_d(t; T_j)$$

$$= \frac{\phi^d(T_{j-1}; T_j)}{\phi^x(T_{i-1}; T_j)} P_d(t; T_{j-1}) - P_d(t; T_j,) \qquad \forall j.$$

$\square$

Therefore the price of the Swap can be written as

$$\textbf{Swap}^{\text{MC}}(t; \mathbf{T}, \mathbf{S}, K, \omega)$$

$$= N\omega \left[ \sum_{j=1}^{n} \left[ \psi(T_{j-1}; T_j)P_d(t; T_{j-1}) - P_d(t; T_j) \right] - \sum_{i=1}^{m} K\tau_K(S_{i-1}, S_i)P_d(t; S_i) \right], \qquad (\text{B.4})$$

with
$$\psi(T_{j-1};T_j) = \frac{\phi^d(T_{j-1};T_j)}{\phi^x(T_{j-1};T_j)} = \frac{P_d^M(0;T_j)}{P_d^M(0;T_{j-1})} \frac{P_x^M(0;T_{j-1})}{P_x^M(0;T_j)}, \tag{B.5}$$

where $P_c^M(0;T)$ is the currently observed ZCB maturing at $T$ and the second equality follows from

$$\exp\left\{ -\int_{T_{j-1}}^{T_j} \varphi^c(u)du \right\} = \frac{P_c^M(0;T_j)}{P_c^M(0;T_{j-1})} \exp\left\{ -\frac{1}{2} \left[ V(0;T_j) - V(0;T_{j-1}) \right] \right\}, \tag{B.6}$$

where $V(t;T_j)$ is the variance of the random variable $I(t;T_j) = \int_t^{T_j} [x(s) + y(s)]ds$, which is normally distributed with mean $M(t;T_j)$ (see [39] for the proof). By considering the piece-wise constant volatility parameters introduced in sec. 2.3.1 we obtain the following equation

$$\begin{aligned}
V(t;T_j) = &\frac{\sigma^2}{a^2} \sum_{i=u}^{v} \Gamma_i^2 \left[ T_{i+1} - T_i - \frac{2e^{-aT_j}}{a} \left( e^{aT_{i+1}} - e^{aT_i} \right) - \frac{e^{-2aT_j}}{2a} \left( e^{2aT_{i+1}} - e^{2aT_i} \right) \right] \\
&+ \frac{\eta^2}{b^2} \sum_{i=u}^{v} \Gamma_i^2 \left[ T_{i+1} - T_i - \frac{2e^{-bT_j}}{b} \left( e^{bT_{i+1}} - e^{bT_i} \right) - \frac{e^{-2bT_j}}{2b} \left( e^{2bT_{i+1}} - e^{2bT_i} \right) \right] \\
&+ \frac{2\rho\eta\sigma}{ab} \sum_{i=u}^{v} \Gamma_i^2 \left[ T_{i+1} - T_i - \frac{e^{-aT_j}}{a} \left( e^{aT_{i+1}} - e^{aT_i} \right) - \frac{e^{-bT_j}}{b} \left( e^{bT_{i+1}} - e^{bT_i} \right) \right] \\
&+ \frac{2\rho\eta\sigma}{ab} \sum_{i=u}^{v} \Gamma_i^2 \left[ \frac{e^{-(a+b)T_j}}{a+b} \left( e^{(a+b)T_{i+1}} - e^{(a+b)T_i} \right) \right],
\end{aligned} \tag{B.7}$$

where here we assumed that $T_u = t$ and $T_{v+1} = T_j$.

Now we are able to write the multi-curve Swap price in terms of the single-curve one assuming the existence of a vector of coefficient $\widehat{c}$ such that

$$\begin{aligned}
\mathbf{Swap}^{\mathrm{MC}}(t;\mathbf{T},\mathbf{S},K,\omega) &= c_0 \, \mathbf{Swap}^{\mathrm{SC}}(t;\mathbf{T},\mathbf{S},K,\omega,\widehat{c}) \\
&= c_0 \, \omega \left( P(t;T_0) - \sum_{i=1}^{m} \widehat{c}_i P(t;T_i) \right).
\end{aligned} \tag{B.8}$$

These coefficients are defined as follows

$$\begin{aligned}
c_0 &= \psi(T_0;T_1), \\
\widehat{c}_j &= c_0^{-1} \left[ 1 - \psi(T_j;T_{j+1}) \mathbb{1}_{\{T_j \neq T_n\}} + K\tau_K(S_i,S_{i+1}) \mathbb{1}_{\{T_j = S_i\}} \right], \quad j = 1,\dots,n.
\end{aligned} \tag{B.9}$$

Consider for example a payer Swap with unitary notional and maturity 2 years with semi-annual floating leg and annual fixed leg, characterized by the schedules $\mathbf{T} = \{T_0,T_1,T_2,T_3,T_4\}$ and $\mathbf{S} = \{S_0,S_1,S_2\}$, where $T_0 = S_0$, $T_2 = S_1$ and $T_4 = S_2$. The price in multi-curve framework is given by

$$\begin{aligned}
\mathbf{Swap}^{\mathrm{MC}}(t;\mathbf{T},\mathbf{S},K,1) = \,& P_d(t;T_0)\psi(T_0;T_1) - P_d(t;T_1)\left[ 1 - \psi(T_1;T_2) \right] \\
& - P_d(t;T_2)\left[ 1 - \psi(T_2;T_3) + K\tau_K(S_0,S_1) \right] - P_d(t;T_3)\left[ 1 - \psi(T_3;T_4) \right] \\
& - P_d(t;T_4)\left[ 1 + K\tau_K(S_1,S_2) \right],
\end{aligned} \tag{B.10}$$

from which it is possible to recognize the following coefficients

$$\begin{aligned}
c_0 &= \psi(T_0;T_1) \\
\widehat{c}_1 &= c_0^{-1} \left[ 1 - \psi(T_1;T_2) \right] \\
\widehat{c}_2 &= c_0^{-1} \left[ 1 - \psi(T_2;T_3) + K\tau_K(S_0,S_1) \right] \\
\widehat{c}_3 &= c_0^{-1} \left[ 1 - \psi(T_3;T_4) \right] \\
\widehat{c}_4 &= c_0^{-1} \left[ 1 + K\tau_K(S_1;S_2) \right].
\end{aligned} \tag{B.11}$$

52

At this point we are able to write the G2++ pricing formula for an European Swaption in multi-curve framework and with piece-wise constant volatility parameters ensuring the preservation of the proof in [39]

**Swaption**$(t; \mathbf{T}, \mathbf{S}, K, \omega)$

$$= N\omega P_d(t; T_e) \int_{-\infty}^{+\infty} \frac{e^{-\frac{1}{2}\left(\frac{x-\mu_x}{\sigma_x}\right)^2}}{\sigma_x\sqrt{2\pi}} \left[\Phi(-\omega h_1(x)) - \sum_{j=1}^{n} \lambda_j(x) e^{\mathcal{K}_j(x)} \Phi(-\omega h_2(x))\right] dx, \tag{B.12}$$

where

$$h_1(x) = \frac{\bar{y} - \mu_y}{\sigma_y\sqrt{1-\rho_{xy}^2}} - \frac{\rho_{xy}(x-\mu_x)}{\sigma_x\sqrt{1-\rho_{xy}^2}}, \tag{B.13}$$

$$h_2(x) = h_1(x) + \mathcal{B}(b, T_e, T_j)\sigma_y\sqrt{1-\rho_{xy}^2}, \tag{B.14}$$

$$\lambda_j(x) = \widehat{c}_j \mathcal{A}_d(T_e; T_j) e^{-\mathcal{B}(a,T_e,T_j)x}, \tag{B.15}$$

$$\mathcal{K}_j(x) = -\mathcal{B}(b, T_e, T_j)\left[\mu_y - \frac{1}{2}(1-\rho_{xy}^2)\sigma_y^2\mathcal{B}(b, T_e, T_j) + \rho_{xy}\sigma_y\frac{x-\mu_x}{\sigma_x}\right], \tag{B.16}$$

$$\mathcal{A}_c(t; T_j) = \frac{P_c^M(0; T_j)}{P_c^M(0; T_j)}\exp\left(-\frac{1}{2}V(0; T_j) + \frac{1}{2}V(0; t) + \frac{1}{2}V(t; T_j)\right), \tag{B.17}$$

$$\mathcal{B}(z, t; T_j) = \frac{1 - e^{-z(T_j-t)}}{z}, \quad z \in \{a, b\}. \tag{B.18}$$

$\bar{y} = \bar{y}(x)$ is the solution of the following equation

$$\sum_{j=1}^{n} \widehat{c}_j \mathcal{A}_d(T_e; T_j) e^{-\mathcal{B}(a,T_e,T_j)x - \mathcal{B}(b,T_e,T_j)\bar{y}} = 1, \tag{B.19}$$

and by setting $T_u = t$ and $T_{v+1} = T_e$

$$\mu_x = -M_x^T(t; T_e), \tag{B.20}$$

$$\mu_y = -M_y^T(t; T_e), \tag{B.21}$$

$$\sigma_x = \sqrt{\frac{\sigma^2}{2a}\sum_{i=u}^{v}\Gamma_i^2 e^{-2aT_e}e^{2a(T_{i+1}-T_i)}}, \tag{B.22}$$

$$\sigma_y = \sqrt{\frac{\eta^2}{2b}\sum_{i=u}^{v}\Gamma_i^2 e^{-2bT_e}e^{2b(T_{i+1}-T_i)}}, \tag{B.23}$$

$$\rho_{xy} = \frac{\rho\sigma\eta}{(a+b)\sigma_x\sigma_y}\left[1 - e^{-(a+b)T_e}\right]\sum_{i=u}^{v}\Gamma_i^2 e^{(a+b)(T_{i+1}-T_i)}, \tag{B.24}$$

where $M_x^T(t; T_e)$ and $M_y^T(t; T_e)$ are drift components stemming from the dynamics of the pro-

cesses $x$ and $y$ under the forward measure $T$

$$M_x^T(t; T_e) = \frac{\sigma^2}{a} \sum_{i=u}^{v} \Gamma_i^2 \left[ \frac{e^{-aT_e}}{a} \left( e^{aT_{i+1}} - e^{aT_i} \right) - \frac{e^{-a(T_e+T)}}{2a} \left( e^{2aT_{i+1}} - e^{2aT_i} \right) \right]$$
$$- \frac{\rho\sigma\eta}{b(a+b)} \sum_{i=u}^{v} \Gamma_i^2 \left[ \frac{e^{-aT_e}}{a} \left( e^{aT_{i+1}} - e^{aT_i} \right) - \frac{e^{-(aT_e+bT)}}{a+b} \left( e^{(a+b)T_{i+1}} - e^{(a+b)T_i} \right) \right],$$
$$\text{(B.25)}$$

$$M_y^T(t; T_e) = \frac{\eta^2}{b} \sum_{i=u}^{v} \Gamma_i^2 \left[ \frac{1}{b} e^{-bT_e} \left( e^{bT_{i+1}} - e^{bT_i} \right) - \frac{e^{-b(T_e+T)}}{2b} \left( e^{2bT_{i+1}} - e^{2bT_i} \right) \right]$$
$$- \frac{\rho\sigma\eta}{a(a+b)} \sum_{i=u}^{v} \Gamma_i^2 \left[ \frac{e^{-bT_e}}{b} \left( e^{bT_{i+1}} - e^{bT_i} \right) - \frac{e^{-(aT_e+bT)}}{a+b} \left( e^{(a+b)T_{i+1}} - e^{(a+b)T_i} \right) \right].$$
$$\text{(B.26)}$$

# C ISDA-SIMM for Swaps and European Swaptions

We describe the application of the Standard Initial Margin Model to Swaps and European Swaptions at trade level. We considered ISDA-SIMM Version 2.1 in order to be consistent with the valuation date considered (28 December 2018) [19] used in our analyses. Further details may be found in [42]. As shown in sec. 3.3.1, IM for a Swap and an European Swaption is given by

$$\text{IM}^{\text{Swap}} = \text{DeltaMargin}^{\text{IR}}, \tag{C.1}$$

$$\text{IM}^{\text{Swpt}} = \text{DeltaMargin}^{\text{IR}} + \text{VegaMargin}^{\text{IR}} + \text{CurvatureMargin}^{\text{IR}}. \tag{C.2}$$

The details on the calculation process for the three IM components are given in paragraphs below.

## C.1 Delta Margin for Interest Rate Risk Class

Delta Margin for IR Risk Class is computed through the following step-by-step process.

1. Calculation of IR Delta sensitivities vector

$$\Delta^c = [\Delta_{2w}^c, \Delta_{1m}^c, \Delta_{3m}^c, \Delta_{6m}^c, \Delta_{1y}^c, \Delta_{2y}^c, \Delta_{3y}^c, \Delta_{5y}^c, \Delta_{10y}^c, \Delta_{15y}^c, \Delta_{20y}^c, \Delta_{30y}^c], \tag{C.3}$$

where $c \in \{f, d\}$. See sec. 3.3.2 for details on definition and calculation methodology.

2. Calculation of Weighted Sensitivity $\text{WS}_{j,c}$ for the $j$-th SIMM tenor through the following formula

$$\text{WS}_{j,c} = \text{RW}_j \cdot \Delta_j^c \cdot \text{CR}_b, \tag{C.4}$$

where:

- $\text{RW}_j$ is the Risk Weight for the $j$-th SIMM tenor (tab. 14). ISDA specifies three different vectors based upon the volatility of the currency in which the instrument is denominated[20];

- $\Delta_j^c$ is Delta sensitivity corresponding to the $j$-th SIMM tenor for the interest rate curve $c$;

---

[19]Version 2.1 was effective from 1 December 2018 to 30 November 2019 when Version 2.2 was published.

[20]Low Volatility currencies: JPY; Regular Volatility currencies: USD, EUR, GBP, CHF, AUD, NZD, CAD, SEK, NOK, DKK, HKD, KRW, SGD and TWD; High Volatility currencies: all other currencies.

- $CR_b$ is the Concentration Risk Factor for the Currency Group $b$. In this case ISDA specifies four Currency Groups based upon the volatility of the currency in which the instrument is denominated[21]. $CR_b$ is calculated as follows

$$CR_b = \max\left\{1, \left(\frac{|\sum_{j,c} \Delta_j^c|}{T_b}\right)^{\frac{1}{2}}\right\}, \tag{C.5}$$

where $T_b$ is the Concentration Threshold for the Currency Group $b$. For Regular Volatility well-traded currencies $T_b = 210$ USD Mio/bp.

3. Calculation of Delta Margin through the aggregation of Weighted Sensitivities

$$\text{DeltaMargin}^{\text{IR}} = \sqrt{\sum_{c,j} \text{WS}_{j,c}^2 + \sum_{c,j} \sum_{(k,l) \neq (c,j)} \phi_{c,k} \rho_{j,l} \text{WS}_{j,c} \text{WS}_{l,k}}, \tag{C.6}$$

where:

- $\phi_{c,k} = 98\%$ is the correlation between interest rate curves of the same currency;
- $\rho_{j,l}$ is the correlation matrix between SIMM tenors (tab. 15).

## C.2 Vega Margin for Interest Rate Risk Class

Vega Margin for IR Risk Class is computed through the following step-by-step process.

1. Calculation of Vega Risks vector

$$\text{VR} = [\text{VR}_{2\text{w}}, \text{VR}_{1\text{m}}, \text{VR}_{3\text{m}}, \text{VR}_{6\text{m}}, \text{VR}_{1\text{y}}, \text{VR}_{2\text{y}}, \text{VR}_{3\text{y}}, \text{VR}_{5\text{y}}, \text{VR}_{10\text{y}}, \text{VR}_{15\text{y}}, \text{VR}_{20\text{y}}, \text{VR}_{30\text{y}}], \tag{C.7}$$

where:

$$\text{VR}_j = \nu_j \cdot \sigma_j^{\text{Blk}}, \tag{C.8}$$

is the Vega Risk for an European Swaption with expiry equal to tenor $j$, with $\nu_j$ and $\sigma_j^{\text{Blk}}$ being, respectively, IR Vega sensitivity and Black implied volatility. See sec. 3.3.2 for details on definition and calculation methodology.

2. Calculation of Vega Risk Exposure $\text{VRE}_j$ for the $j$-th SIMM expiry through the following formula

$$\text{VRE}_j = \text{VRW}^{\text{IR}} \cdot \text{VR}_j \cdot \text{VCR}_b, \tag{C.9}$$

where:

- $\text{VRW}^{\text{IR}} = 0.16$ is the Vega Risk Weight for IR Risk Class;
- $\text{VCR}_b$ is the Vega Concentration Risk Factor for the Currency Group $b$ calculated as[22]

$$\text{VCR}_b = \max\left\{1, \left(\frac{|\sum_j \text{VR}_j|}{\text{VT}_b}\right)^{\frac{1}{2}}\right\}, \tag{C.10}$$

where $\text{VT}_b$ is the Concentration Threshold for the Currency Group $b$. For Regular Volatility well-traded currencies $T_b = 2200$ USD Mio.

---

[21]Low Volatility currencies: JPY; Regular Volatility well-traded currencies: USD, EUR, GBP; Regular Volatility less well-traded currencies: CHF, AUD, NZD, CAD, SEK, NOK, DKK, HKD, KRW, SGD, TWD; High Volatility currencies: all other currencies.

[22]See footnote 21.

3. Calculation of Vega Margin through the aggregation of the Vega Risk Exposures

$$\text{VegaMargin}^{\text{IR}} = \sqrt{\sum_j \text{VRE}_j^2 + \sum_j \sum_{l \neq j} \rho_{j,l} \text{VRE}_j \text{VRE}_l}, \qquad \text{(C.11)}$$

where $\rho_{j,l}$ is the correlation matrix between expiries (tab. 15).

## C.3  Curvature Margin for Interest Rate Risk Class

Curvature Margin for IR Risk Class is computed through the following step-by-step process.

1. Calculation of Curvature Risk vector by applying a Scaling Function (tab. 16) to Vega Risk vector calculated for Vega Margin, in particular, for the $j$-th element

$$\text{CVR}_j = \text{SF}(t_j) \cdot \text{VR}_j, \qquad \text{(C.12)}$$

the value of the scaling function $\text{SF}(t_j)$ is defined as

$$\text{SF}(t_j) = 0.5 \, \min \left\{ 1, \frac{14 \text{ days}}{t_j \text{ days}} \right\}, \qquad \text{(C.13)}$$

where $t_j$ is the time (in calendar days) from the valuation date to the $j$-th SIMM expiry. The values of the Scaling Function for all SIMM expiries are reported in tab. 16.

2. Aggregation of Curvature Risk vector elements

$$K = \sqrt{\sum_j \text{CVR}_j^2 + \sum_j \sum_{l \neq j} \rho_{j,l}^2 \text{CVR}_j \text{CVR}_l}, \qquad \text{(C.14)}$$

where $\rho_{j,l}$ is the correlation matrix between expiries (tab. 15).

3. Calculation of Curvature Margin through the following formula

$$\text{CurvatureMargin}^{\text{IR}} = \max \left\{ 0, \sum_j \text{CVR}_j + \lambda K \right\} \text{HVR}_{\text{IR}}^{-2}, \qquad \text{(C.15)}$$

where:

- $\text{HVR}_{\text{IR}} = 0.62$ is the Historical Volatility Ratio for the IR Risk Class;
- $\lambda = (\Phi^{-1}(0.995)^2 - 1)(1 + \theta) - \theta$, with $\Phi^{-1}(0.995)$ is the 99.5[th] percentile of the standard normal distribution, and

$$\theta = \min \left\{ 0, \frac{\sum_j \text{CVR}_j}{\sum_j |\text{CVR}_j|} \right\}. \qquad \text{(C.16)}$$

Risk Weights vector for Regular Volatility currencies

| Tenor | 2w | 1m | 3m | 6m | 1y | 2y | 3y | 5y | 10y | 15y | 20y | 30y |
|---|---|---|---|---|---|---|---|---|---|---|---|---|
| Risk Weight | 114 | 115 | 102 | 71 | 61 | 52 | 50 | 51 | 51 | 51 | 54 | 62 |

**Table 14:** Risk Weights $\text{RW}_j$ parameters which apply to IR Delta tenors for Regular Volatility currencies.

Correlation matrix between tenors/expiries

| Tenor/Expiry | 2w | 1m | 3m | 6m | 1y | 2y | 3y | 5y | 10y | 15y | 20y | 30y |
|---|---|---|---|---|---|---|---|---|---|---|---|---|
| 2w | | 63% | 59% | 47% | 31% | 22% | 18% | 14% | 9% | 6% | 4% | 5% |
| 1m | 63% | | 79% | 67% | 52% | 42% | 37% | 30% | 23% | 18% | 15% | 13% |
| 3m | 59% | 79% | | 84% | 68% | 56% | 50% | 42% | 32% | 26% | 24% | 21% |
| 6m | 47% | 67% | 84% | | 86% | 76% | 69% | 60% | 48% | 42% | 38% | 33% |
| 1y | 31% | 52% | 68% | 86% | | 94% | 89% | 80% | 67% | 60% | 57% | 53% |
| 2y | 22% | 42% | 56% | 76% | 94% | | 98% | 91% | 79% | 73% | 70% | 66% |
| 3y | 18% | 37% | 50% | 69% | 89% | 98% | | 96% | 87% | 81% | 78% | 74% |
| 5y | 14% | 30% | 42% | 60% | 80% | 91% | 96% | | 95% | 91% | 88% | 84% |
| 10y | 9% | 23% | 32% | 48% | 67% | 79% | 87% | 95% | | 98% | 97% | 94% |
| 15y | 6% | 18% | 26% | 42% | 60% | 73% | 81% | 91% | 98% | | 99% | 97% |
| 20y | 4% | 15% | 24% | 38% | 57% | 70% | 78% | 88% | 97% | 99% | | 99% |
| 30y | 5% | 13% | 21% | 33% | 53% | 66% | 74% | 84% | 94% | 97% | 99% | |

**Table 15:** Correlation parameters $\rho_{j,l}$ between tenors/expiries.

Scaling Function values for SIMM standard expiries

| Expiry | 2w | 1m | 3m | 6m | 12m | 2y | 3y | 5y | 10y | 15y | 20y | 30y |
|---|---|---|---|---|---|---|---|---|---|---|---|---|
| SF | 50.0% | 23.0% | 7.7% | 3.8% | 1.9% | 1.0% | 0.6% | 0.4% | 0.2% | 0.1% | 0.1% | 0.1% |

**Table 16:** Scaling Function values for SIMM expiries calculated through eq. C.13, where expiries have been converted to calendar days using the convention that 12m = 365 days, with pro-rata scaling for other tenors, e.g. 1m = $\frac{365}{12}$ days and 5y = $365 \cdot 5$ days.

# References

[1] Marc P. A. Henrard. The Irony in the Derivatives Discounting. *Wilmott Magazine*, July-August 2007.

[2] Marco Bianchetti. Two Curves, One Price. *Risk Magazine*, pages 74–80, August 2010.

[3] Ferdinando M. Ametrano and Marco Bianchetti. Smooth Yield Curves Bootstrapping For Forward Libor Rate Estimation and Pricing Interest Rate Derivatives. In Fabio Mercurio, editor, *Modelling Interest Rates: Latest Advances for Derivatives Pricing*, pages 3–42. Risk Books, May 2009.

[4] Fabio Mercurio. Post Credit Crunch Interest Rates: Formulas and Market Models, 2009.

[5] Marc P. A. Henrard. The Irony in the Derivatives Discounting Part II: The Crisis, July 2009.

[6] Chris Kenyon. Short-Rate Pricing after the Liquidity and Credit Shocks: Including the Basis, February 2010.

[7] Vladimir V. Piterbarg. Cooking With Collateral. *Risk Magazine*, August 2012.

[8] Marco Scaringi and Marco Bianchetti. No Fear of Discounting-How to Manage the Transition from EONIA to €STR. *Available at SSRN 3674249*, 2020.

[9] Damiano Brigo and Massimo Masetti. Risk Neutral Pricing of Counterparty Risk. 2005.

[10] Damiano Brigo, Andrea Pallavicini, and Vasileios Papatheodorou. Arbitrage-Free Valuation of Bilateral Counterparty Risk for Interest-Rate Products: Impact of Volatilities and Correlations. *International Journal of Theoretical and Applied Finance*, 14(06):773–802, 2011.

[11] Damiano Brigo, Agostino Capponi, and Andrea Pallavicini. Arbitrage-Free Bilateral Counterparty Risk Valuation Under Collateralization and Application to Credit Default Swaps. *Mathematical Finance: An International Journal of Mathematics, Statistics and Financial Economics*, 24(1):125–146, 2014.

[12] International Accounting Standards Board. International Financial Reporting Standard 13 - Fair Value Measurement, May 2011.

[13] Christoph Burgard and Mats Kjaer. In the Balance, March 2011.

[14] Massimo Morini and Andrea Prampolini. Risky Funding with Counterparty and Liquidity Charges. *Risk Magazine*, March 2011.

[15] Andrea Pallavicini, Daniele Perini, and Damiano Brigo. Funding, Collateral and Hedging: uncovering the mechanics and the subtleties of funding valuation adjustments. *SSRN eLibrary*, December 2012.

[16] Jon Gregory. *The xVA Challenge: Counterparty Risk, Funding, Collateral, Capital and Initial Margin*. Wiley Finance. John Wiley & Sons Inc, April 2020.

[17] Andrew David Green and Chris Kenyon. MVA: Initial Margin Valuation Adjustment by Replication and Regression. *Available at SSRN 2432281*, 2015.

[18] Basel Committee on Banking Supervision. Basel II: International Convergence of Capital Measurement and Capital Standards: A Revised Framework - Comprehensive Version, June 2006.

[19] Basel Committee on Banking Supervision. Basel III: A global regulatory framework for more resilient banks and banking systems, June 2011.

[20] Andrew David Green, Chris Kenyon, and Chris Dennis. KVA: Capital Valuation Adjustment. *Risk, December*, 2014.

[21] Basel Committee on Banking Supervision and Board of the International Organization of Securities Commissions. Margin requirements for non-centrally cleared derivatives, March 2015.

[22] Basel Committee on Banking Supervision and Board of the International Organization of Securities Commissions. Second consultative document, margin requirements for non-centrally cleared derivatives, February 2013.

[23] International Swaps and Derivatives Association. Standard Initial Margin Model for Non-Cleared Derivatives, December 2013.

[24] Damiano Brigo, Massimo Morini, and Andrea Pallavicini. *Counterparty Credit Risk, Collateral and Funding, With Pricing Cases for all Asset Classes*. Wiley Finance, March 2013.

[25] Damiano Brigo, Cristin Buescu, Marco Francischello, Andrea Pallavicini, and Marek Rutkowski. Risk-neutral valuation under differential funding costs, defaults and collateralization, 2018.

[26] Damiano Brigo, Marco Francischello, and Andrea Pallavicini. Nonlinear valuation under credit, funding, and margins: Existence, uniqueness, invariance, and disentanglement. *European Journal of Operational Research*, 274(2):788–805, 2019.

[27] Jon Gregory. The Impact of Initial Margin. *Available at SSRN 2790227*, 2016.

[28] Leif BG Andersen, Michael Pykhtin, and Alexander Sokol. Rethinking the margin period of risk. *Journal of Credit Risk*, 13(1), 2017.

[29] Mariano Zeron and Ignacio Ruiz. Dynamic Initial Margin via Chebyshev Spectral Decomposition. Technical report, 2018.

[30] A. Maran, A. Pallavicini, and S. Scoleri. Chebyshev Greeks: Smoothing Gamma without Bias. *arXiv:2106.12431*, 2021.

[31] Luca Capriotti and Michael Giles. Adjoint Greeks made easy. *Risk*, 25(9):92, 2012.

[32] Antoine Savine. *Modern Computational Finance: AAD and Parallel Simulations*. John Wiley & Sons, 2018.

[33] Fabrizio Anfuso, Daniel Aziz, Paul Giltinan, and Klearchos Loukopoulos. A Sound Modelling and Backtesting Framework for Forecasting Initial Margin Requirements. *Available at SSRN 2716279*, 2017.

[34] Peter Caspers, Paul Giltinan, Roland Lichters, and Nikolai Nowaczyk. Forecasting Initial Margin Requirements: A Model Evaluation. *Journal of Risk Management in Financial Institutions*, 10(4):365–394, 2017.

[35] European Parliament and Council of the European Union. Regulation (EU) No 575/2013 of the European Parliament and of the Council of 26 June 2013 on prudential requirements for credit institutions and investment firms and amending Regulation (EU) No 648/2012. *Official Journal of the European Union*, June 2013.

[36] European Commission. Commission Delegated Regulation (EU) 2016/101 of 26 October 2015 supplementing Regulation (EU) No 575/2013 of the European Parliament and of the Council with regard to regulatory technical standards for prudent valuation under Article 105(14). *Official Journal of the European Union*, January 2016.

[37] Ferdinando M. Ametrano and Marco Bianchetti. Everything You Always Wanted to Know About Multiple Interest Rate Curve Bootstrapping but Were Afraid to Ask. *SSRN eLibrary*, April 2013.

[38] Massimo Morini. Solving the Puzzle in the Interest Rate Market, 2009.

[39] Damiano Brigo and Fabio Mercurio. *Interest-Rate Models - Theory and Practice*. Springer, 2nd edition, 2006.

[40] Paul Glasserman. *Monte Carlo Methods in Financial Engineering*. Springer, 2003.

[41] Leif BG Andersen, Michael Pykhtin, and Alexander Sokol. Credit Exposure in the Presence of Initial Margin. *Available at SSRN 2806156*, 2016.

[42] International Swaps and Derivatives Association. ISDA SIMM Methodology, version 2.1, December 2018.

[43] International Swaps and Derivatives Association. ISDA SIMM: From Principles to Model Specification, March 2016.

[44] Patrick S. Hagan, Deep Kumar, Andrew S. Lesniewski, and Diana E. Woodward. Managing Smile Risk. *Wilmott Magazine*, November 2002.